



Calhoun: The NPS Institutional Archive DSpace Repository

Theses and Dissertations

1. Thesis and Dissertation Collection, all items

1973-06

Secondary electron emission from monocrystalline metal and alkali-halide crystals

Allen, Kristin Lloyd

Monterey, California. Naval Postgraduate School

<http://hdl.handle.net/10945/16786>

Downloaded from NPS Archive: Calhoun



<http://www.nps.edu/library>

Calhoun is the Naval Postgraduate School's public access digital repository for research materials and institutional publications created by the NPS community.

Calhoun is named for Professor of Mathematics Guy K. Calhoun, NPS's first appointed -- and published -- scholarly author.

**Dudley Knox Library / Naval Postgraduate School
411 Dyer Road / 1 University Circle
Monterey, California USA 93943**

SECONDARY ELECTRON EMISSION FROM
MONOCRYSTALLINE METAL AND ALKALI-HALIDE
CRYSTALS

Kristin Lloyd Allen

Library
Naval Postgraduate School
Monterey, California 93940

NAVAL POSTGRADUATE SCHOOL

Monterey, California



THESIS

SECONDARY ELECTRON EMISSION
FROM MONOCRYSTALLINE METAL
AND ALKALI-HALIDE CRYSTALS

by

Kristin Lloyd Allen

Thesis Advisor:

D. E. Harrison, Jr.

June 1973

T153781

Approved for public release; distribution unlimited.

Secondary Electron Emission from Monocrystalline
Metal and Alkali-Halide Crystals

by

Kristin Lloyd Allen
Ensign, United States Navy
B.S.N.E., University of Virginia, 1972

Submitted in partial fulfillment of the
requirements for the degree of

MASTER OF SCIENCE IN PHYSICS

from the

NAVAL POSTGRADUATE SCHOOL
June 1973

ABSTRACT

This thesis is a computer simulation of secondary electron emission (SEE) from monocrystalline metals and alkali-halides using a modified version of the Harrison, Carlston and Magnuson single collision theory of SEE. Three cases of SEE are investigated: the angular dependence of SEE from Cu bombarded by Ar^+ , the dependence of SEE as a function of energy for rare gas ions normally incident on the (100), (110) and (111) faces of metal single crystals, and the dependence of SEE as a function of energy for Ar^+ and Ne^+ ions normally incident on the (100), (110) and (111) faces of KCl. The theory does not accurately describe the angular dependence of SEE for monocrystalline Cu targets, but does accurately predict the modified $\sec \theta$ dependence found experimentally in polycrystalline studies. For the metal targets, the difference between the theoretical kinetic secondary emission result and the experimental datum is identified as potential secondary emission. The alkali-halide SEE simulation agrees reasonably well with experiment.

TABLE OF CONTENTS

I. INTRODUCTION - - - - -	10
II. STUDY OBJECTIVES - - - - -	12
III. SECONDARY ELECTRON EMISSION THEORY - - - - -	13
IV. THEORIES CONCERNING SECONDARY ELECTRON EMISSION- -	19
A. THEORY OF PARILIS AND KISHINEVSKII - - - - -	19
B. THEORY OF HARRISON, CARLSTON AND MAGNUSON- - -	25
1. Inelastic Energy Transfer- - - - -	28
2. Collision Parameters - - - - -	30
3. Number of Electrons Emitted - Russek Model- - - - -	36
4. HCM Results- - - - -	38
V. MODIFICATIONS TO THE HCM THEORETICAL MODEL - - - -	41
A. INTERATOMIC POTENTIAL- - - - -	41
B. THE BASIC INTERACTION- - - - -	43
C. THE DISTRIBUTION OF IMPACT PARAMETERS- - - -	44
VI. NUMERICAL METHODS AND COMPUTER PROGRAMS- - - - -	53
VII. RESULTS- - - - -	60
A. ANGULARLY DEPENDENT RESULTS- - - - -	61
B. METAL TARGET RESULTS - - - - -	61
1. Copper Bombarded by Ar, Ne, Kr and Xe Ions- - - - -	61
2. Silver Bombarded by Ar, Ne and Kr Ions - -	72
3. Molybdenum Bombarded by Ar, Ne, Kr and Xe Ions- - - - -	80
4. Aluminum Bombarded by Ar, Kr and Xe Ions- - - - -	80

C. ALKALI-HALIDE RESULTS - - - - -	80
1. Potassium-Chloride Bombarded by Ar Ions - - - - -	102
2. Potassium-Chloride Bombarded by Ne Ions - - - - -	109
VIII. CONCLUSIONS AND RECOMMENDATIONS - - - - -	112
APPENDIX A - COMPUTER PROGRAM PARAMETERS - - - - -	116
COMPUTER PROGRAM - HERMAN-SKILLMAN RADIAL ELECTRON DENSITY PROGRAM - - - - -	121
COMPUTER PROGRAM - POTENTIAL PROGRAM - - - - -	139
COMPUTER PROGRAM - DISTRIBUTION OF IMPACT PARAMETERS PROGRAM- - - - -	149
COMPUTER PROGRAM - KSE PROGRAM - - - - -	155
LIST OF REFERENCES - - - - -	170
INITIAL DISTRIBUTION LIST- - - - -	172
FORM DD 1473 - - - - -	173

LIST OF FIGURES

Figure	Page
1. Potential energy diagram for a helium ion as it undergoes Auger neutralization at a tungsten surface. (3)	16
2. Potential energy diagram for a metastable atom (He) as it undergoes Auger de-excitation at a tungsten surface. (3)	17
3. Relationships between various quantities appearing in the Dynamic Integral	31
4. Representative areas for normal incidence. After (2)	33
5. Distribution of impact parameters for normal incidence on face-centered cubic crystals	34
6. Distribution of impact parameters for normal incidence on body-centered cubic crystals	35
7. Ar ⁺ - Cu results obtained from the HCM original model	39
8. Representative area of a (100) FCC crystal face rotated about <110> in either a positive or negative sense	47
9. Representative area of the (100) face of an FCC crystal rotated in a positive sense about the <110> direction	48
10. Rotation geometry for a (100) face of an FCC crystal about an arbitrary crystallographic direction	49
11. Unnormalized distribution of impact parameters for FCC (100) rotated through various angles about <110>	52
12. Deck setup for running the Electron Density Program	55
13. Deck setup for running the Potential Program	56

14. Deck setup for running the Distribution of Impact Parameters Program- - - - -	57
15. Deck setup for running the Interpolation Program - - - - -	58
16. Deck setup for running the KSE Program- - - - -	59
17. SEE coefficient vs. angle of rotation for (100) FCC Copper crystal. Direction of rotation was about $\langle 110 \rangle$ - - - - -	62
18. Cu bombarded by Ar^+ ions normally incident on the (100), (110) and (111) planes- - - - -	64
19. Cu bombarded by Ne^+ ions normally incident on the (100), (110) and (111) faces - - - - -	65
20. Cu bombarded by Kr^+ ions normally incident on the (100), (110) and (111) faces - - - - -	66
21. Cu bombarded by Xe^+ ions normally incident on the (100), (110) and (111) faces - - - - -	67
22. PSE contribution to secondary electron emission for the $\text{Ar}^+ - \text{Cu}$ system- - - - -	68
23. PSE contribution to secondary electron emission for the $\text{Ne}^+ - \text{Cu}$ system- - - - -	69
24. PSE contribution to secondary electron emission for the $\text{Kr}^+ - \text{Cu}$ system- - - - -	70
25. PSE contribution to secondary electron emission for the $\text{Xe}^+ - \text{Cu}$ system- - - - -	71
26. Ag bombarded by Ar^+ ions normally incident on the (100), (110) and (111) faces - - - - -	73
27. Ag bombarded by Ne^+ ions normally incident on the (100), (110) and (111) faces - - - - -	74
28. Ag bombarded by Kr^+ ions normally incident on the (100), (110) and (111) faces - - - - -	75
29. PSE contribution to secondary electron emission for the $\text{Ar}^+ - \text{Ag}$ system- - - - -	76
30. PSE contribution to secondary electron emission for the $\text{Ne}^+ - \text{Ag}$ system- - - - -	77

31. PSE contribution to γ secondary electron emission for the Kr ⁺ - Ag system - - - - -	78
32. Effect of varying target atom ionization in the HCM model on γ secondary electron emission from the Ar ⁺ - Mo system - - - - -	81
33. Effect of varying target atom ionization in the HCM model on γ secondary electron emission from the Ar ⁺ - Mo system - - - - -	82
34. Effect of varying target atom ionization in the HCM model on γ secondary electron emission in the Ar ⁺ - Mo system - - - - -	83
35. Effect on varying target atom ionization in the HCM model on secondary electron emission from the Ne ⁺ - Mo system - - - - -	84
36. Effect of varying target atom ionization in the HCM model on γ secondary electron emission from the Ne ⁺ - Mo system - - - - -	85
37. Effect of varying target atom ionization in the HCM model on γ secondary electron emission from the Ne ⁺ - Mo system - - - - -	86
38. Effect of varying target atom ionization in the HCM model on γ secondary electron emission from the Kr ⁺ - Mo system - - - - -	87
39. Effect of varying target atom ionization in the HCM model on γ secondary electron emission from the Kr ⁺ - Mo system - - - - -	88
40. Effect of varying target atom ionization in the HCM model on γ secondary electron emission from the Kr ⁺ - Mo system - - - - -	89
41. Effect of varying target atom ionization in the HCM model on γ secondary electron emission from the Xe ⁺ - Mo system - - - - -	90
42. Effect of varying target atom ionization in the HCM model on γ secondary electron emission from the Xe ⁺ - Mo system - - - - -	91
43. Effect of varying target atom ionization in the HCM model on γ secondary electron emission from the Xe ⁺ - Mo system - - - - -	92

44. Effect of varying target atom ionization in the HCM model on secondary electron emission from the Ar - Al system - - - - -	93
45. Effect of varying target atom ionization in the HCM model on secondary electron emission from the Ar - Al system - - - - -	94
46. Effect of varying target atom ionization in the HCM model on secondary electron emission from the Ar - Al system - - - - -	95
47. Effect of varying target atom ionization in the HCM model on secondary electron emission from the Kr - Al system - - - - -	96
48. Effect of varying target atom ionization in the HCM model on secondary electron emission from the Kr - Al system - - - - -	97
49. Effect of varying target atom ionization in the HCM model on secondary electron emission from the Kr - Al system - - - - -	98
50. Effect of varying target atom ionization in the HCM model on secondary electron emission from the Xe - Al system - - - - -	99
51. Effect of varying target atom ionization in the HCM model on secondary electron emission from the Xe - Al system - - - - -	100
52. Effect of varying target atom ionization in the HCM model on secondary electron emission from the Xe - Al system - - - - -	101
53. Representative area KC1 (100) - - - - -	103
54. Representative area KC1 (110) - - - - -	104
55. Representative area KC1 (111) - - - - -	105
56. Potassium distribution of impact parameters in KC1 - - - - -	106
57. Chlorine distribution of impact parameters in KC1 - - - - -	107
58. SEE coefficient as a function of energy for KC1 bombarded by Ar ions - - - - -	108
59. SEE coefficient as a function of energy for KC1 bombarded by Ne ions - - - - -	111

ACKNOWLEDGEMENT

I would like to thank Dr. Don E. Harrison, Jr. of the Naval Postgraduate School for his assistance in the preparation of this manuscript and for the many hours of conversation that resulted in a better understanding of the theories presented here. To my wife, Sarah, I express my sincere appreciation for her patience and understanding during the long hours spent in gathering data and writing this manuscript.

I. INTRODUCTION

Secondary electron emission is the release of electrons from target materials bombarded by primary ions. The first observation of secondary electron emission in 1889 was by Villard who noticed electrons being ejected from the cathode in a discharge tube. Secondary electron emission (SEE) is characterized by the coefficient of ion-electron emission, γ , which is defined as the number of electrons liberated per incident ion.

Secondary electron emission can be produced by two mechanisms, potential emission (PSE) and kinetic emission (KSE). Potential emission arises from the fact that as an ion approaches a target material it may become energetically feasible for a free electron to be emitted from the target surface either by Auger neutralization or Auger recombination. On the other hand, kinetic emission arises from the actual collision between the electrons of the impinging ion and the electrons in the target atom. In general, γ depends primarily upon the PSE mechanism at ion energies below one Kev and the KSE begins to contribute at ion energies above one Kev. Although this is a fairly good rule of thumb, variables such as the work function of the target material, ion charge, surface state of the target, target temperature, and whether the monocrystalline or polycrystalline nature of the target affect the value of the KSE threshold.

Medved et al. [1] have shown that potential emission from Ar^+ and Ar° on Mo increases with energy, with the total SEE at higher energies consisting partly of a KSE component and partly of a PSE component. In general there exists a transition region that is not sharply defined and for this reason it is felt that PSE contributes to secondary emission in the energy range above one Kev, even though the KSE should be the dominant emission mechanism in the one to ten Kev energy range. Both types of emission are investigated in this thesis.

II. STUDY OBJECTIVES

In 1964 Harrison, Carlston and Magnuson [2] proposed a single collision theory of secondary electron emission from monocrystalline target materials in the one to ten Kev primary ion energy range. The original paper develops a theory applicable to monocrystalline targets bombarded by inert gas ion beams directed normal to the (100), (110) and (111) crystal faces. This thesis will extend this theory to explain the following phenomena in the one to ten Kev primary ion energy range:

1. Secondary electron emission from a single crystal plane rotated arbitrarily about a crystallographic axis,
2. Secondary electron emission from metal single crystals, and
3. Secondary electron emission from alkali-halide monocrystals.

III. SECONDARY ELECTRON EMISSION THEORY

Secondary electron ejection mechanisms are either of the potential or kinetic type. Potential ejection can be caused by resonance neutralization, resonance ionization, Auger neutralization, or Auger de-excitation. Kinetic ejection requires the direct transfer of the ion's kinetic energy to the electrons of the target atom. Both mechanisms are discussed below.

Resonance neutralization occurs when it is energetically feasible for an electron in the target material to "tunnel" through its potential barrier and approach the position of the incoming ion. This stage of the process increases the energy of the ion and target atom system by an amount equal to the energy needed to remove an electron from the metal. This energy can range from near zero to ϕ , the work function of the target material. In the second stage of resonance neutralization, the electron and the ion combine, effectively at infinity, to reduce the system energy to an amount V_i , the ionization potential of the ion. This mechanism is not quite as simple as it seems, since it is affected by the image potential and coulombic forces of the electronic structure of the atoms in the crystal. According to the Franck-Condon principle, the electronic transition of the electron from the target material to the ion can only occur with appreciable probability when the position and velocity

of the ion are not affected by the transition. By this principle we expect a crossover of the initial and final potential energy curves of the system. Taking the image potential into account, resonance neutralization can occur for reasonable separations of ion and target atom when

$$(V_i - V_e) - \phi + I_s < W_a - \phi ,$$

and

$$(V_i - V_e) + I_s > \phi .$$

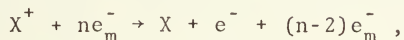
Therefore $\phi < (V_i - V_e) + I_s < W_a ,$

where ϕ is the work function of the target material, V_i , the ionization potential of the ion, V_e , the excitation potential of the primary ion, I_s , the surface image potential and W_a , the initial kinetic energy of the primary ion.

The second possible potential ejection mechanism is resonance ionization which is essentially the reverse process of resonance neutralization. In resonance ionization an excited atom at infinity is ionized into an electron and an ion. The electron then proceeds to the metal surface and occupies any of the unfilled available states above the Fermi level of the metal. As in resonance neutralization, there is a range of ion-target atom separation for which the process is most likely to occur. There is also the possibility that a highly excited atom will be ionized very close to the target surface with a subsequent high probability that a secondary electron will be produced.

Although the above processes are possible, they are not the ones that make the largest contributions to secondary electron emission at low energies. Auger processes, which occur at distances of approach of 3 \AA or less, are the primary mechanisms contributing to PSE in the low Kev energy range. These can be summarized as follows [3]:

Auger neutralization:



and

Auger de-excitation:



where X^+ and X^m refer to the bombarding ion or metastable atom, respectively, and ne_m^- is the number of free electrons initially in the target material. In both cases, the final state of the system is such that a free electron and a neutral atom are produced. Auger neutralization occurs when the energy of the initial system, target and ion, is greater than the resulting system, $X + e^- + (n-2)e_m^-$, at infinite separation. Schematically the process is shown in Figure 1 [3]. Auger de-excitation, on the other hand, involves a metastable atom which approaches the target material. As a result, the initial energy curve, shown in Figure 2 [3], is not modified by an image potential and hence the initial and final energy states never cross.

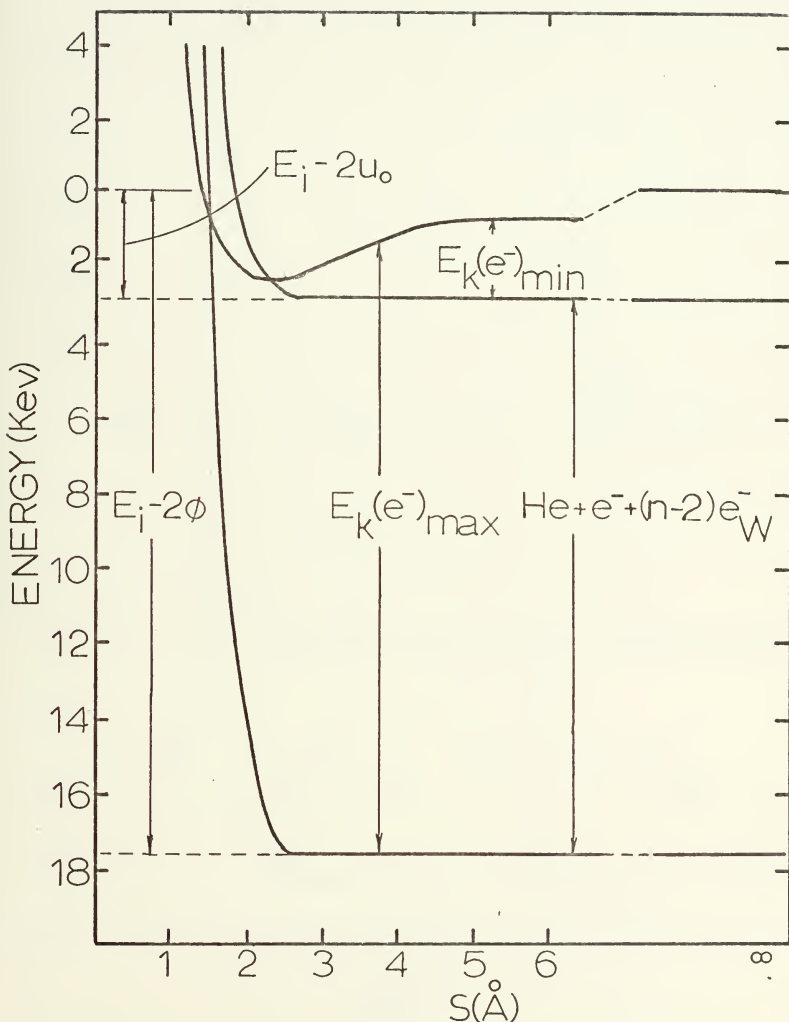


Figure 1. Potential energy diagram for a helium ion as it undergoes Auger neutralization at a tungsten surface (3).

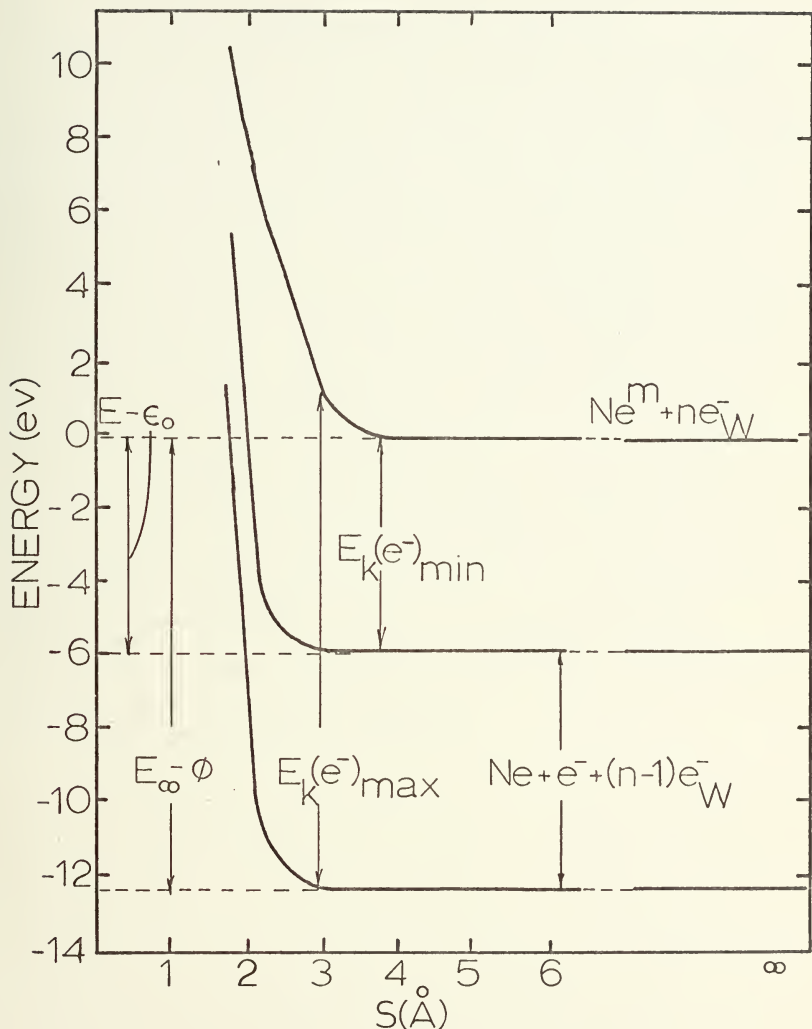


Figure 2. Potential energy diagram for a metastable atom (He) as it undergoes Auger de-excitation at a tungsten surface (3).

These two processes, to a great extent, account for low energy (ev range) secondary electron emission.

Kinetic emission is the result of the direct transfer of the incoming ion's kinetic energy to the atom's electrons. Part of this energy is absorbed in the recoil of the atom, while some of the remaining energy is transferred to the electrons of both the ion and target atom, causing an excitation of both of their electronic structures. As the two nuclei separate, some of the perturbed electrons are liberated as secondary electrons. The ion and recoiling target atom are slowed down within the crystal structure of the target material and are likely to undergo Auger neutralization or de-excitation. If this process occurs sufficiently close to the surface of the target material, there is a probability that these electrons also will escape from the target materials surface and contribute to kinetic secondary electron emission.

IV. THEORIES CONCERNING SECONDARY ELECTRON EMISSION

A. THEORY OF PARILIS AND KISHINEVSKII

Of all the theories proposed to explain kinetic secondary electron emission, the theory of Parilis and Kishinevskii (PK) seemed to be one of the most promising [4]. PK divided the secondary electron emission problem into two separate subproblems which were analyzed separately and subsequently collated to develop the theory of KSE. These two subproblems included:

1. The search for a sufficiently effective mechanism of transfer of the kinetic energy of a moving particle to the (target) electron; and
2. The description of the yield of excited electrons from the target. [4]

PK assumed that the solution to the first problem was of the form proposed by O. B. Firsov for inelastic scattering of ion-atom collisions in the Kev range [5]. Secondly, PK visualized the secondary electron emission process as one in which the primary ion ionizes many atoms as it progresses along its trajectory in the crystal. Electrons produced in this manner, or by further ionization of the primary ion, then proceed to the surface suffering collisions and energy losses as well as possible capture in route. The combination of the electron production phase and the electron escape phase then yields the KSE from the crystal.

The actual collision between the ion and the atom was seen by PK as being accompanied by an overlap of the

electron shell structure of the two collision partners, during which time there occurred an electronic interaction. Energy was transferred between colliding particles, exciting their electrons to a higher energy state. To calculate this excitation energy, a statistical picture of the electron distribution of the particles was used. The theoretical relationship, based on the Thomas-Fermi (TF) model of the atom, leads to the following formula for the energy transferred between the colliding particles:

$$E = \frac{m^2 e^2}{4\pi^2 \hbar^3} \int (\int_S \phi^2 dS) \underline{R} \cdot d\underline{R} ,$$

where \underline{R} is the radius vector connecting the centers of the colliding particles, S is the surface separating the domain of action for the potential of the two particles, and ϕ is the potential on this surface given by:

$$\phi = \left[\frac{(z_1 + z_2)e}{r} \right] \times \left[\frac{1.13(z_1 + z_2)^{1/3} r}{a_{TF}} \right] ,$$

where z_i is the charge on each particle, $a_{TF} = h^2/m e^2$ and χ is the TF screening function [8]. Physically, the interaction can be thought of as analogous to the collision of two tennis balls. As they impact, both deform, with the vector joining their centers being perpendicular to the area S of the plane of interaction which separates them. Obviously the total energy transferred is a function of the relative velocity with which the ion and atom impact and

the electron distribution associated with each. In terms of the tennis ball analogy, the greater the relative impact velocity, the larger the deformed area S , the shorter the radius vector distance R , and the greater the number of electrons involved.

The analysis was rewritten by PK in terms of the impact parameter associated with the collision. Hence by changing variables

$$E(p) = \frac{\hbar u_0}{\pi a^2} (z_1 + z_2)^2 \int_{R_0}^{\infty} \frac{(1 - V(r))}{[1 - \frac{V(r)}{E} - \frac{p^2}{R^2}]} dR$$

$$\int_{R/2}^{\infty} \frac{\chi^2(\rho) d\rho}{\rho},$$

where u_0 is the initial velocity of the ion, E is the excitation energy of the colliding particles, p is the impact parameter and $V(r)$ is the potential of repulsion between the particles.

To obtain the correct behavior of the emission curve, the cross section of electron ejection into the conduction band had to be calculated. Because more than one electron may be lifted from the valence band to the conduction band, the cross section was determined to be

$$\sigma = \Sigma \text{ (constant)} \cdot (\text{Probability of ionization})$$

$$p \cdot (\text{Impact parameter})$$

which in the integral limit approaches

$$\sigma = 2\pi \int_0^{P_1} \frac{E(p)}{J} p \, dp .$$

Here P_1 is the impact parameter at which $E(P_1) = \delta - \phi$, where δ is the energy depth of the filled conduction band, ϕ is the work function of the target material and J is the average ionization potential for the outer shells of the atom. For $1/4 < Z_1/Z_2 < 4$ PK found the cross section to be given by

$$\sigma(u_0) = \frac{1.39 a_{TF} h}{J} \frac{(Z_1 + Z_2)^2}{(Z_1^{1/2} + Z_2^{1/2})^2} S(u_0)$$

and $S(u_0)$ is approximated by

$$S(u_0) = 5.25 u_0 \arctan (.6 \times 10^{-7} (u_0 - u_{\min})) ,$$

where u_{\min} is the threshold velocity. After determining the probability that an electron will be promoted from a filled band to the conduction band, PK assumed that most of these electrons remained in the conduction band because of the surface potential of the metal target. However, because a hole is left in the valence band, an Auger recombination is possible with subsequent emission of an electron from the metal. The probability that this process occurs is given by PK as

$$w(\delta) = 0.016 (\delta - 2\phi) .$$

PK assumed that both PSE and KSE were due to Auger processes [4].

After the secondary electrons have been produced, they suffer collisions as they proceed to the surface of the metal. These collisions degrade their energy and increase the probability that they will be lost through recombination. PK assumed that the number of electrons which reach the surface is given by an exponential law of the form $\exp(-x/\lambda)$ where x is the depth at which the electrons are formed in the crystal and λ is the mean free path of the electrons in the material. Specifically, the number of electrons emitted per ion incident on the surface is given by

$$\gamma = \sum_x \left(\text{Number of atoms per cubic centimeter} \cdot \left(\begin{array}{l} \text{Prob. that an electron} \\ \text{will be ejected into} \\ \text{the conduction band} \\ \text{and a hole left in} \\ \text{valence band} \end{array} \right) \cdot \left(\begin{array}{l} \text{Prob. that an electron} \\ \text{will escape to the} \\ \text{surface of the crystal} \end{array} \right) \right)$$

which in the limit goes to

$$\gamma = \int_0^{x_n} N \sigma(u) w(\delta) \exp(-x/\lambda) dx ,$$

where x_n is the maximum depth at which the ion retains sufficient energy to ionize a target atom. Upon taking into account the degradation of energy of the primary ion as it suffers multiple collisions and the diffusion cross

section of the electrons, PK arrived at the final expression for γ :

$$\gamma = N w(\delta) \lambda [\sigma(u_o) - \Delta\sigma(u_o)] ,$$

where

$$\Delta\sigma(u_o) = \exp(-u_o/(K\lambda)) \int_{u_{\min}}^{u_o} \exp(u^2/(K\lambda)) \frac{d\sigma(u)}{du} du$$

and

$$K = \frac{2.48\pi N \cdot a_{TF} e^2 z_1 z_2}{(M_1 + M_2) (z_1^{1/2} + z_2^{1/2})^{2/3}}$$

The PK theory predicts the following trends [3]:

1. Low velocity region: $u_o = u_{\min}$, $\Delta\sigma(u_o)$ term is important..., γ increases slowly with u_o , $(\sigma(u_o) - \Delta\sigma(u_o)) = u_o^2 - (3/2 u_{\min})^2$. Hence initially $\gamma \propto u_o^2$, i.e., γ is a linear function of energy...
2. High velocity region: $(\sigma(u_o) - \Delta\sigma(u_o)) = u_o \tan^{-1}(0.6 \times 10^{-7}(u_o - u_{\min}))$. This expression asymptotically approaches the straight line $\sigma(u_o) = c(u_o - u_{\min})$ and therefore increases linearly with velocity. Extrapolating the linear portion back to $\sigma(u_o) = 0$ a value of the intercept $u_1 = 1.05 \times 10^7$ cm/sec is obtained; this is independent of ion target combination.
3. Very high velocities: Here ion penetration depths are greater so that electrons are formed further

from the surface. The number escaping to the surface and therefore the yield is expected to pass through a maximum. This is confirmed experimentally.

4. No yield dependence on ion charge is predicted.
5. A dependence of yield on the ion target combination of the form $((z_1 + z_2) / (z_1^{1/2} + z_2^{1/2}))^2$ for heavy ions and $((z_1^{1/2} + z_2^{1/2}) (z_1^{1/6} + z_2^{1/6}))^3$ for light ions. If the term $\Delta\sigma(u_0)$ is important...the yield is independent of ion-target combination to a first approximation.
6. Dependence of yield on the angle of incidence θ is expected to be of the form $\gamma_i = \sec \theta$ since the probability of electron escape is a function of the shortest distance to the surface and the probability of formation of electrons is a function of the actual distance traversed.
7. The effect of the isotopic mass on yield is anticipated to be connected with the different retardation rates for the isotopic pairs." [3]

All of these conclusions are approximately confirmed by the experimental results.

B. THE THEORY OF HARRISON, CARLSTON AND MAGNUSON

The PK theory uses many simplifying assumptions which introduce approximations into the results obtained. In

particular, the PK theory predicts secondary electrons of only average energy, two to five ev, and data obtained by Wolff [6] of SEE from copper bombarded by ten Kev argon ions indicates some secondary electrons emitted have energies greater than 140' ev.

In the PK theory secondary electron emission was viewed as a two-step process in which ions were first produced along a path in the target material and subsequently diffused to the surface with possible scattering or Auger emission occurring along the path. This model does not yield the high-energy secondary electrons which are reported experimentally. In an effort to explain this discrepancy between experimental and theoretical result, Harrison, Carlston and Magnuson [2] (HCM) proposed a "single collision" theory of secondary emission. This theory, though in many respects similar to the PK theory, has as its basic philosophy an electron production mechanism which differs from the model proposed above.

HCM proposed a model in which an ion approaching a target surface first undergoes resonance neutralization and subsequently collides with the first layer of atoms in the target material in the un-ionized state. Even though the primary particle is neutralized before the collision, the terminology of "ion" is retained here to distinguish between the primary particle and the target atom after collision. For simplicity HCM assumed that the electrons liberated due to the inelastic energy transferred between the electronic structures of the

ion and the atom all come from the ion, which allowed them to ignore the energy partition between collision partners. Theoretical work by Harrower [7] indicates that the Auger process requires a time on the order of 10^{-14} seconds while in the one to ten Kev energy range the collision process takes on the order of 5×10^{-14} seconds. This indicates that, statistically, the ion usually does not have time to neutralize before its next collision and for all practical purposes cannot contribute further to the secondary electron emission process. These results lend credence to the single collision model. Mathematically HCM proposed:

$$\gamma_{\text{KSE}}^{(hkl)} = K \int_0^{s_{\text{MAX}}} n_e(s, E_{\text{TFF}}) P^{(hkl)}(s) ds ,$$

where $\gamma_{\text{KSE}}^{(hkl)}$ is the number of electrons emitted per incident

ion when the ions are normally incident upon the (hkl) surface; s is the impact parameter of the ion on the atom; E_{TFF} is the inelastic energy transfer between the ion and the atom; $n_e^{(hkl)}(s, E_{\text{TFF}})$ is the number of electrons this energy will produce; and $P^{(hkl)}(s)$ is the probability that the impact parameter s will occur in the (hkl) surface. This equation contains three adjustable parameters, the constant K and two constants which enter into the calculation of ϕ , the electron density, and the interaction potential $V(r)$. By symmetry, these last two constants must be the same for all orientations of the particular crystal plane, (hkl) , in question.

According to HCM, the constant K is a factor which accounts for three physical processes:

1. The probability that an electron will be emitted from the surface (a value close to 1/2);
2. The probability of additional emission by an Auger process; and
3. The probability that a high energy electron escapes before it is scattered back into a conduction band. [2]

All of these processes are orientation independent. The factors which appear in the formulation of the HCM secondary electron emission equation are discussed in detail below.

1. The Inelastic Energy Transfer

In the HCM theory E_{TFF} is the inelastic energy transferred in the collision process and is basically the same as $E(p)$ in the PK theory. However, as HCM point out, because the interaction involves atoms spaced regularly in a lattice array, the inelastic energy integral does not have an infinite upper limit as was assumed by PK. Specifically,

$$E_{TFF}(s, E_0) = K_{TFF} \int_{r_{\min}}^{r_{\max}} \frac{(1-V(r)/E_0) dr}{(1-V(r)/E_0 - s^2/r^2)^{1/2}}$$

$$\int_{r/2}^{r_{EM}} \phi^2 \frac{(\rho) d\rho}{\rho}$$

where

$$K_{TFF} = \frac{h}{\pi a_H^2} (E_0 / (2m_1))^{1/2} (z_1 + z_2)^2 ,$$

$$a_H = h^2 / (me^2) = .529 \text{ \AA}$$

and E_0 is the energy of the ion in the center of mass system; z_1 and z_2 are the ion and atom nuclear charges, respectively; r_{min} is the distance of closest approach; and ϕ is the Thomas-Fermi (TF) screening function:

$$\phi(\rho) = [1 + (a_F \rho)^{0.8034}]^{-3.734}$$

where

$$a_F = \frac{a_{TF} ((z_1 + z_2) / 144)^{1/3}}{0.8853}$$

and a_{TF} is one of the adjustable constants introduced above. By experimenting with different sets of potentials, in conjunction with the screened electron distribution, HCM found that the best agreement with experiment was obtained when the potential $V(r)$ was of the Born-Mayer form [2]:

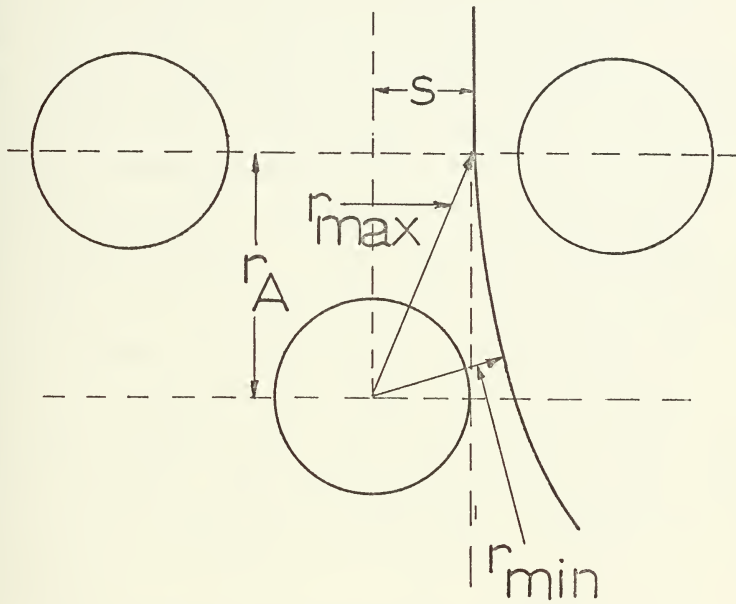
$$V(r) = \exp (A + Br) = A' \exp (Br)$$

with B always negative, and where A is the second of the above mentioned arbitrary constants. HCM referred to the integral containing $d\rho$ as the electron integral. The convention is retained here.

Several important results were noted by HCM in the formulation of their original model. First, the dynamical integral was extremely sensitive to its upper limit $r_{\max}^{(s)}$, whereas the electron integral was not sensitive to variations in r_{EM} . For this reason r_{EM} was set at a value somewhat larger than the nearest neighbor distance R_0 , in the crystal lattice, and retained this value for all orientations of the crystal lattice. On the other hand, the upper limit of the dynamical integral was extremely sensitive to the nearest neighbor distance. Such a behavior is expected because as each ion collision with a particular atom terminates, another must begin with one of its neighbors. From a particle dynamics point of view, HCM found that by treating the actual collision with the lattice as a binary collision between the incoming ion and any single atom within the first repeat distance of the crystal plane, the theory yielded results which approximated those obtained by experiment. Figure 3 indicates the geometrical relationship between various quantities associated with the dynamical integral [2].

2. Collision Parameters

Because of the repetitive nature of the lattice, or lattice plane, it is not unreasonable to think of a "representative area" which characterizes the lattice plane as a whole and hence its distribution of impact parameters. If no lattice were present, and only one target atom, there would be no characteristic area and the occurrence of a



DYNAMICAL INTEGRAL GEOMETRY

FCC (100)

Figure 3. Relationships between various quantities appearing in the Dynamical Integral.

collision with any impact parameter would be possible, yielding an infinite collision cross section. As an ion approaches a plane of atoms in a crystal, however, there exists an allowable set of impact parameters for the ion-atom collision. Specifically, in a lattice there exists an impact probability distribution, $p^{(hkl)}(s)$, for each crystal orientation. For normal incidence HCM proposed the areas shown in Figure 4. These areas are representative of the normal impact of an ion with any atom on the specified crystal surface, *viz.*, by symmetry operations they fill plane space and are representative under any of these symmetry operations of what an ion "sees" as it approaches the planar surface normally. There are many distributions which could be considered probability distributions. HCM considered the following:

1. The distribution of values of s measured to the nearest surface atom;
2. The distribution of all values measured to all atoms which project their area into the representative area;
3. The distribution of smallest impact parameters when all atoms are considered [2].

The third case was the only one which yielded results in agreement with the experimental data. The distributions for normal incidence on FCC and BCC metal targets are shown in Figures 5 and 6.

Operationally, the distributions are determined as follows: First, the representative area is chosen. "Points" are shot at the representative area, and the distances

FACE CENTERED CUBIC

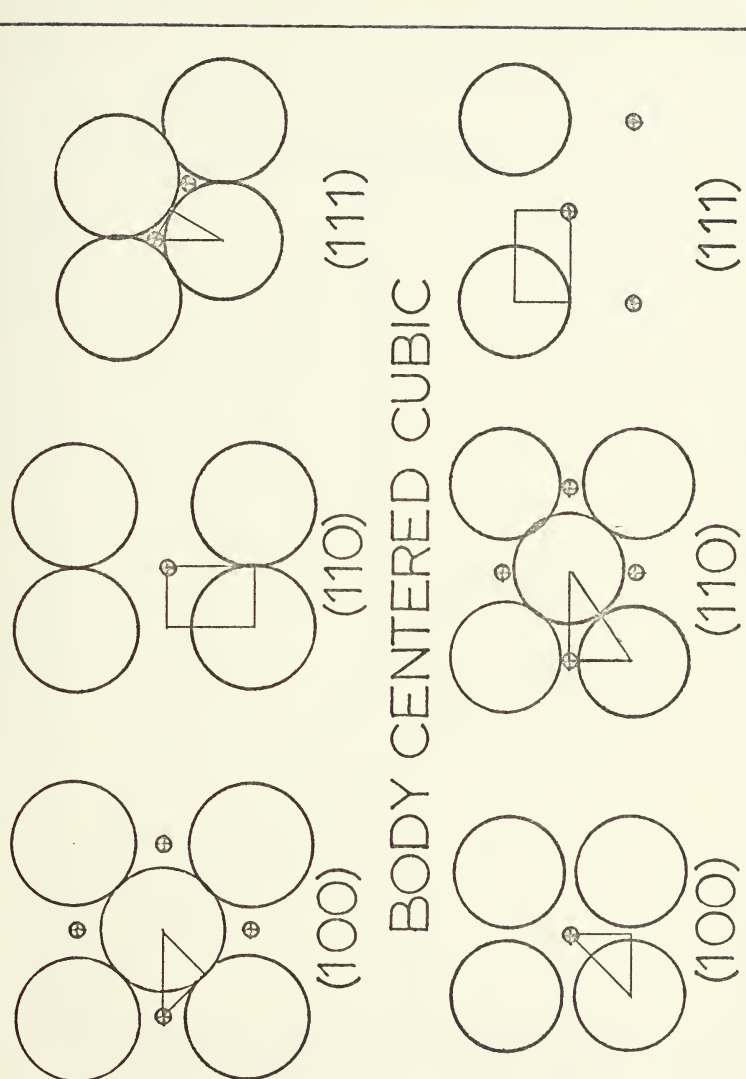


Figure 4. Representative areas for normal incidence.
After (2).



Figure 5. Distribution of impact parameters for normal incidence on face-centered cubic crystals.

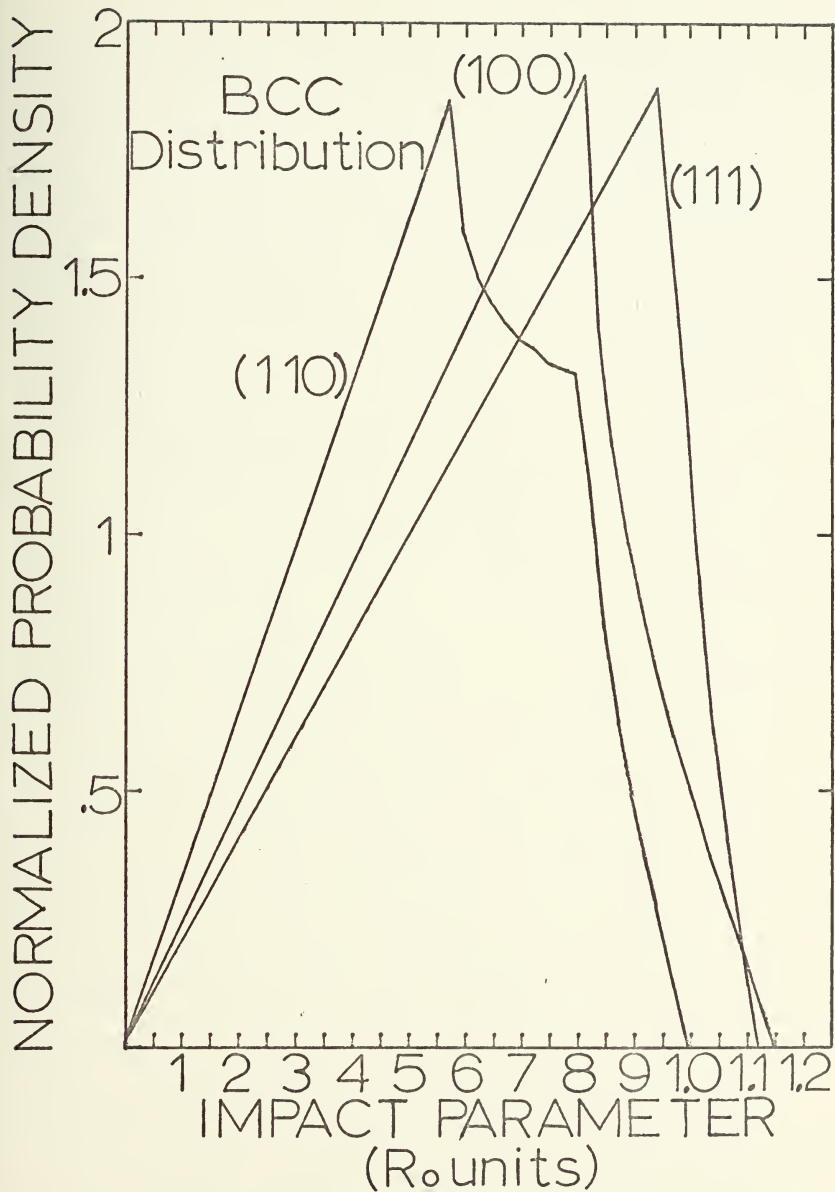


Figure 6. Distribution of impact parameters for normal incidence on body-centered cubic crystals.

between the impact point and the centers of the atoms lying in the representative area are measured. For each atom the distances for points that are measured to be closest to it are tallied. After a sufficient number of points are tallied to yield good statistics, the distribution for each atom is weighted by a factor to account for the fractional portion of atom lying in the representative area. The atoms' distributions are then added and scaled so that the total area under the resulting curve is unity.

3. Number of Electrons Emitted--Russek Model

One of the major shortcomings of the PK theory was that it used average ionization energies to obtain an ionization cross section. This is to say the PK theory did not consider the electronic structure of the target atom. HCM adopted a model proposed by Russek [9] to obtain the number of electrons liberated per collision, $n_e^{(hkl)}(s, E_{TFF})$. In his original paper, Russek proposed two ionization models of interest, the uniform ionization model (UI), and the staggered ionization model (SI). The UI model assumed that as electrons were liberated by the collision process, the amount of energy required to liberate any one electron was the same as that required to liberate any other electron. On the other hand, the SI model assumed that each electron liberated required more energy than was required to liberate the preceding electron. For the SI case Russek shows that the probability that n electrons will be liberated from a shell, which contains M electrons is given by:

$$p_n^{(M)} \sim \binom{M}{n} \sum_{i=0}^k (-1)^i \binom{M-n}{i} \left(\frac{\frac{1-nE_n^{ION}}{n} + \frac{iE_n^{ION}}{n+1}}{E_{TFF}} \right)^{M-1}$$

where $k \leq (E_{TFF}/E_{n+1}^{ION} - nE_{n+1}^{ION}/E_n^{ION}) \leq k+1$ and M is the number

of electrons available in the outermost shell of the atom;

E_n^{ION} is the energy required to remove the n^{th} of these electrons and E_{TFF} is the energy available to cause this removal. Two things should be noted. First, the impact parameter enters this calculation through the inelastic energy transfer. Second, when $E_{n+1}^{ION} = E_n^{ION}$ one obtains the UI model. After normalizing the function, $p_n^{(M)}$, viz.,

$$\sum_{n=0}^N p_n^{(M)} = 1$$

then, from probability arguments, the number of electrons liberated is:

$$\frac{n_e}{E_{TFF}} = \sum_{n=0}^M p_n^{(M)} n_e .$$

HCM were unable to obtain good results with the Russek UI model. In all cases, γ increased much too rapidly as a function of energy. On the other hand, the SI model yielded reasonably good results, where spectroscopic values for E_n^{ION} were used.

4. HCM Results

HCM investigated the Ar - Cu system in detail.

They first examined the E_{TFF} dynamical integral for various types of potential functions and found that the PK potential which was of the Thomas-Fermi-Firsov type was too hard for small values of E_0 , viz., the hard core radius of the target atom was too large, in this energy range, to yield acceptable results. Attempts at softening the potential by decreasing a_{TF} failed. For this reason HCM assumed a potential function of the Born-Mayer type. The potential function used in each case was found by matching the exponential to the TF screening function at some separation.

HCM assumed that the experimental data contained both potential, γ_{PSE} , and kinetic, γ_{KSE} , contributions to the total secondary electron emission coefficient. Therefore, HCM identified the γ at which KSE begins to contribute as γ_{PSE} and assumed this value remains constant for all energies. This value for γ_{PSE} was then subtracted from the experimentally determined γ for the (111) surface at 10 Kev. The (111) value of γ_{KSE} at 10 Kev, obtained from theory, was scaled to this point, and all other points were multiplied by the scale factor used in performing this operation. Finally the constant value of γ_{PSE} was added to all the scaled theoretical values. The result is the HCM value for the total secondary electron emission. The results of the HCM theory for the $\text{Ar}^+ - \text{Cu}$ system are presented in Figure 7.

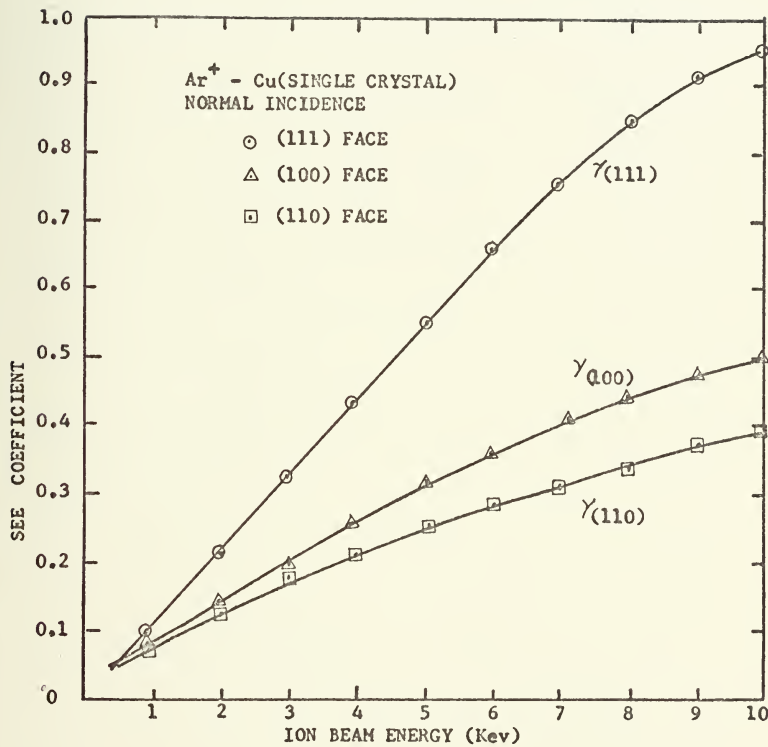


Figure 7. $\text{Ar}^+ - \text{Cu}$ results obtained from the HCM original model. Taken from (2).

In general, HCM's theory agrees reasonably well with experimental results for all systems studied except Ar - Mo.

V. MODIFICATIONS TO THE HCM THEORETICAL MODEL

A. INTERATOMIC POTENTIAL

Independent of the philosophy behind the basic interaction, the HCM theory, like the PK theory, is highly dependent on two specific assumptions. First, both assume that the inelastic energy transferred is of the form proposed by Firsov. Second, both theories must assume an interatomic potential function which is consistent with the electron distributions of the ion and atom. Since the Firsov model is presently the only comprehensive model available for the inelastic energy transfer, it has been retained here as an approximate model of the inelastic collision process and is assumed to be sufficiently accurate for our purposes. However, the interaction potential used in the Firsov model need not be of the Thomas-Fermi form, but may be derived from a more accurate representation of the electron distributions of the ion and atom.

The interaction potential is derived from the electron distributions of the collision partners. These potentials exist on three general levels of sophistication: (1) The Bohr and Born-Mayer potentials which are derived from electron distributions which provide screening of the nucleus in a self-consistent, but not necessarily accurate, manner; (2) Thomas-Fermi and Thomas-Fermi-Dirac potentials which are derived from statistical pictures of the electron

distributions of the collision partners; and

(3) Potentials generated from electron densities derived numerically from Schroedinger's equation.

Parilis and Kishinevskii used a Thomas-Fermi potential function in the theory they proposed. Statistical models of the atomic electron distribution, such as in the TF model, are based on studies of inhomogeneous gases and approximate solutions of Schroedinger's equation consistent with this picture [10, 11]. They require that the total electron energy be a minimum and that the electron density integrate to the total number of electrons in the system. Approximations may be made to evaluate the exchange and correlation energies. When the exchange and correlation energies are omitted and the kinetic energy is approximated by a plane wave, the TF atomic model results [11]. If the exchange energy is retained and the kinetic energy is approximated by a plane wave, the TFD atomic model results [11]. The TF model of the atom has been used extensively by Firsov, whereas the TFD model appears in papers by Abrahamson [13].

Potential functions based on Hartree-Fock solutions of the atomic Schroedinger equation have been discussed by Wedepohl [12], Harrison [13], and Wilson [14]. These potentials assume the adiabatic approximation, use spherically symmetric electron distributions which have shell structure, and take into account the correlation,

kinetic and exchange energies through various approximations. They appear to lead to improved calculations of the interaction potential [8, 14, 15]. The present investigation utilizes an interaction energy calculation similar to that proposed by Wedepohl [12]. However, the electron densities from which the potential is derived are calculated from the Hartree-Fock-Slater self-consistent wave functions calculated from the Herman-Skillman [16] computer program. The reader is referred to the original book [16] for detailed information on the calculation of the atomic electron distribution functions and to the work by Torrens [8] for a general discussion of the interaction potential.

B. THE BASIC INTERACTION

Harrison, Carlston and Magnuson assumed that all of the secondary electrons produced in the single collision model came from the ion. This assumption was tested by choosing various values of E_n^{ION} in the Russek model and noting the dependence of $n_e(E_{\text{TFF}})$ on E_1^{ION} . This experiment was carried out for the $\text{Ar}^+ - \text{Cu}$ system. The results were most favorable for E_1^{ION} equal to 15.8 ev, the first ionization potential of argon, and least favorable for neutral copper's first ionization potential. This approximation was an attempt to simplify the model so that detailed models of energy sharing mechanisms could be avoided. In this present investigation, this assumption has been relaxed to include contributions to the secondary emission by the target atom.

Theoretically, the interaction is viewed as the collision of two atoms having spherically-symmetric, shell structured electron distributions. As the atoms collide, they are assumed to form a "molecular" structure whose electron ionization potential distribution is comprised of the separate ionization potentials of the electrons of the atoms involved in the collision. Since electrons are ejected on a "least energy" principle, the values of E_n^{ION} used in the Russek model have been modified by include both primary ion and target atom ionization energies which are arranged in increasing order of magnitude, irrespective of the atom to which they belong. The mean number of electrons is a complicated function of the inelastic energy transfer and the energy necessary to effect each electron's removal.

C. THE DISTRIBUTION OF IMPACT PARAMETERS

To accomplish the objectives of this present investigation, one additional modification to HCM's original paper had to be made. Since the angular dependence of γ was to be studied, a new distribution of impact parameters had to be calculated. Fortunately, according to the HCM paper, this modification to the mathematical model is the only change required to take into account rotations of the crystal plane around an arbitrary crystallographic direction. No other factor entering into the secondary electron emission equation is orientation dependent [2].

Two possible solutions to this problem are proposed below. First, a crystal plane normal to the direction of incidence of the ion beam can be found, from which a representative area can be constructed. Such a formulation would be analogous to cutting the crystal in such a manner that it presented a planar area normal to the incident ion beam and finding an area on this plane which would be representative of that orientation. Alternatively, a representative area constructed from the crystal face which was experimentally rotated can be used and mathematically rotated about the specified crystallographic axis. In practice, the first method is computationally restrictive because it requires that a representative area on a plane normal to the incident ion beam be found for each orientation. For this reason it is not pursued further here.

The second method mentioned above yields a result that is more in line with the reasoning behind HCM's original definition of the distribution of impact parameters. Practically speaking, a representative area is found for each crystal face which fills plane space and is representative of what an ion sees as it approaches the crystal plane from an arbitrary direction. Unlike the representative areas for normal incidence, angularly dependent representative areas must be truly representative for all possible rotations of the plane and not simply for one particular orientation. The representative area for the FCC (100) surface which can be rotated in either a positive or negative

sense about the $\langle\bar{1}10\rangle$ crystallographic axis is shown in Figure 8. Note that atoms which lie within the first repeat distance of the crystal plane are eligible target atoms in the representative area by HCM's definition of representative area. Also note that these atoms from the lower atomic plane appear to move as the crystal plane is rotated in a positive sense about the $\langle\bar{1}10\rangle$ axis (see Figure 9). This behavior can be verified by physically rotating a stick and ball model of the lattice structure about the indicated axis.

Once the representative area is chosen, its rotational properties and corresponding distribution of impact parameters are calculated as follows. The representative area is placed in the first quadrant of a rectangular coordinate system (x,y) (see Figure 10). In this system, the crystallographic axis of rotation is specified by two parameters:

1. The angle of the crystallographic axis makes with the x -axis of the rectangular coordinate system (x,y) ; and
2. The y -axis intercept of the crystallographic axis in the rectangular coordinate system (x,y) .

This system of coordinates is then transformed into a primed rectangular reference frame (x',y') for which the crystallographic axis of rotation is the x' -axis, and whose origin is the point at which the crystallographic axis intercepts the y -axis, (x_R, y_R) (see Figure 10). The equations relating the transformation of points from the (x,y) coordinate

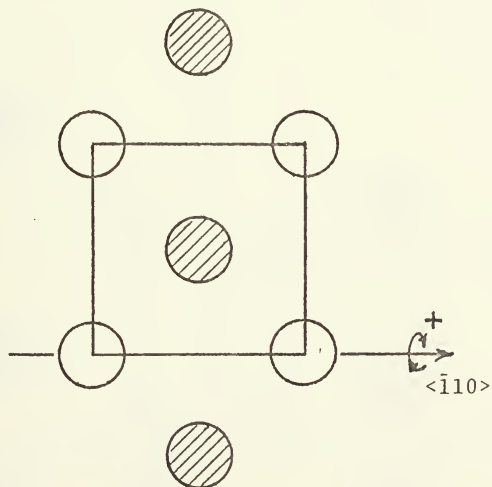
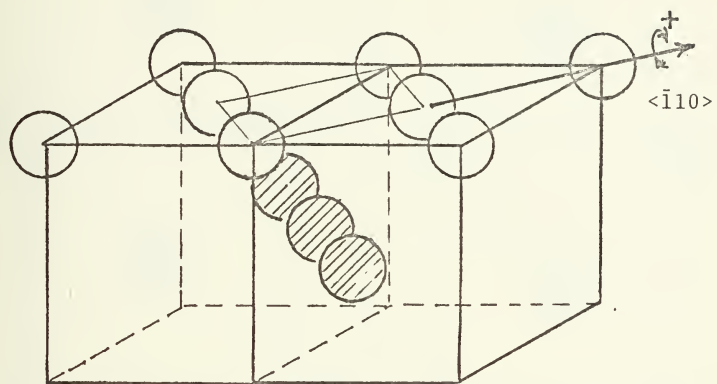


Figure 8. Representative area of a (100) FCC crystal face rotated about $\langle 110 \rangle$ in either a positive or negative sense.

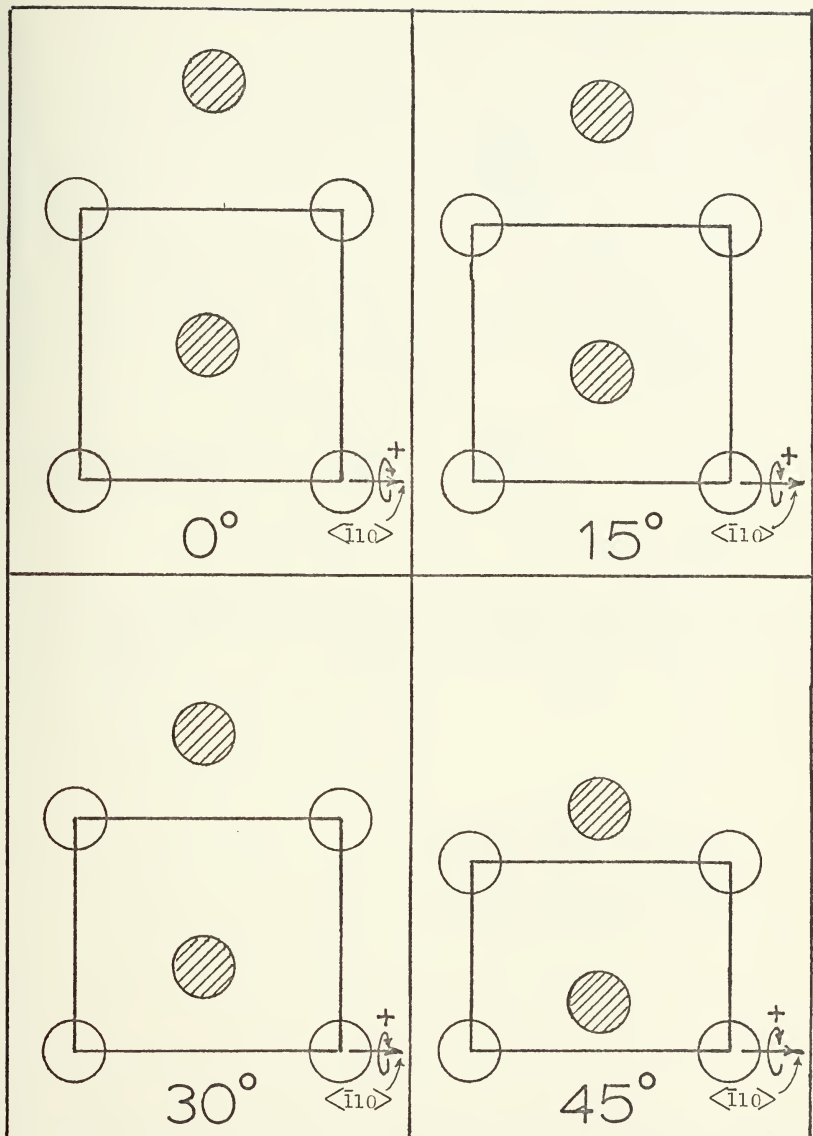


Figure 9. Representative area of the (100) face of an FCC crystal rotated in a positive sense about the $\langle 110 \rangle$ direction.

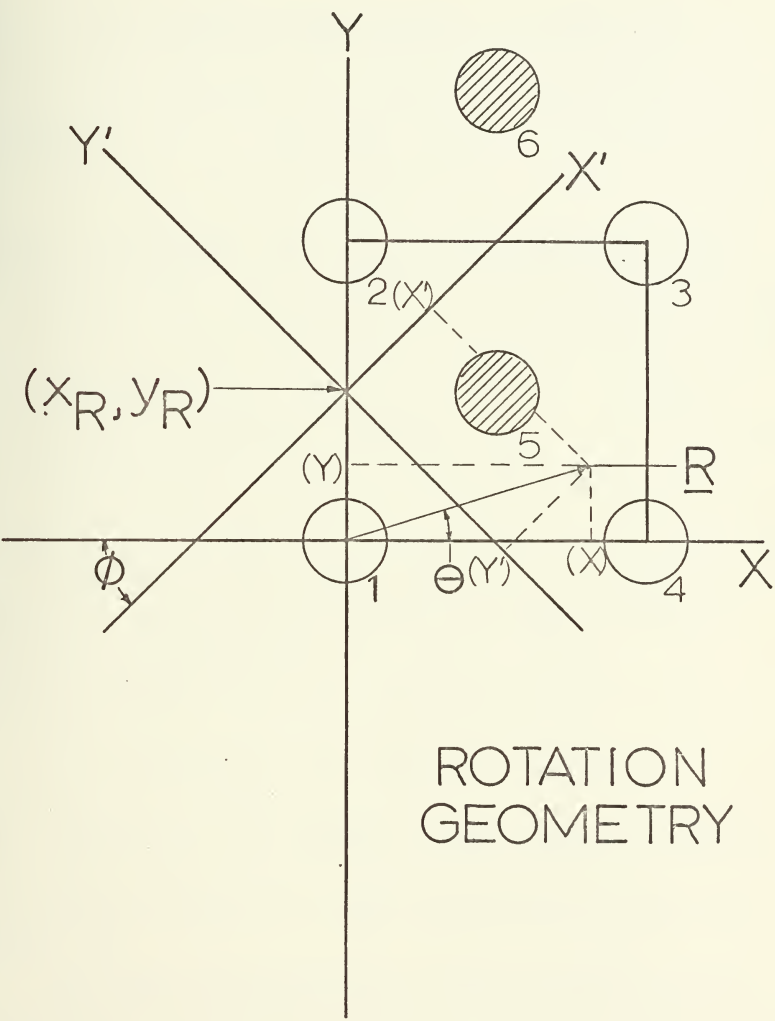


Figure 10. Rotation geometry for a (100) face of an FCC crystal about an arbitrary crystallographic direction.

system to the (x', y') coordinate system are:

$$x' = R \cos (\theta - \phi) - (y_R \sin \phi + x_R \cos \phi),$$

$$y' = R \sin (\theta - \phi) + (x_R \sin \phi - y_R \cos \phi).$$

where

$$R = (x^2 + y^2)^{1/2}$$

$$\theta = \arctan (y/x)$$

and ϕ is the angle that the crystallographic axis makes with the x -axis. If the system is rotated through an angle α about the x' -axis, distances to any point (x', y') appear to be shortened by an amount $\cos \alpha$ in the y' dimension, leaving the x' dimension unchanged. Also, if the atom whose projected position lies at (x', y') before rotation is an atom whose actual position is R_a units below the plane being rotated, then its new apparent position on a plane perpendicular to the direction of incidence after rotation is given by the coordinates $(x', y' \cos \alpha - R_a \sin \alpha)$. In general then the final transformation equations become:

$$x' = R \cos (\theta - \phi) - (y_R \sin \phi + x_R \cos \phi),$$

$$y' = (R \sin (\theta - \phi) + (x_R \sin \phi - y_R \cos \phi)) \cos \alpha - R_a \sin \alpha.$$

The geometry implicit in these calculations is shown in Figure 10.

The actual calculation of the distribution of impact parameters is performed as follows. A mathematically constructed, rectangular grid is placed over the area and points which lie within the representative area are

systematically chosen. Using the transformation equations and the known position of the atoms in the representative area, the distance from the points chosen in the area to each respective atom are calculated in (x', y') coordinates and the shortest distance is chosen. The shortest impact parameter is tallied against the atom with which it is associated, in an array. In the case of equal distances between two atoms, the atom with which the ion impacts is chosen by a uniformly distributed pseudorandom process [17]. The final array contains the distribution of all impact parameters tallied with each atom in the representative area. To obtain the final distribution of impact parameters for the crystal face, the individual distributions are weighted, added, and the area under the curve is normalized to unity. The number of points used in calculating these distributions are on the order of 100,000 per representative area. The final unnormalized distribution of impact parameters for (100) FCC crystals for various angles of rotation is shown in Figure 11. Note that all dimensions used in calculating these distributions are in terms of R_0 , the nearest neighbor distance in the crystal lattice.

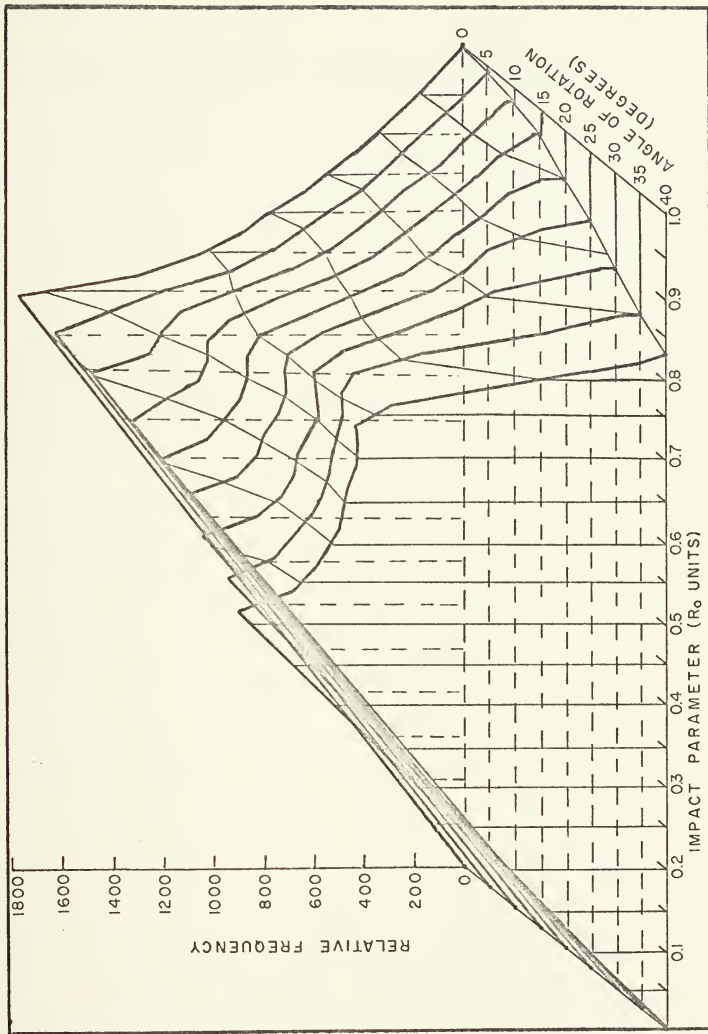


Figure 11. Unnormalized distribution of impact parameters for FCC (100) rotated through various angles about $\langle 110 \rangle$.

VI. NUMERICAL METHODS AND COMPUTER PROGRAMS

The theory presented in the preceding chapters has been incorporated into five FORTRAN IV computer programs which are presented in the appendix to this thesis. They appear in the order of their use. Specifically, these programs are:

1. The Herman-Skillman radial-electron density program,
2. The Harrison potential program,
3. Distribution of impact parameters program,
4. Numerical interpolation program, and
5. The Harrison KSE program.

To calculate the coefficient of ion-electron emission (SEE coefficient), these programs are utilized in the following manner. The ion-atom-radial-electron densities are calculated using the Herman-Skillman computer program [16]. These densities are put into the Harrison potential program which calculates the interatomic potential, $V(r)$, used in the calculation of the inelastic energy transfer, E_{TFF} . The distribution of impact parameters program calculates the distribution of impact parameters for each crystal face under investigation. Since this is a statistical process, the distributions recovered from this program are "smoothed" using a first and tenth degree Legendre orthogonal least squares interpolating polynomial, which is generated by the numerical interpolation program [18]. Finally the

smoothed distribution of impact parameters and potential function are inserted into the Harrison KSE program which has been modified to include all the changes to the original theory presented in the "Modifications" chapter of this thesis. This program performs the actual calculation of the SEE coefficient using the HCM model. The input data format to each of these programs is shown in Figures 12 through 16. The definitions of the input variables used in the programs are presented in Appendix A to this thesis. The results presented in the following chapter were run on the Naval Postgraduate School IBM/360 Computer System.

Data Input for the Electron Density Program

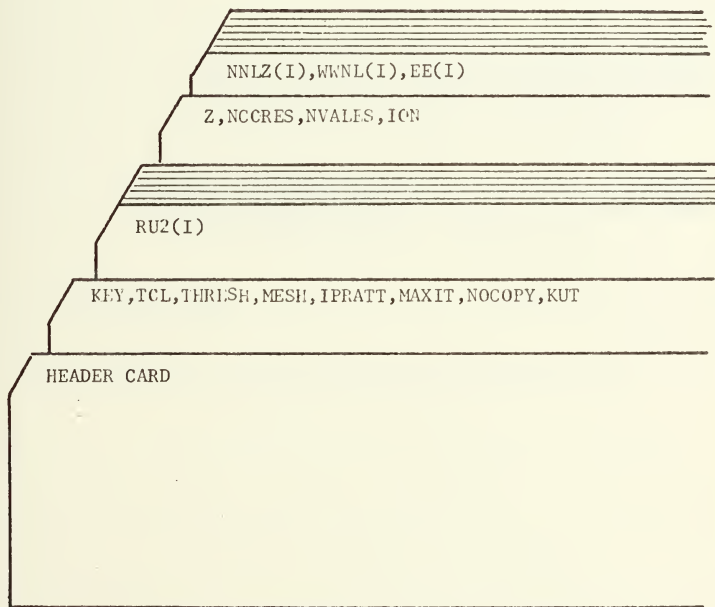


Figure 12. Deck setup for running the Electron Density Program.

Data Input for the Potential Program

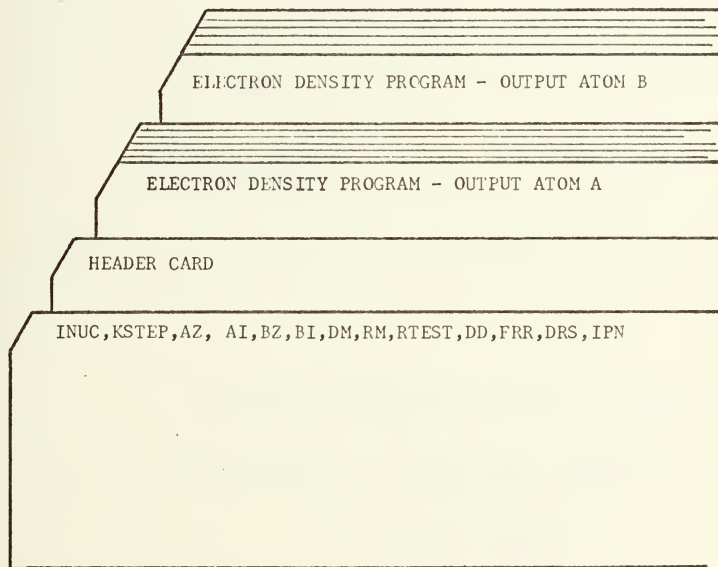
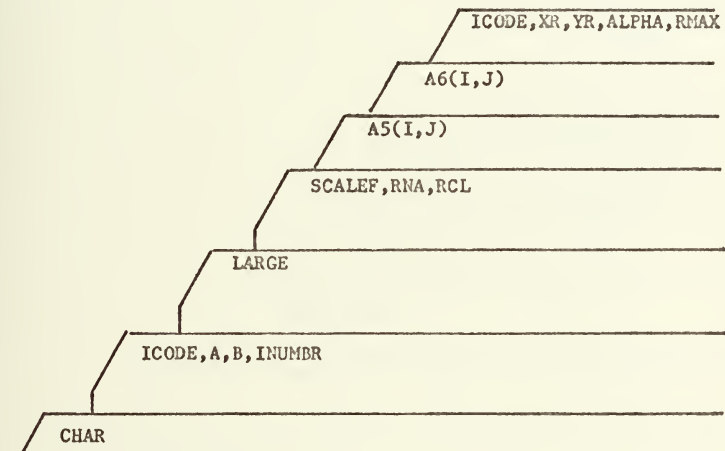
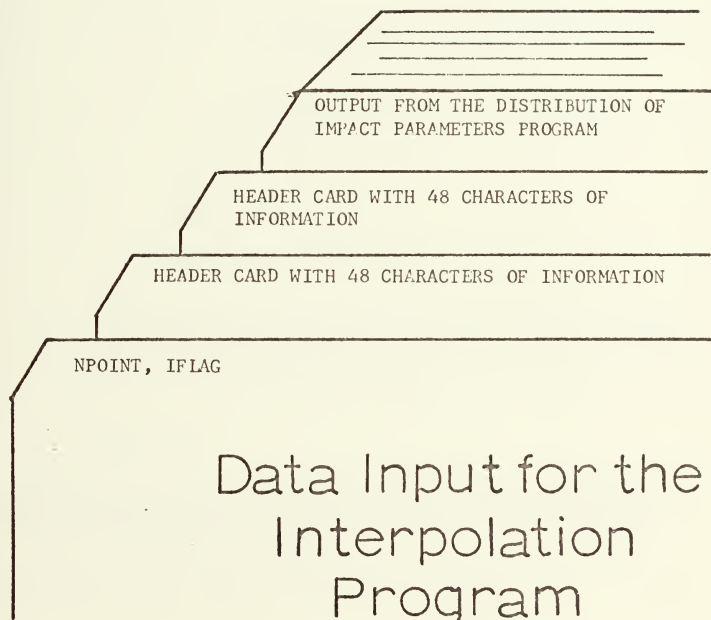


Figure 13. Deck setup for running the Potential Program.



Data Input for the Impact Parameters Program

Figure 14. Deck setup for running the Distribution of Impact Parameters Program.



Data Input for the Interpolation Program

Figure 15. Deck setup for running the Interpolation Program.

Data Input for the KSE Program

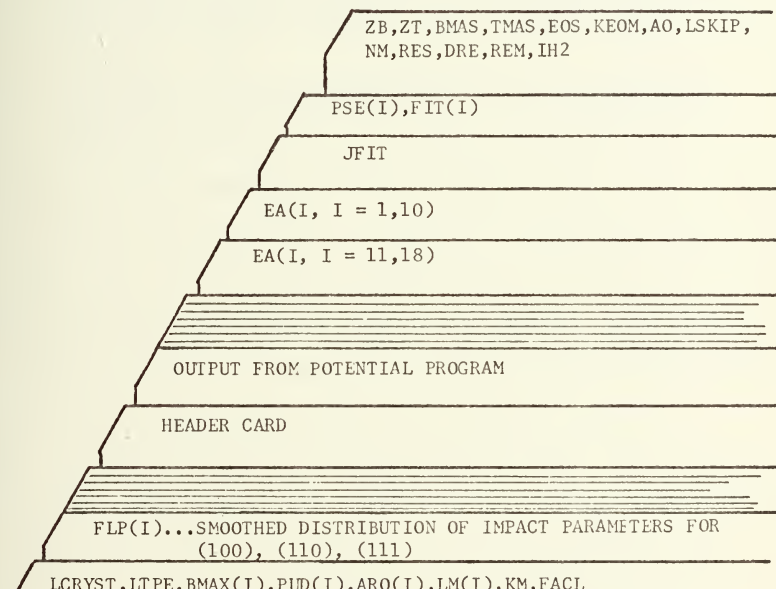


Figure 16. Deck setup for running the KSE Program.

VII. RESULTS

Three separate cases of secondary electron emission were investigated using the modified HCM model. These were:

1. Angularly dependent secondary electron emission from the (100) face of a copper single crystal rotated about a $\langle\bar{1}10\rangle$ axis;
2. Secondary electron emission from Ar, Ne, Kr and Xe ions normally incident on the (100), (110) and (111) faces of Cu, Ag, Mo, and Al single crystals; and
3. Secondary electron emission from Ar and Ne ions normally incident on the (100), (110) and (111) faces of KCl.

In the HCM theoretical model, the primary ion is assumed to be neutralized before it strikes the target surface. The target atoms in the metal are assumed to be ion cores in a sea of valence electrons. For these reasons, the actual results presented here are obtained by modeling the binary collision process as a collision between a neutral, inert gas atom and an ion core of the target atom. In the cases of copper and silver, the ion cores are fairly well defined, since both appear in column I.B. of the periodic table. However, in the cases of molybdenum and aluminum which appear in the VI.B. and III.A. columns of the periodic table, respectively, there are several possible ion core configurations that could be used in the HCM model. For this reason, various degrees of ionization of the molybdenum and aluminum target atoms were used in computing the SEE coefficient for these target atoms by way of the HCM model.

In the cases of copper and silver, results indicate that the best ion core configuration for both target materials is the singly ionized state. Note that all graph titles refer to the HCM model used, whereas the figure captions indicate the physical system actually investigated.

A. ANGULARLY DEPENDENT RESULTS

The results obtained from the bombardment of Cu single crystals by Ar ions for various angles of rotation about the $\langle\bar{1}10\rangle$ crystallographic axis are shown in Figure 17. It is interesting that the HCM model did not predict the correct behavior of the SEE coefficient for monocrystalline, angularly rotated targets, but did accurately reproduce the results obtained for polycrystalline targets [19]. This seems to indicate that the single collision model is not an accurate one for arbitrary rotations about the crystallographic axis, but needs to be modified to account for a more complicated interaction with the crystal lattice.

B. METAL TARGET RESULTS

An attempt was made in this thesis to verify those calculations performed by HCM in their original paper. Not too surprisingly, the results obtained here differ appreciably from those obtained by HCM using their original model. Each system is discussed in detail below.

1. Copper Bombarded by Ar, Ne, Kr and Xe Ions

In HCM's original paper, the $\text{Ar}^+ - \text{Cu}$ system was treated in detail. Using their original model, they

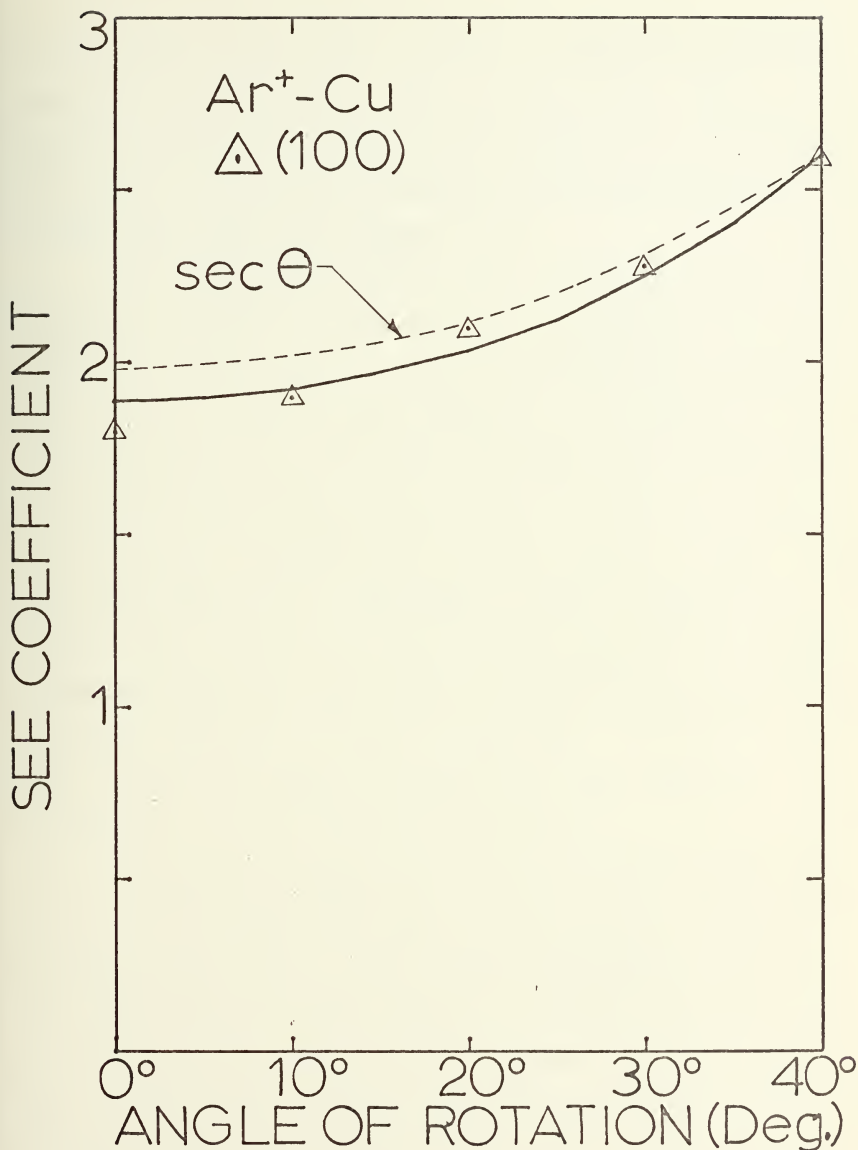


Figure 17. SEE coefficient vs. angle of rotation for (100) FCC Copper crystal. Direction of rotation was about $\langle 110 \rangle$.

obtained the results shown in Figure 7, which show excellent agreement with experiment. After altering their model, using the modifications presented in Chapter IV, the results do not agree so well with experiment as did those obtained by HCM. (See Figures 18 through 21.)

In an attempt to explain this discrepancy, the difference between the experimentally observed SEE coefficient and that obtained here was plotted as a function of energy. Theoretically, if the results obtained in this present investigation are to be physically meaningful, this difference must be due to the potential ejection mechanism operating at higher energies. Experimentally, Medvel et al. [1] have ascertained that for Ar bombardment of polycrystalline Mo targets, the potential ejection mechanism is still operating at energies up to 2.5 Kev, and the PSE contribution is still tending to increase with increasing energy. If this is in fact the case, the results obtained here have physical significance. (See Figures 22 through 25.)

It is interesting to note that the PSE contribution from all three faces investigated exhibit similar behavior in that they all peak at approximately the same energy, and tend to decrease at higher energies. The exact location of the peak, however, varies with the primary ion type. Furthermore, in all four primary ion cases, the PSE contribution curves for the (100) and (110) faces cross at approximately seven to nine Kev, indicating that the PSE mechanism may be somewhat independent of ion type, while showing some

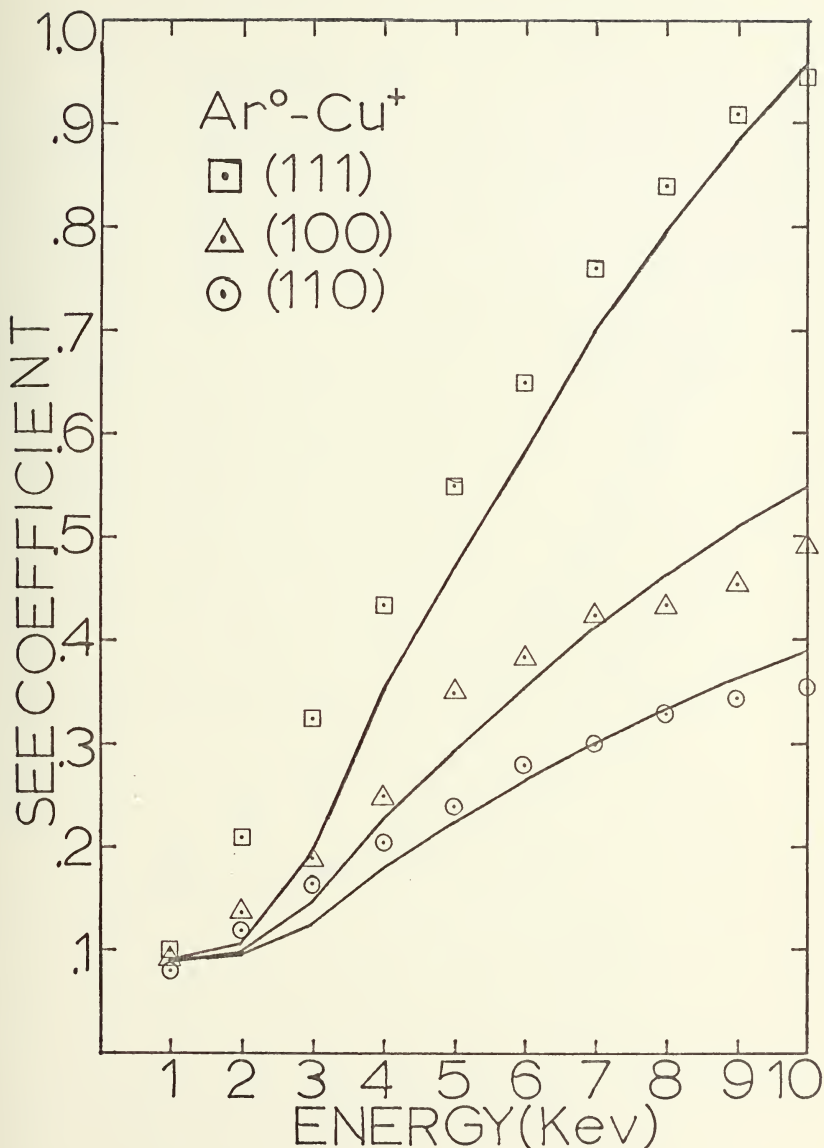


Figure 18. Cu bombarded by Ar^+ ions normally incident on the (100), (110) and (111) planes.

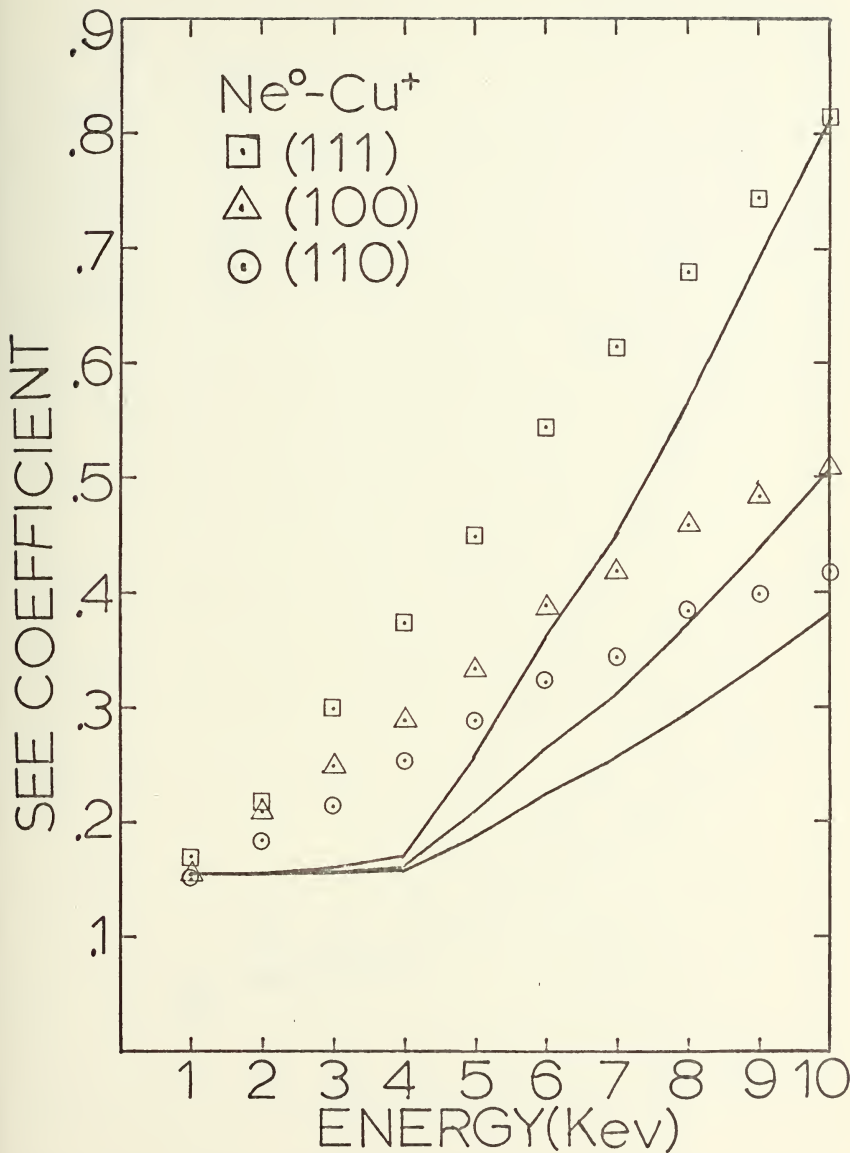


Figure 19. Cu bombarded by Ne^{+} ions normally incident on the (100), (110) and (111) faces.

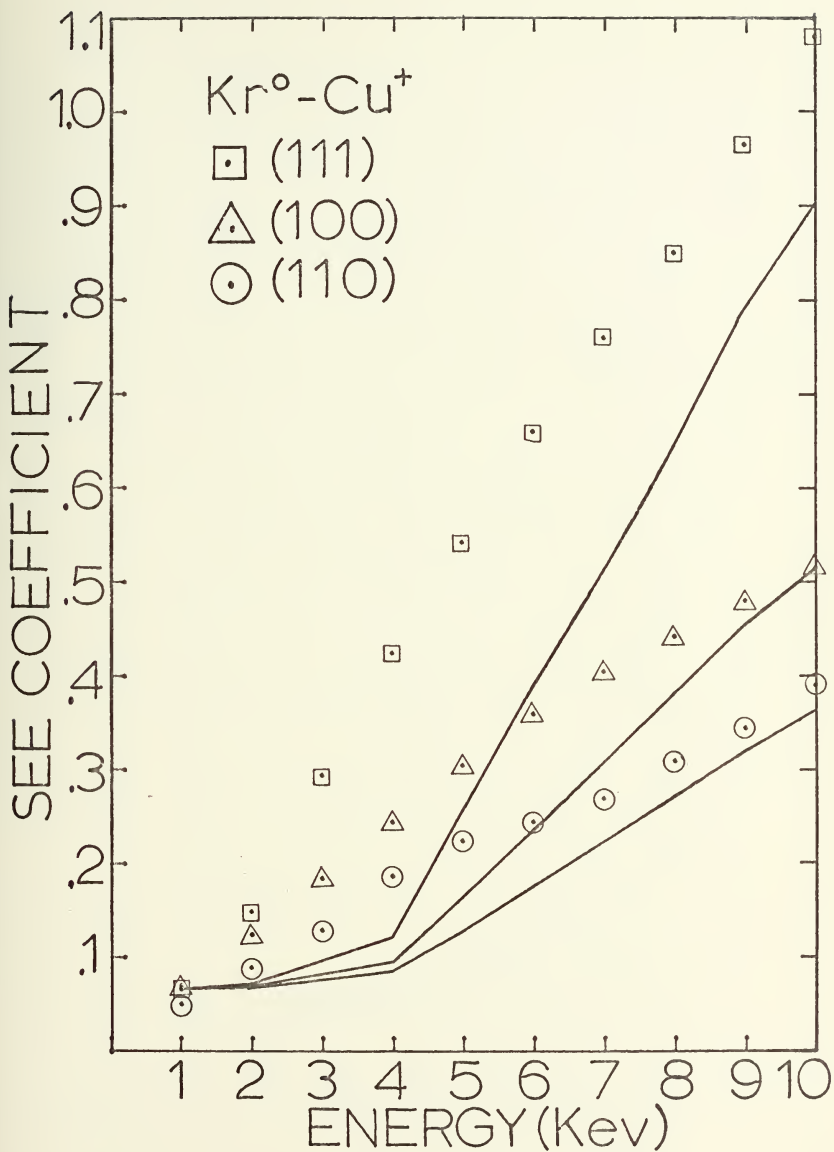


Figure 20. Cu bombarded by Kr^{+} ions normally incident on the (100), (110) and (111) faces.

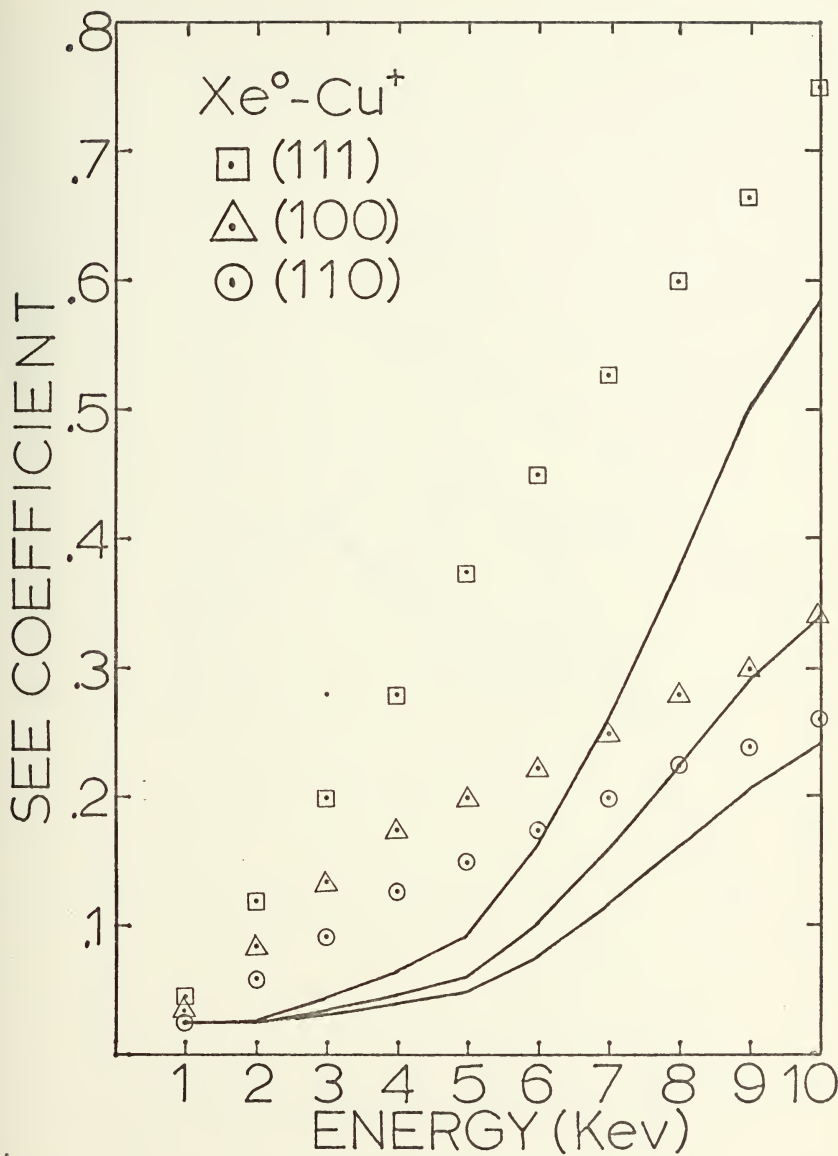


Figure 21. Cu bombarded by Xe^+ ions normally incident on the (100), (110) and (111) faces.

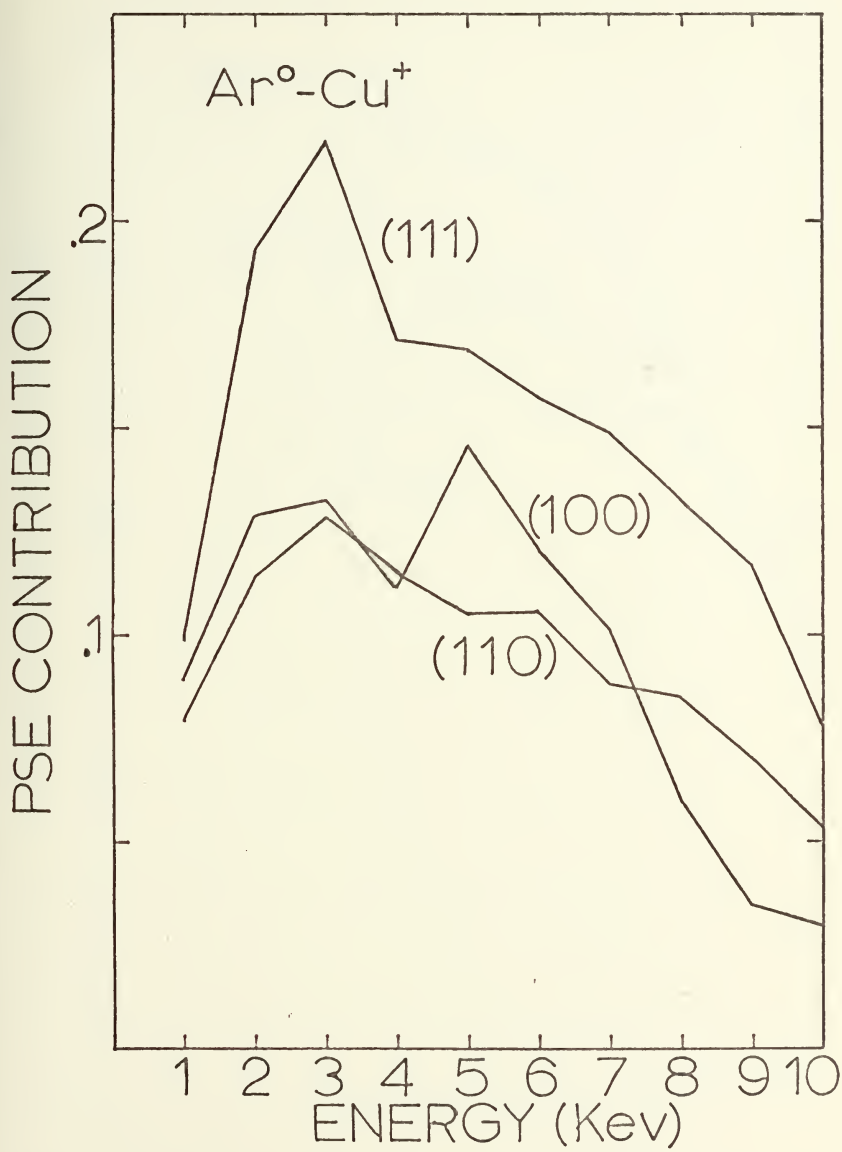


Figure 22. PSE contribution to secondary electron emission for the Ar^o - Cu system.

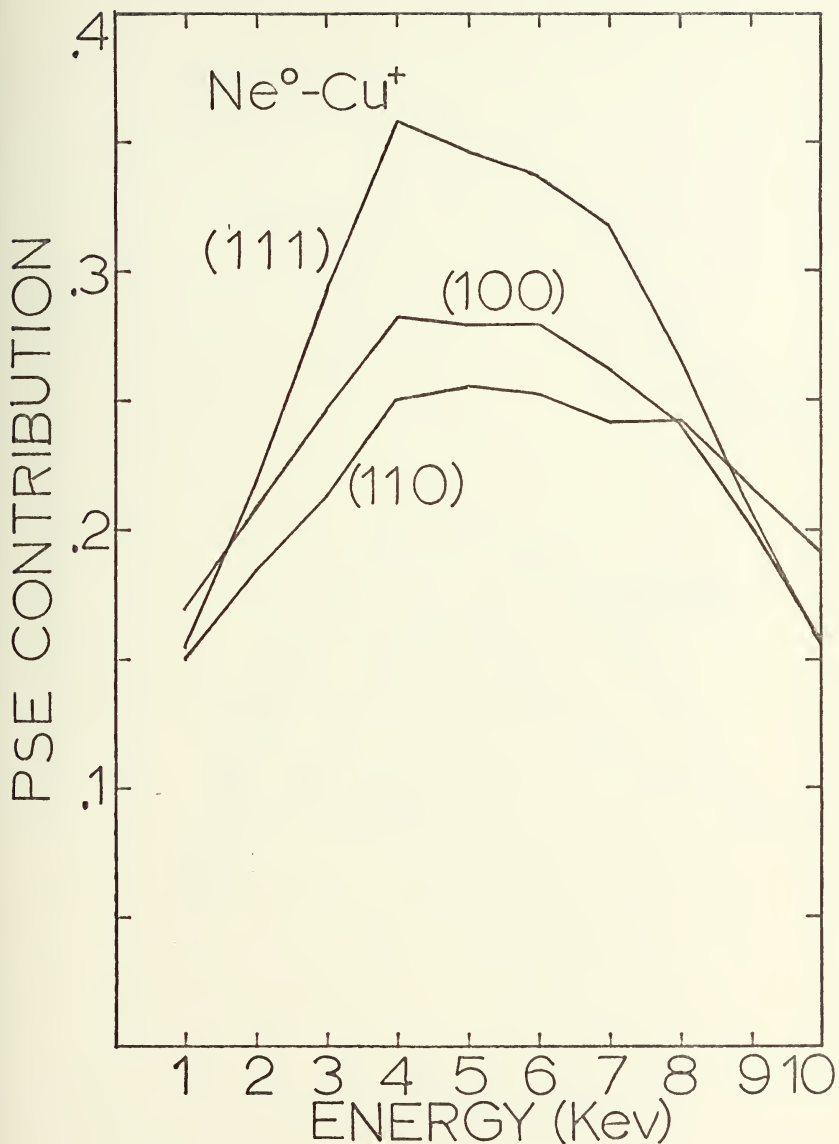


Figure 23. PSE contribution to secondary electron emission for the Ne^o - Cu system.

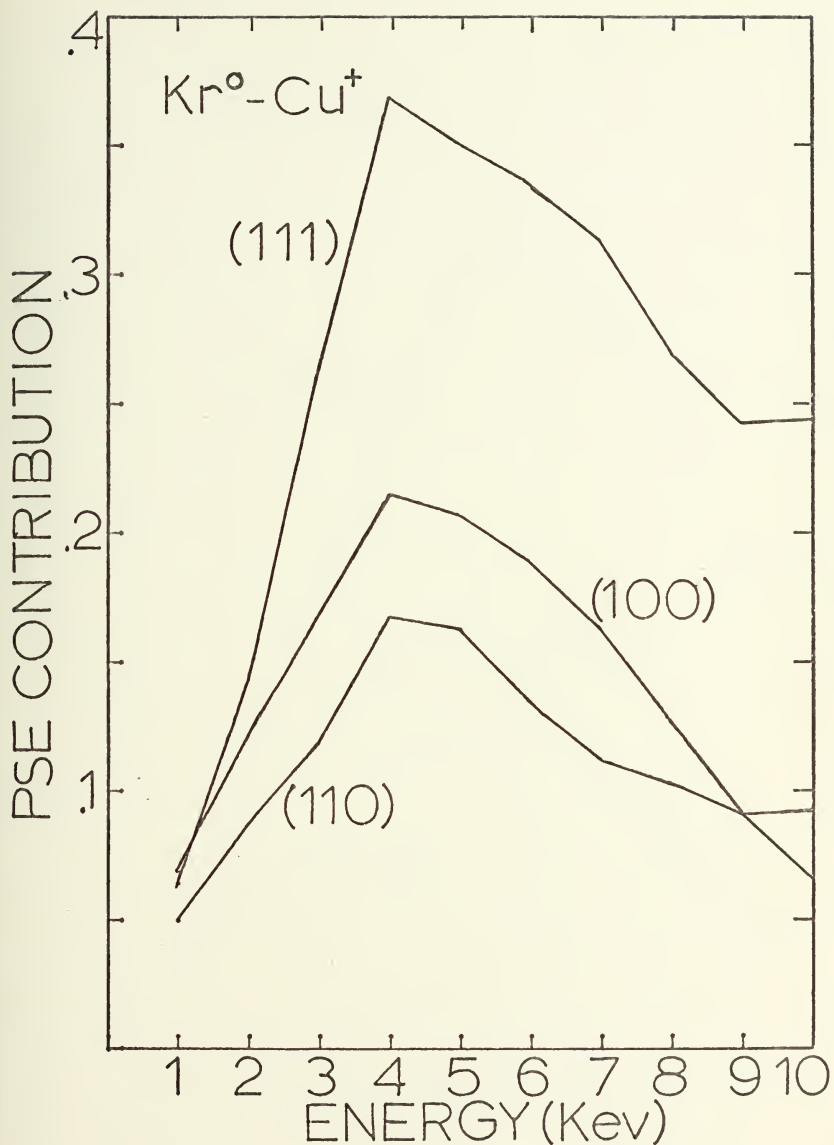


Figure 24. PSE contribution to secondary electron emission for the Kr^o - Cu system.

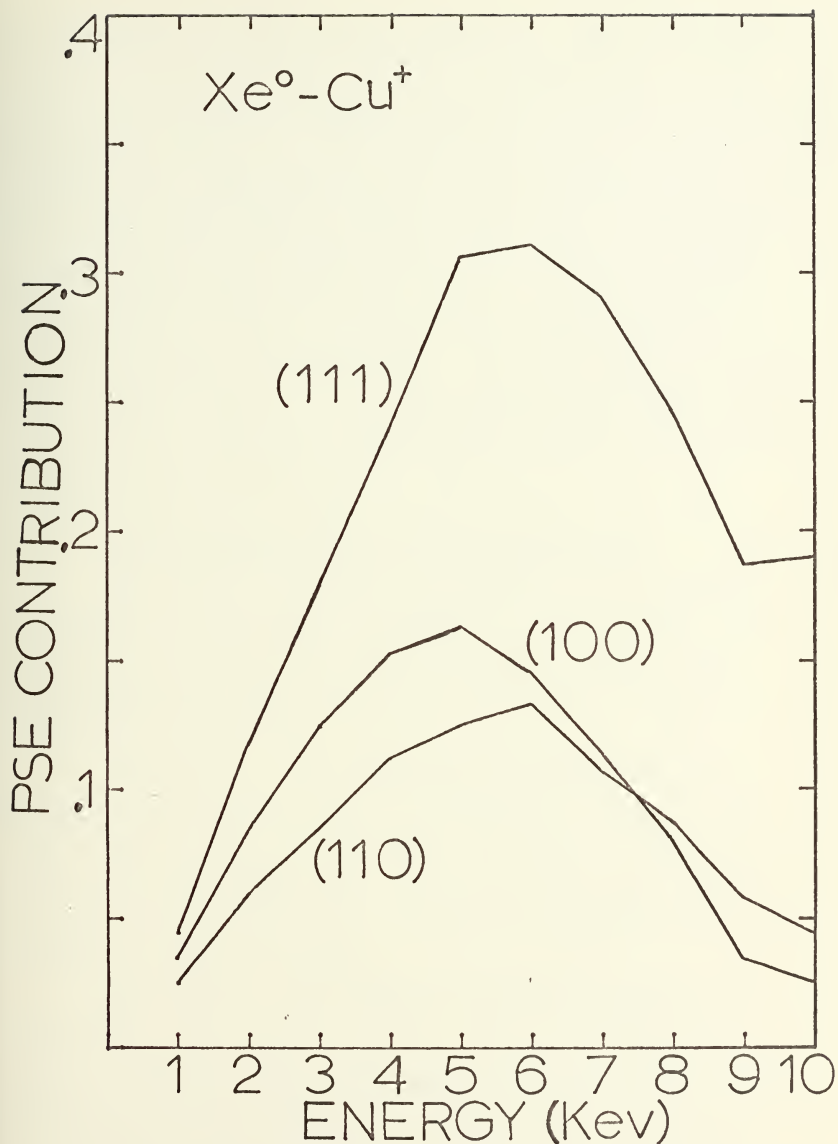


Figure 25. PSE contribution to secondary electron emission for the $\text{Xe}^{\circ} - \text{Cu}^+$ system.

dependence on the plane being bombarded. Such a crossing behavior in the PSE contribution as a function of energy would not be expected simply by analyzing the SEE coefficient curves, since these curves do not cross at any energy. If this is the case, then it would follow that the theoretical results obtained for each crystal face should be independently fitted to the experimental data, without regard to the other planes being bombarded. In most cases this would yield results that are in closer agreement with experiment and yet do not eliminate the PSE contribution to secondary electron emission entirely.

2. Silver Bombarded by Ar, Ne, and Kr Ions

The silver systems also indicate the possibility of the PSE mechanism being dependent on the crystal face being bombarded as well as the primary ion type. (See Figures 26 through 31.)

In the Ar^+ - Ag system the PSE contribution to secondary electron emission is initially largest for the (100) face, followed by the (111) and (110) faces, respectively. In all three cases the PSE contribution decreases slightly at higher energies.

In the Kr^+ - Ag system a different ordering of facial PSE contributions appear. Initially, the (111) face contributes the most to potential emission, followed by the (100) and (110) faces, in that order. At higher energies, the ordering changes, with (100) contributing the largest amount to PSE, followed by (111) and (110),

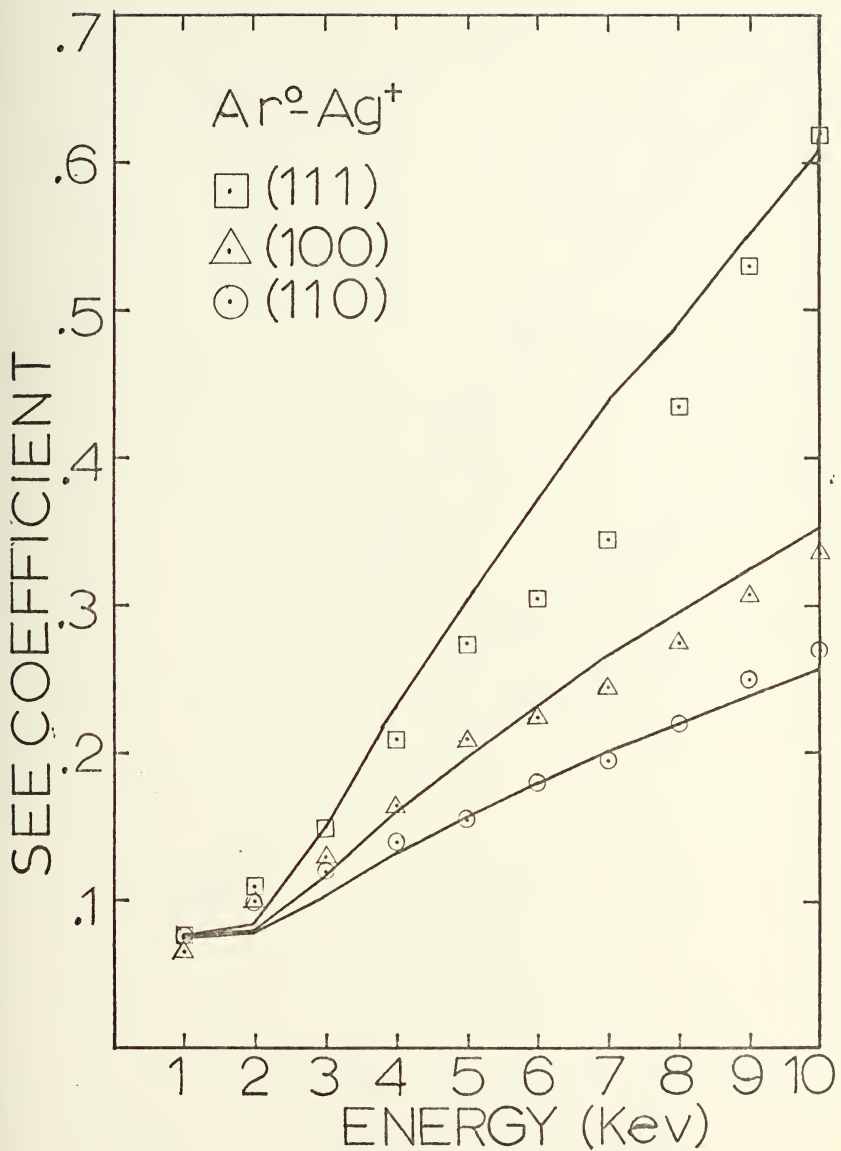


Figure 26. Ag bombarded by Ar^{+} ions normally incident on the (100), (110) and (111) faces.

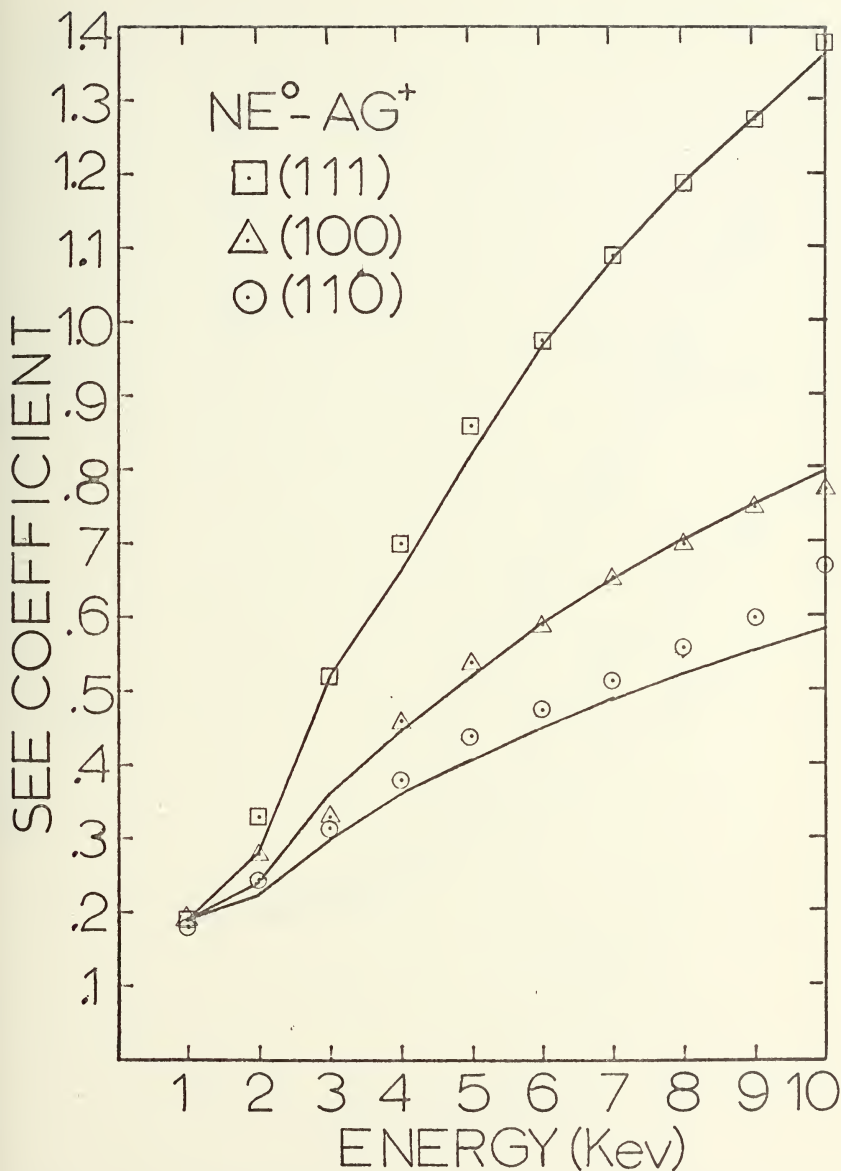


Figure 27. Ag bombarded by Ne^+ ions normally incident on the (100), (110) and (111) faces.

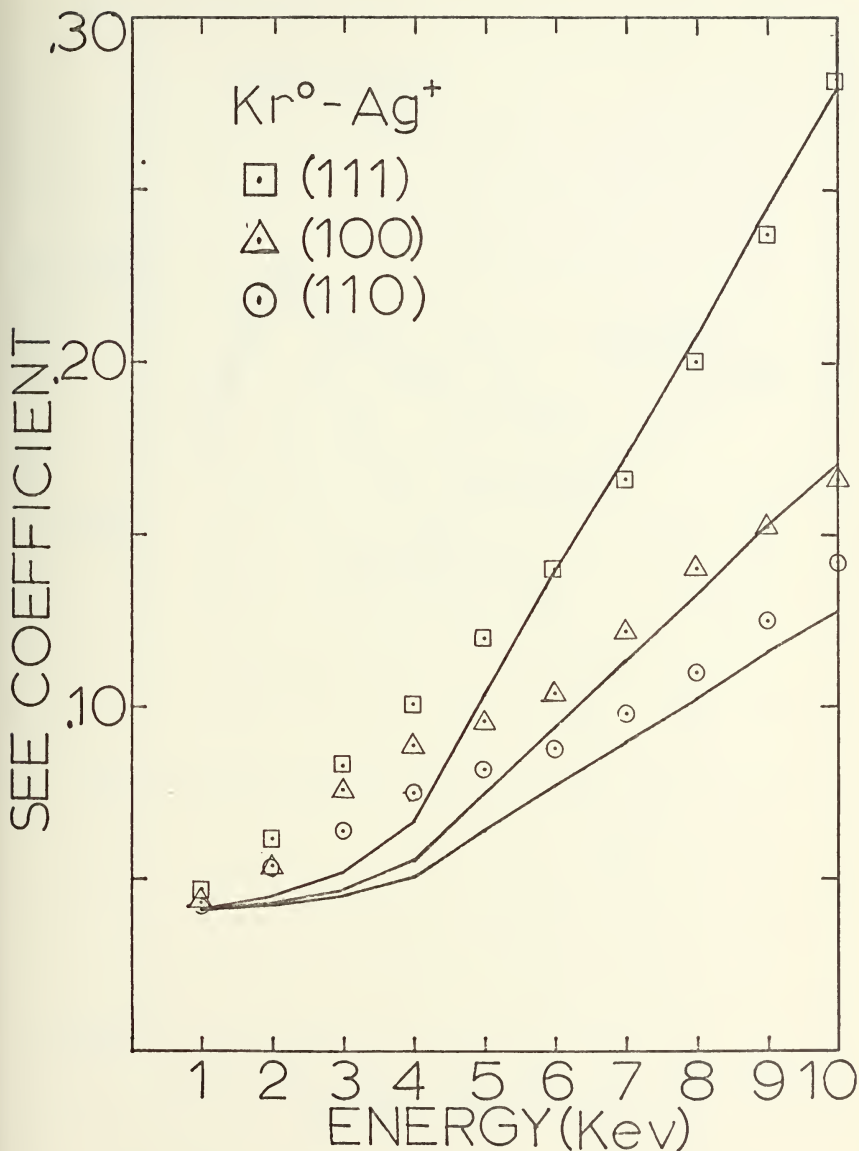


Figure 28. Ag bombarded by Kr^+ ions normally incident on the (100), (110) and (111) faces.

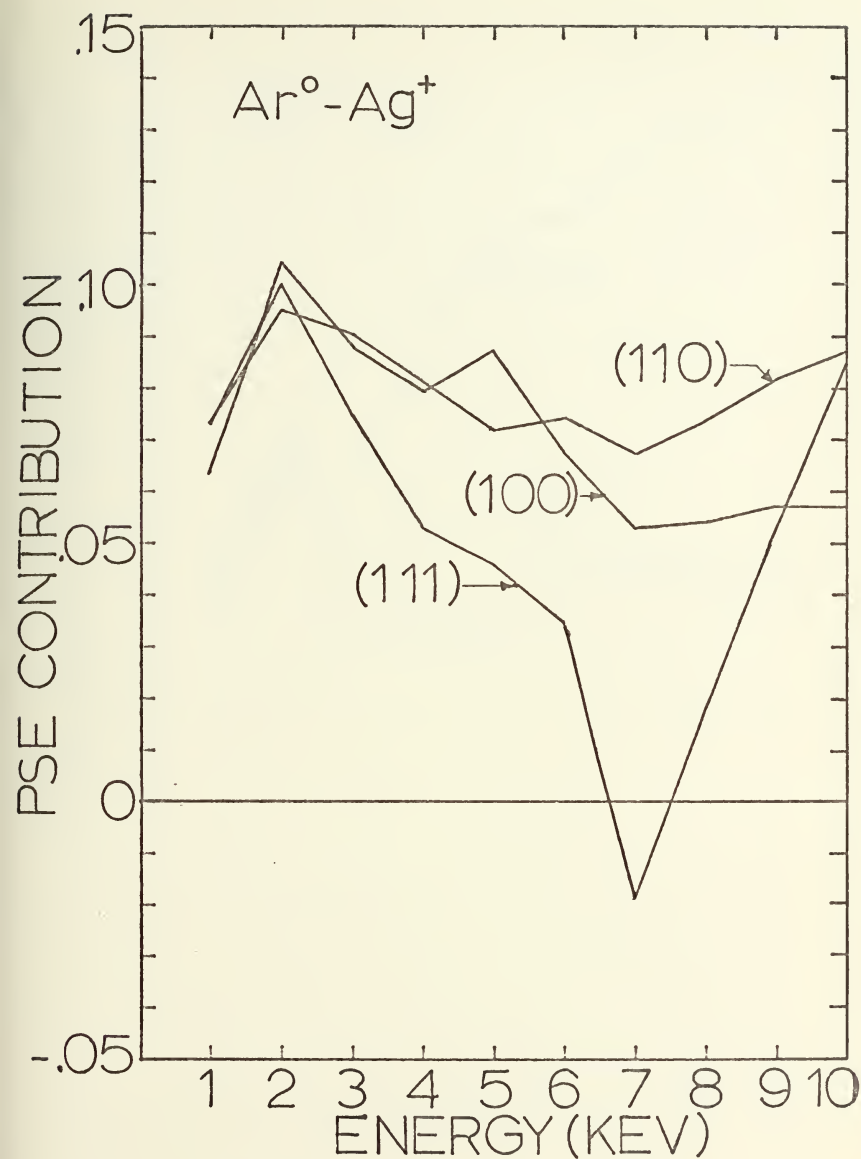


Figure 29. PSE contribution to secondary electron emission for the Ar° - Ag system.

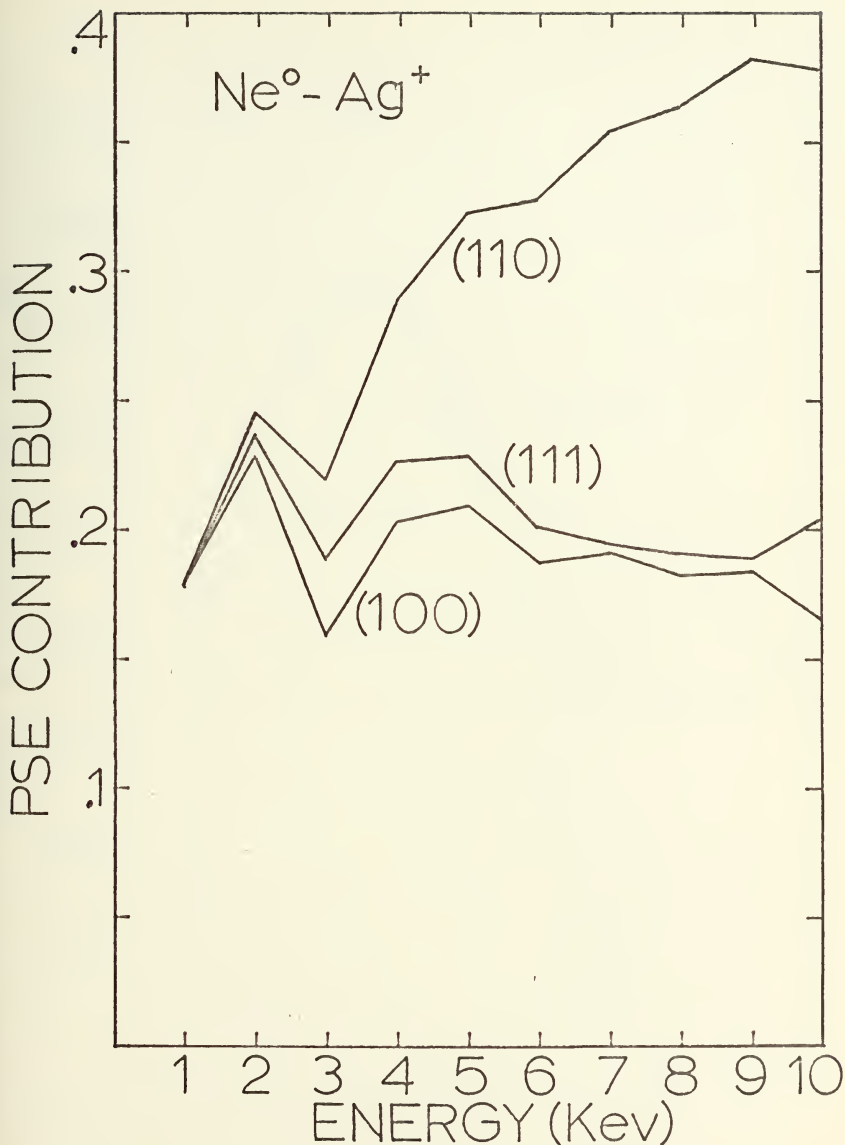


Figure 30. PSE contribution to secondary electron emission for the Ne° - Ag system.

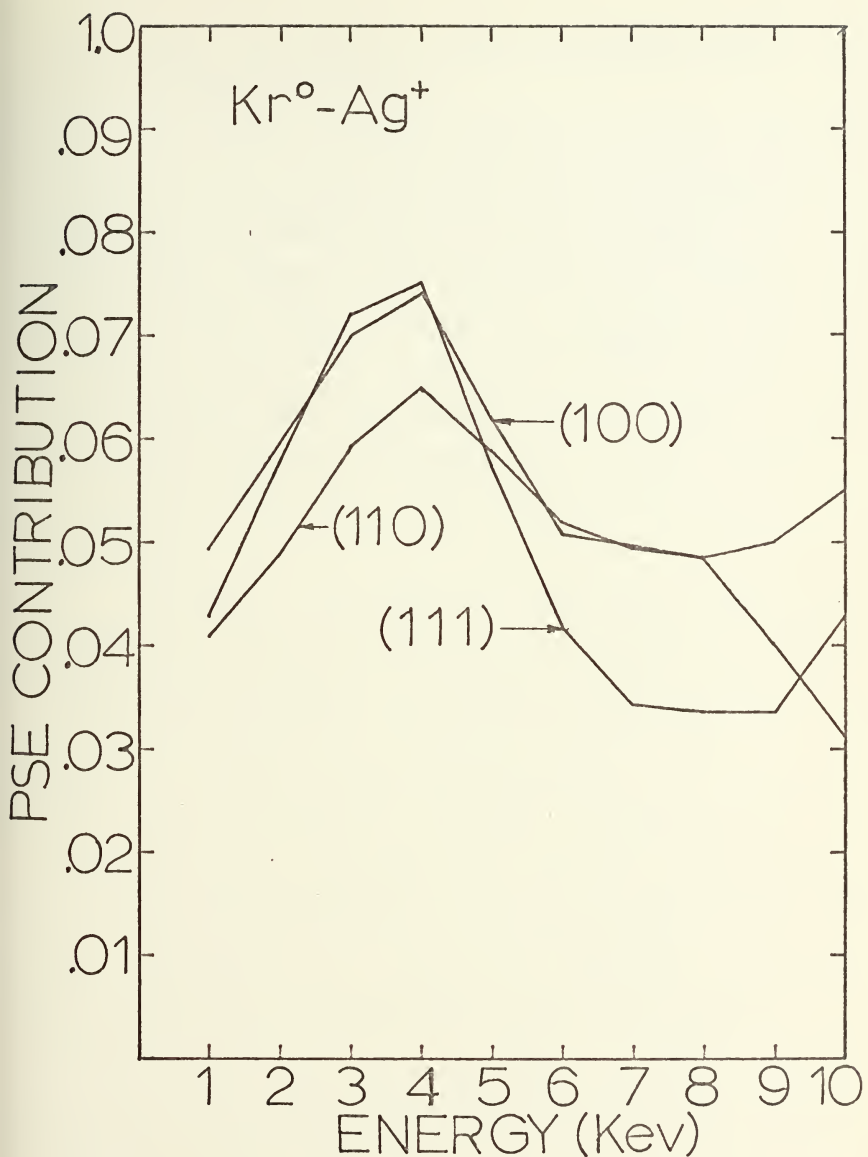


Figure 31. PSE contribution to secondary electron emission for the Kr^o - Ag system.

respectively. Once again, the PSE contribution tends to decrease at higher energies.

In the Ne^+ - Ag system an entirely different picture arises. For all energies, the (110) face contributes the most to PSE, followed by the (111) and (100) faces, respectively. However, even at ten Kev, the potential emission for the (110) face is still rising whereas, over the entire energy range, the PSE contribution from the (111) and (100) face remains fairly constant. These results would seem to indicate, once again, that not only is potential emission dependent on primary ion type, but also on crystal face.

In the Ar^+ - Ag system, the PSE contribution from the (111) face goes to a negative value at seven Kev. The reason for this behavior can be found by analyzing the Ar^+ - Ag SEE coefficient versus energy curves shown in Figure 26. The SEE coefficient experimental data for the (111) face dips downward at seven Kev. This behavior is not demonstrated on the other faces and would tend to indicate that some experimental variation may be present in these experimental data. On the other hand, the interaction being modeled may be sufficiently complicated that the potential contribution cannot be separated simply by scaling the results. No other system investigated displays similar results.

3. Molybdenum Bombarded by Ar, Ne, Kr and Xe Ions

In Figures 32 through 43, Mo^+ initially seems to be the ion core model that best represents secondary electron emission from various target faces. This conclusion holds true for the $\text{Ne}^+ - \text{Mo}$ and $\text{Kr}^+ - \text{Mo}$ systems. However, for the $\text{Xe}^+ - \text{Mo}$ system, the best ion core model is not Mo^+ but Mo^{++} . This would seem to indicate that the primary ion type plays an important role in secondary electron emission.

4. Aluminum Bombarded by Ar, Kr, and Xe Ions

In the case of aluminum bombarded by Ar^+ (Figures 44 through 52) the Al^+ and Al^{++} ion core models for the target atoms yielded results that were almost identical. This system is contrasted with the $\text{Kr}^+ - \text{Al}$ system which shows a distinct preference for Al^{++} as the ion core model, with the Al^+ and Al^{+++} yielding similar and uniformly poor results. Similarly, the $\text{Xe}^+ - \text{Al}$ system shows the same preference for the Al^{++} ion core model and demonstrates a poorer fit when the Al^+ and Al^{+++} models are used. When all cases are considered, it would seem that secondary electron emission is sensitive to the primary ion type, as has been demonstrated by previous results.

C. ALKALI-HALIDE RESULTS

Experimental results for the bombardment of alkali-halide single crystals by inert gas ions have been obtained from experiments by Baboux and Pedrix [21, 22]. Two cases are considered in this present investigation. These include

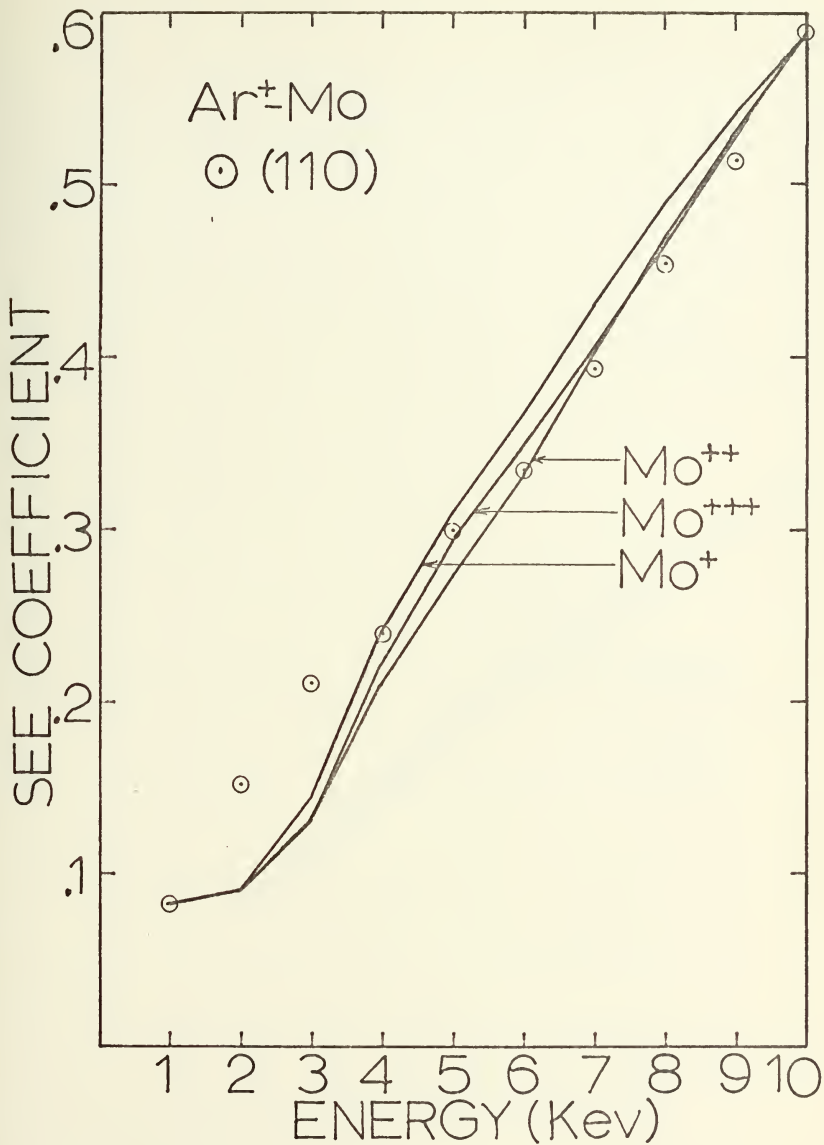


Figure 32. Effect of varying target atom ionization in the HCM model on secondary electron emission from the Ar - Mo system.

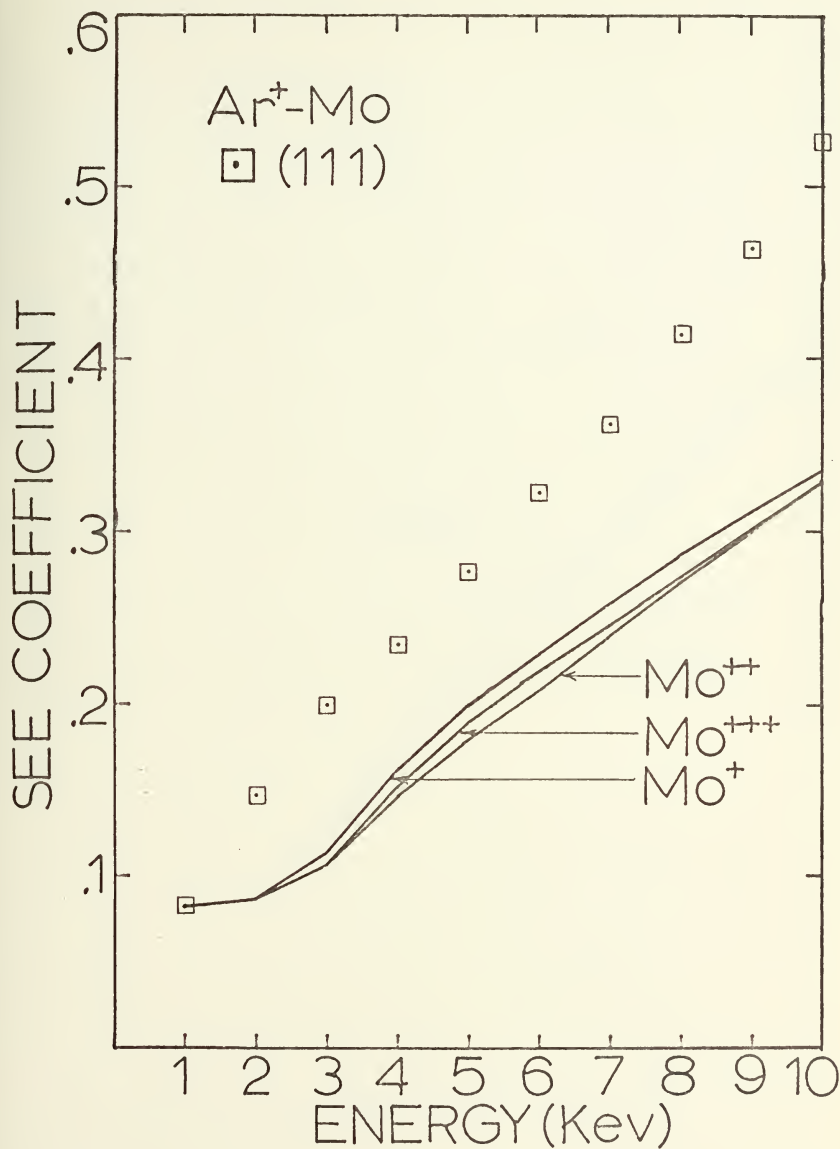


Figure 33. Effect of varying target atom ionization in the HCM model on secondary electron emission from the Ar⁺-Mo system.

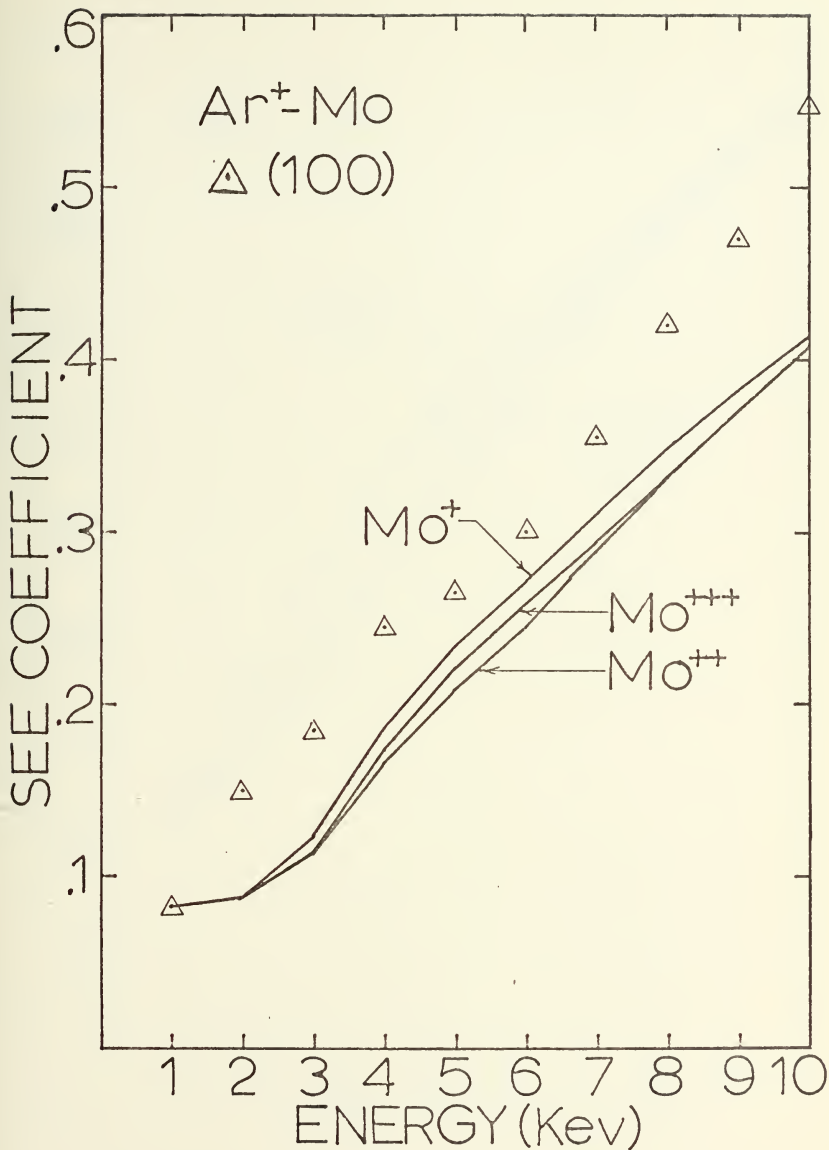


Figure 34. Effect of varying target atom ionization in the HCM model on secondary electron emission in the $\text{Ar}^+ - \text{Mo}$ system.

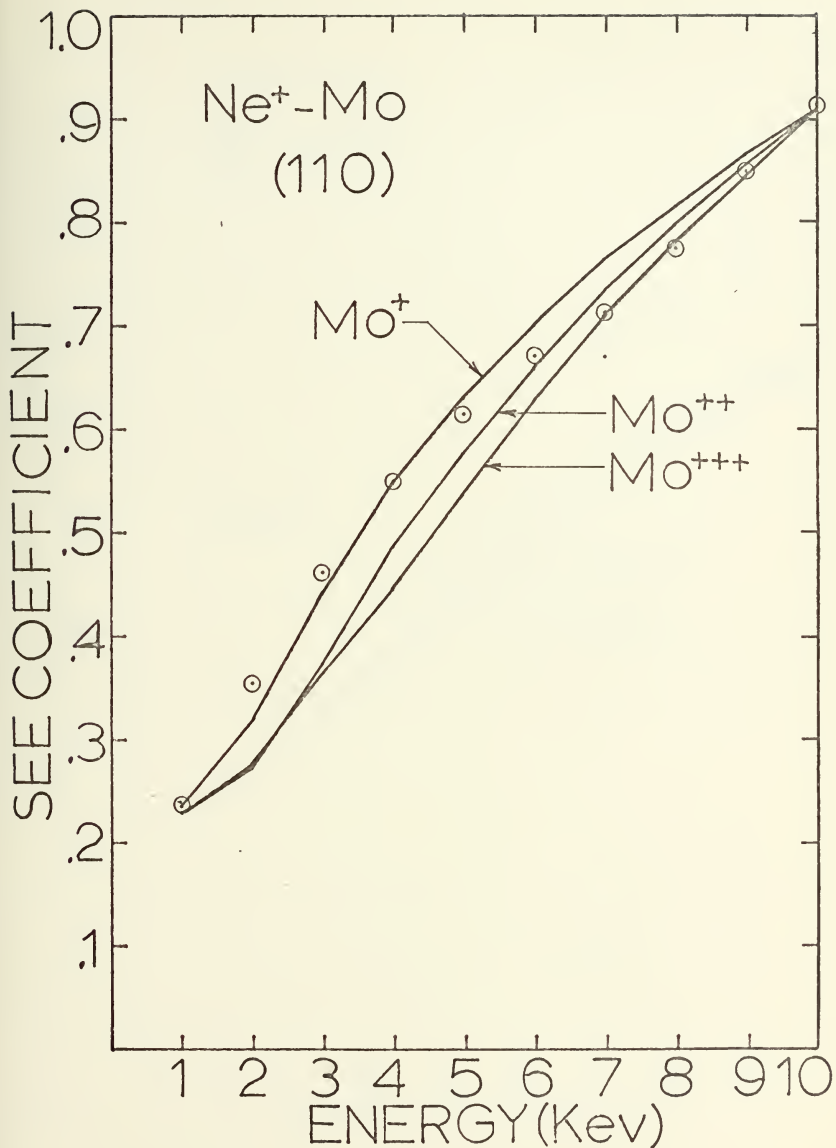


Figure 35. Effect on varying target atom ionization in the HCM model on secondary electron emission from the Ne⁺ - Mo system.

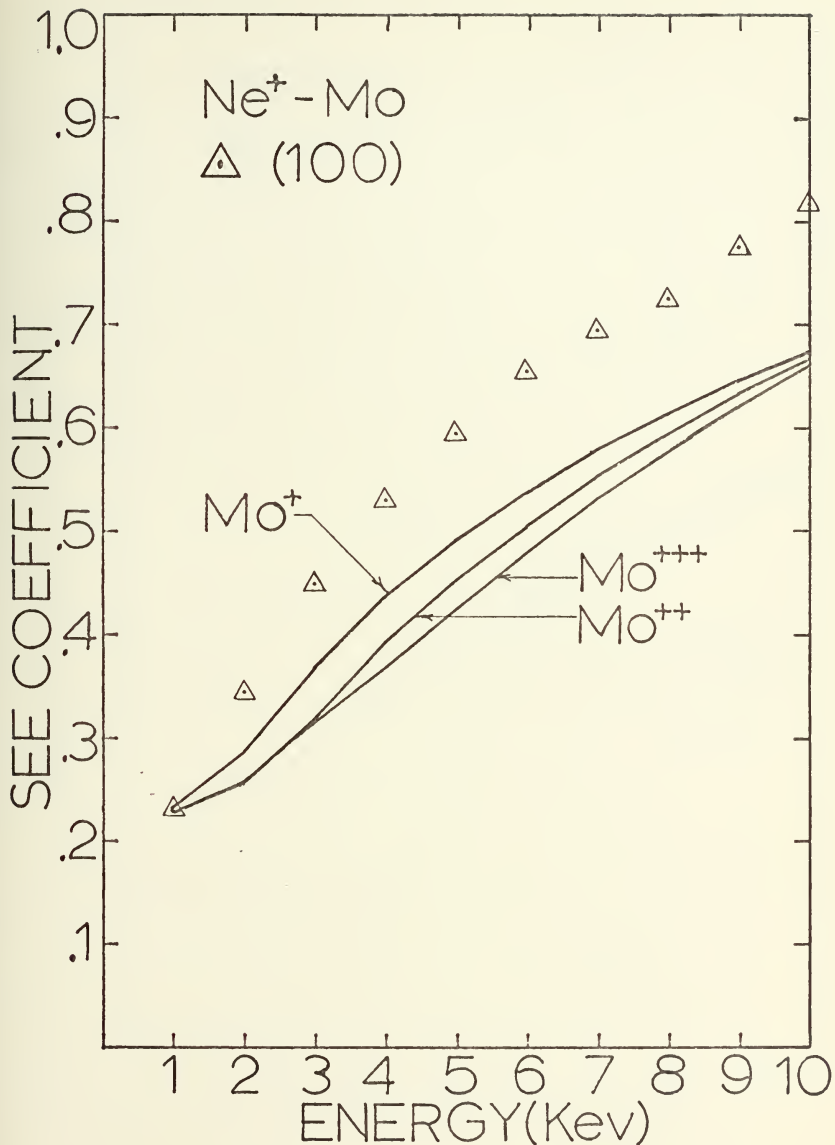


Figure 36. Effect of varying target atom ionization in the HCM model on secondary electron emission from the $\text{Ne}^+ - \text{Mo}$ system.

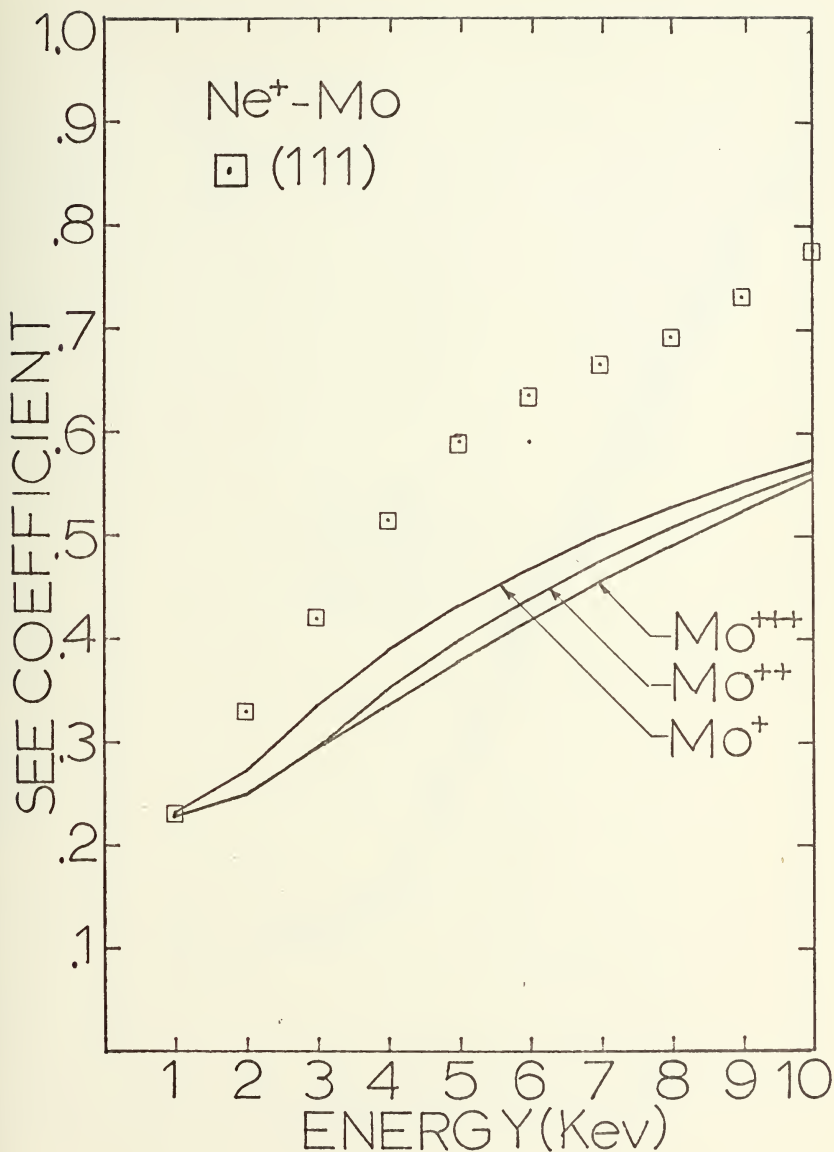


Figure 37. Effect of varying target atom ionization in the HCM model on secondary electron emission from the $\text{Ne}^+ - \text{Mo}$ system.

SEE COEFFICIENT

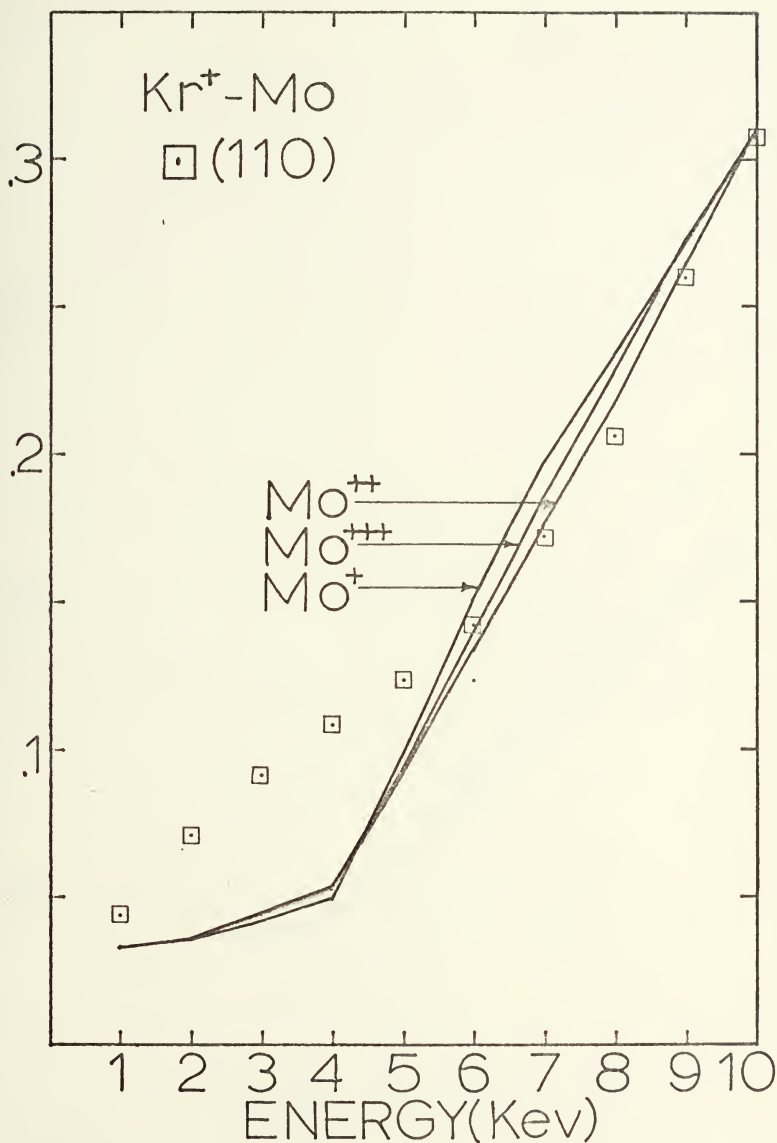


Figure 38. Effect of varying target atom ionization in the HCM model on secondary electron emission from the Kr⁺ - Mo system.

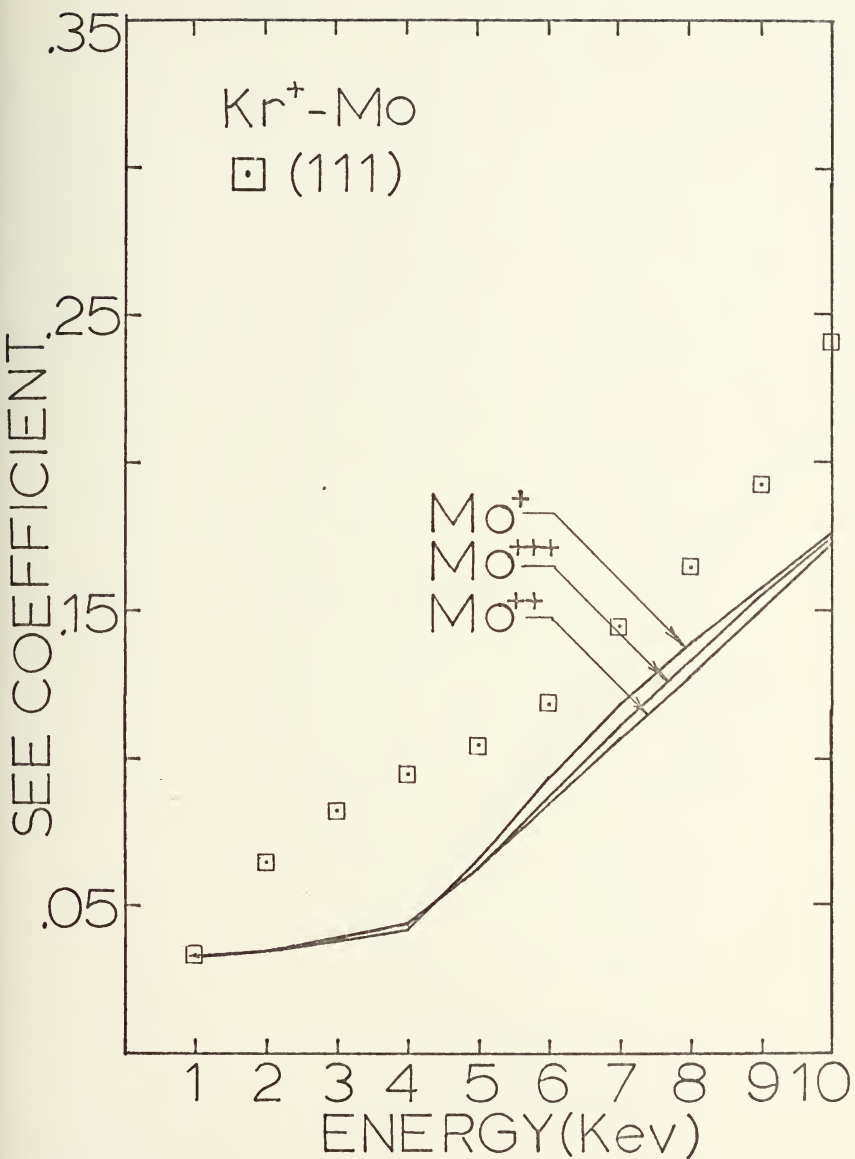


Figure 39. Effect of varying target atom ionization in the HCM model on secondary electron emission from the $\text{Kr}^+ \text{- Mo}$ system.

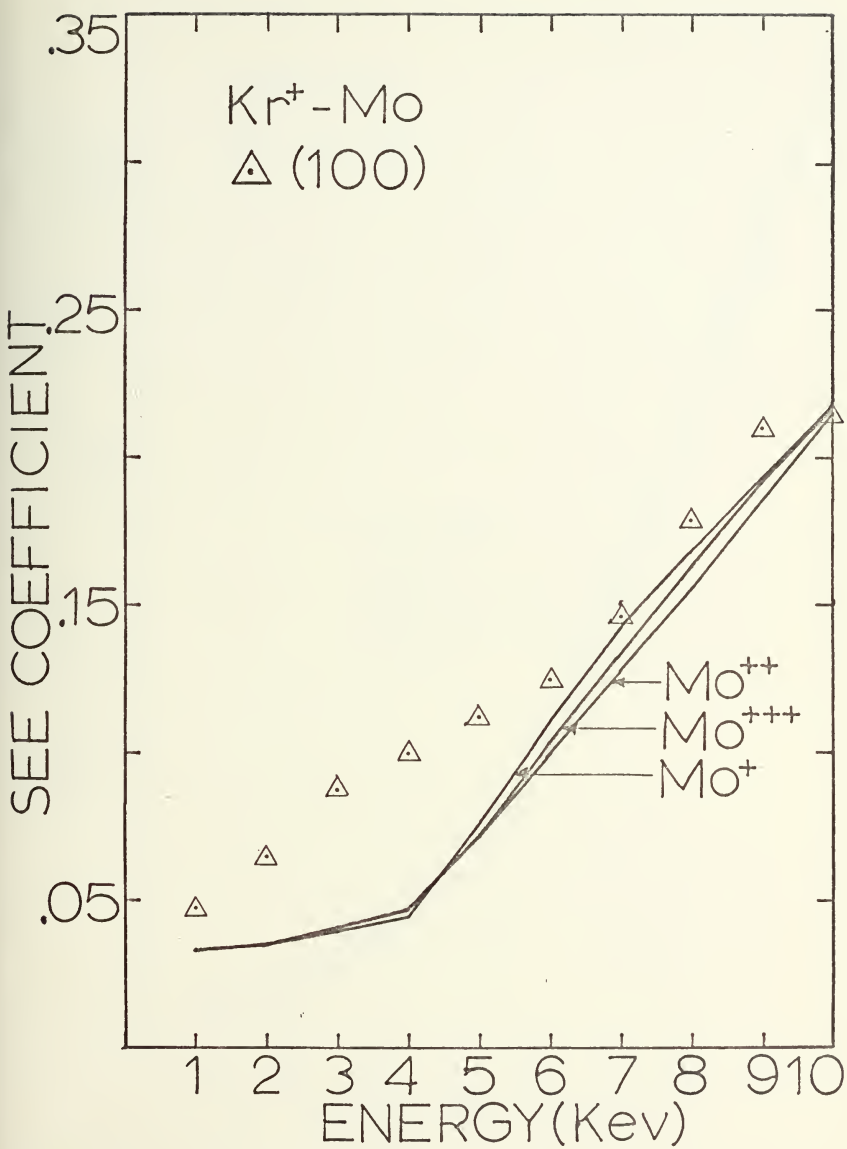


Figure 40. Effect of varying target atom ionization in the HCM model on secondary electron emission from the $\text{Kr}^+ - \text{Mo}$ system.

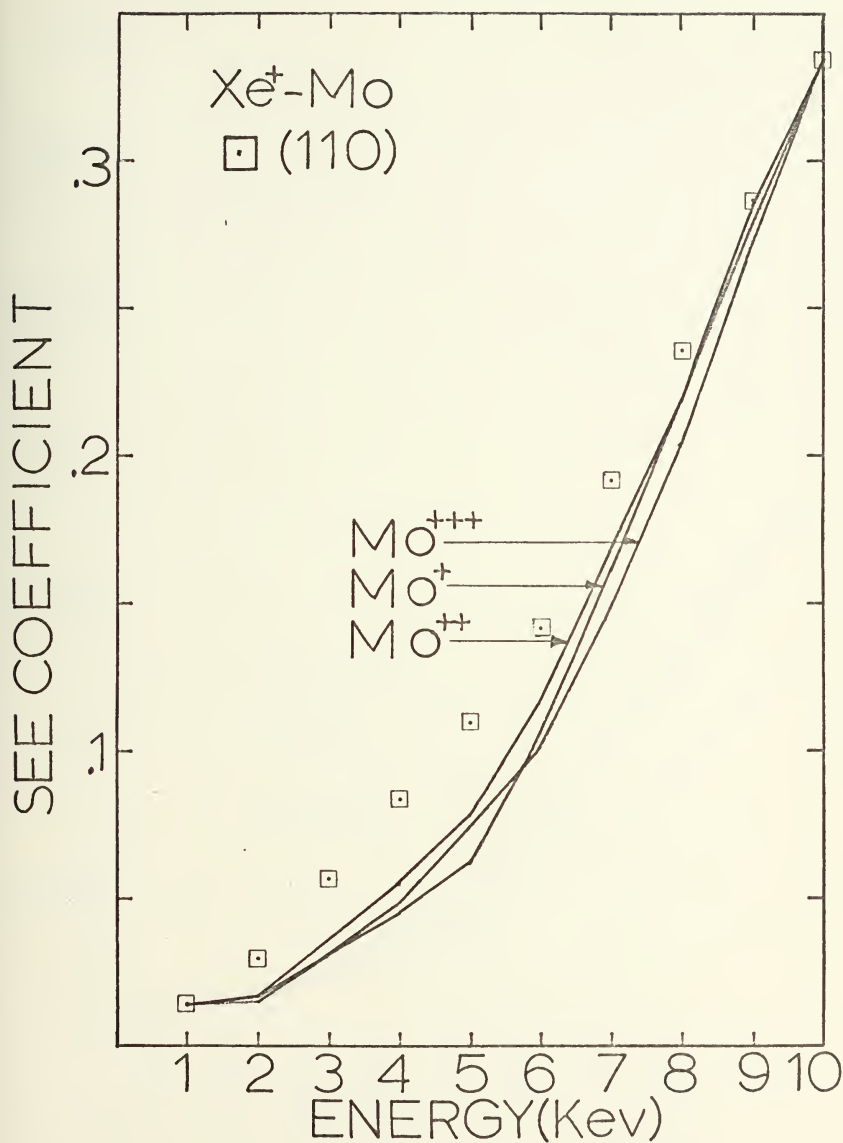


Figure 41. Effect of varying target atom ionization in the HCM model on secondary electron emission from the Xe^+ - Mo system.

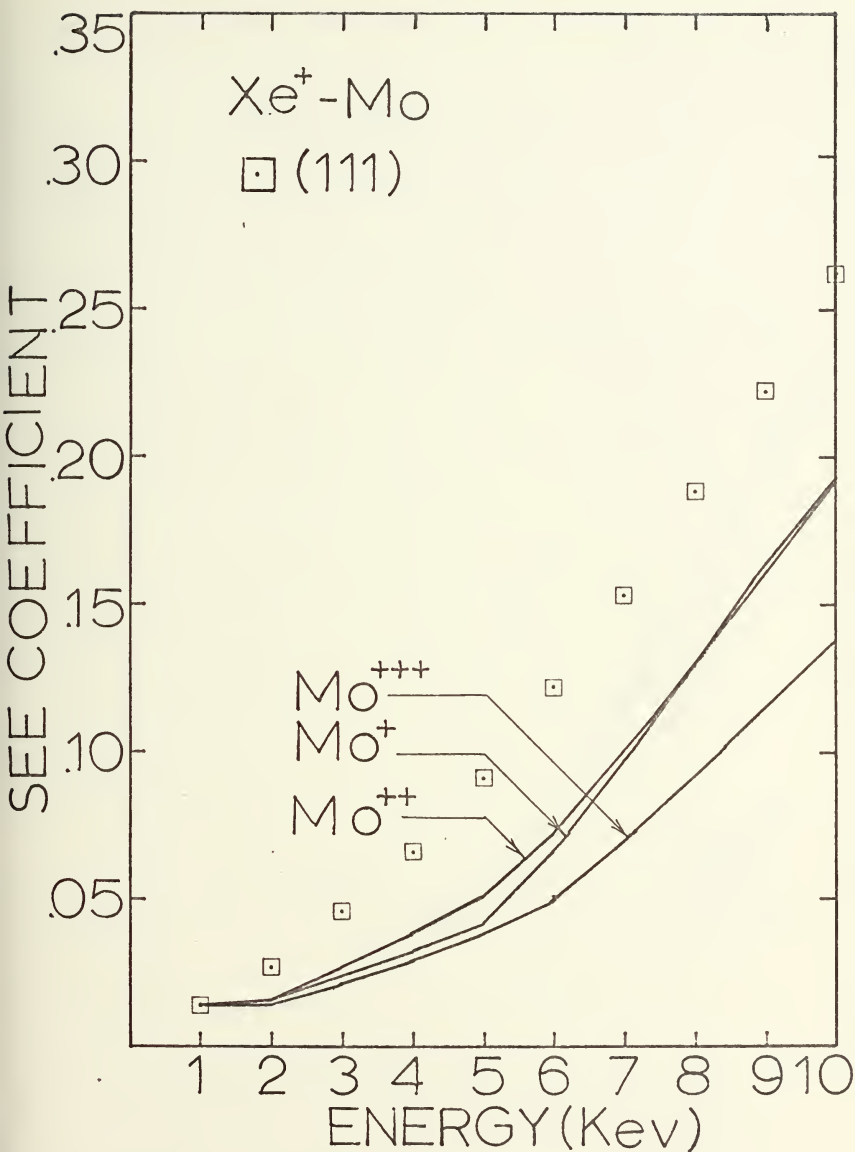


Figure 42. Effect of varying target atom ionization in the HCM model on secondary electron emission from the $Xe^- Mo$ system.

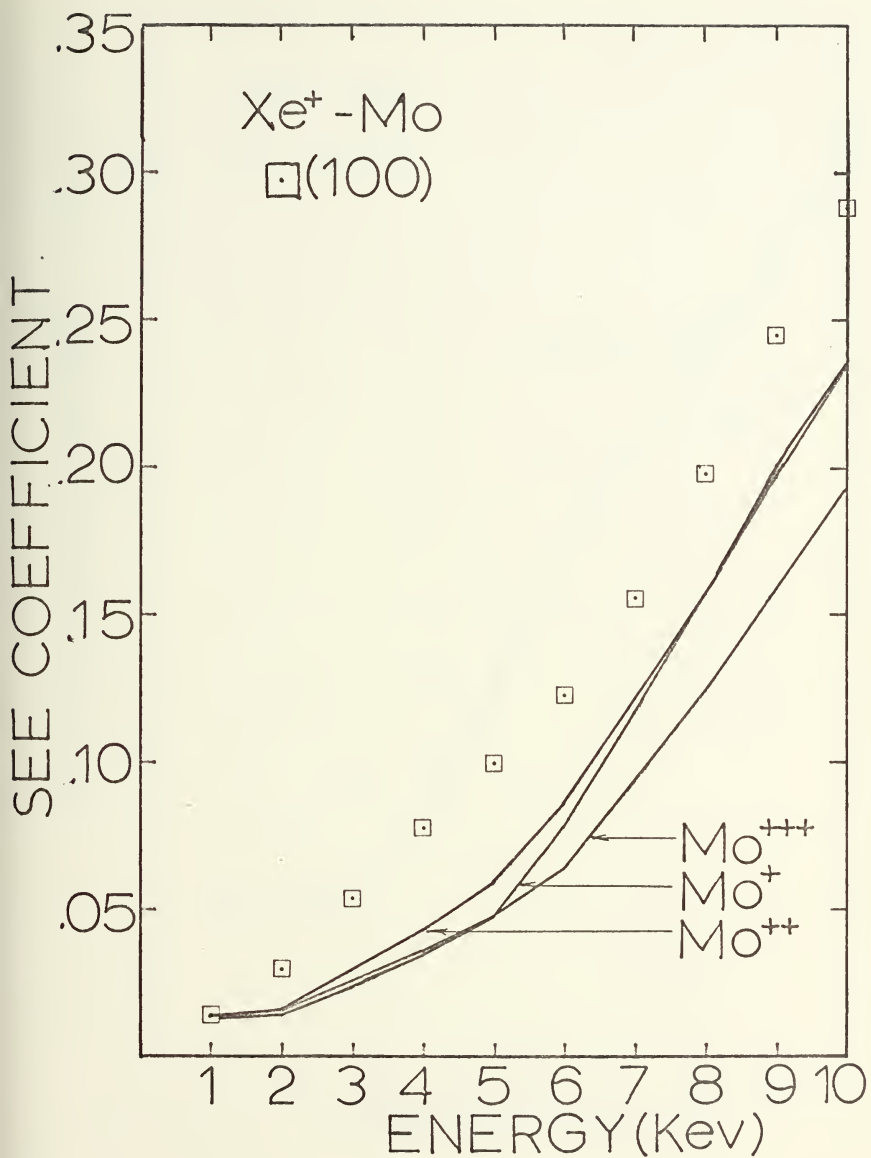


Figure 43. Effect of varying target atom ionization in the HCM model on secondary electron emission from the $Xe^- Mo$ system.

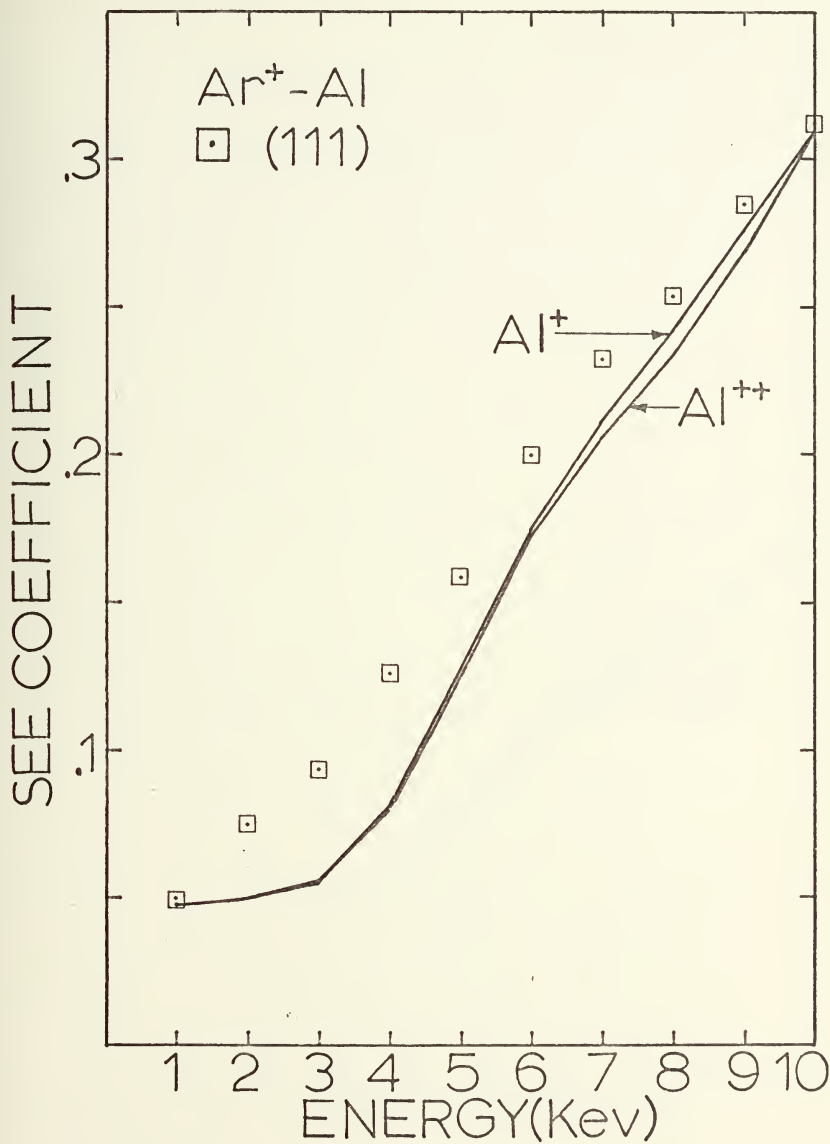


Figure 44. Effect of varying target atom ionization in the HCM model on secondary electron emission from the $\text{Ar} - \text{Al}$ system.

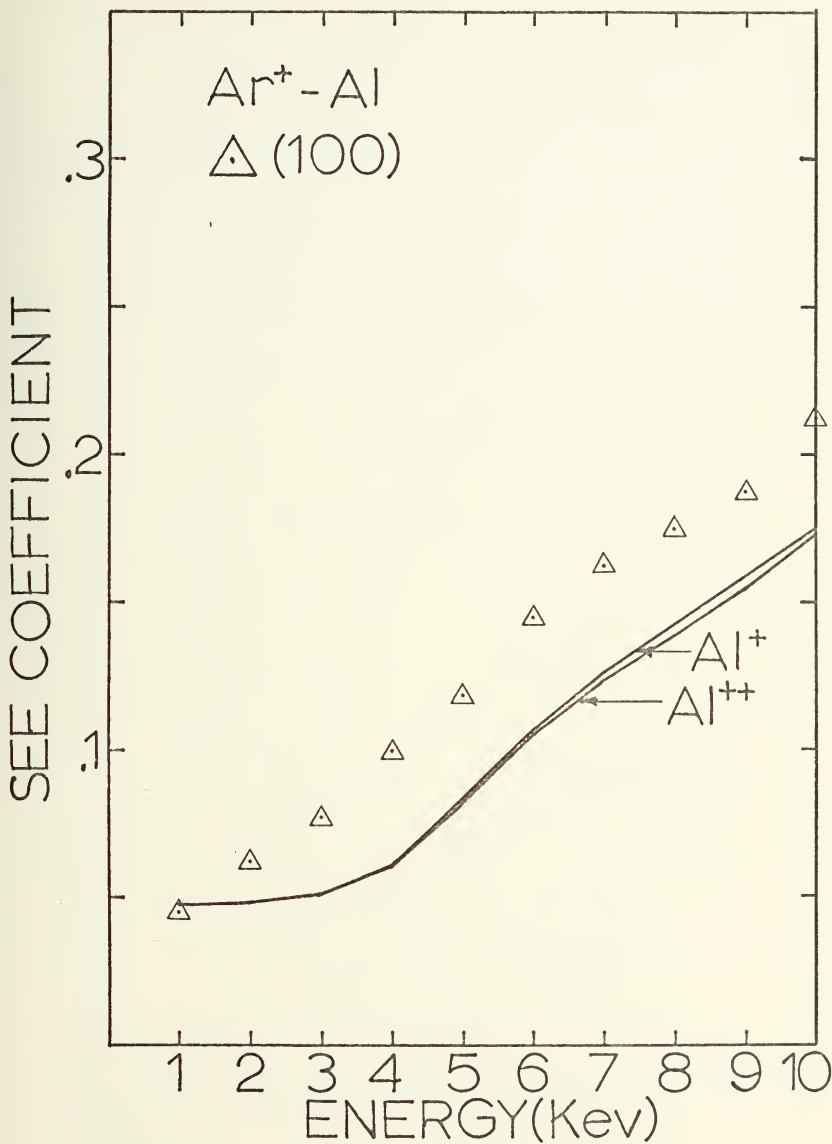


Figure 45. Effect of varying target atom ionization in the HCM model on secondary electron emission from the $\text{Ar}^+ - \text{Al}$ system.

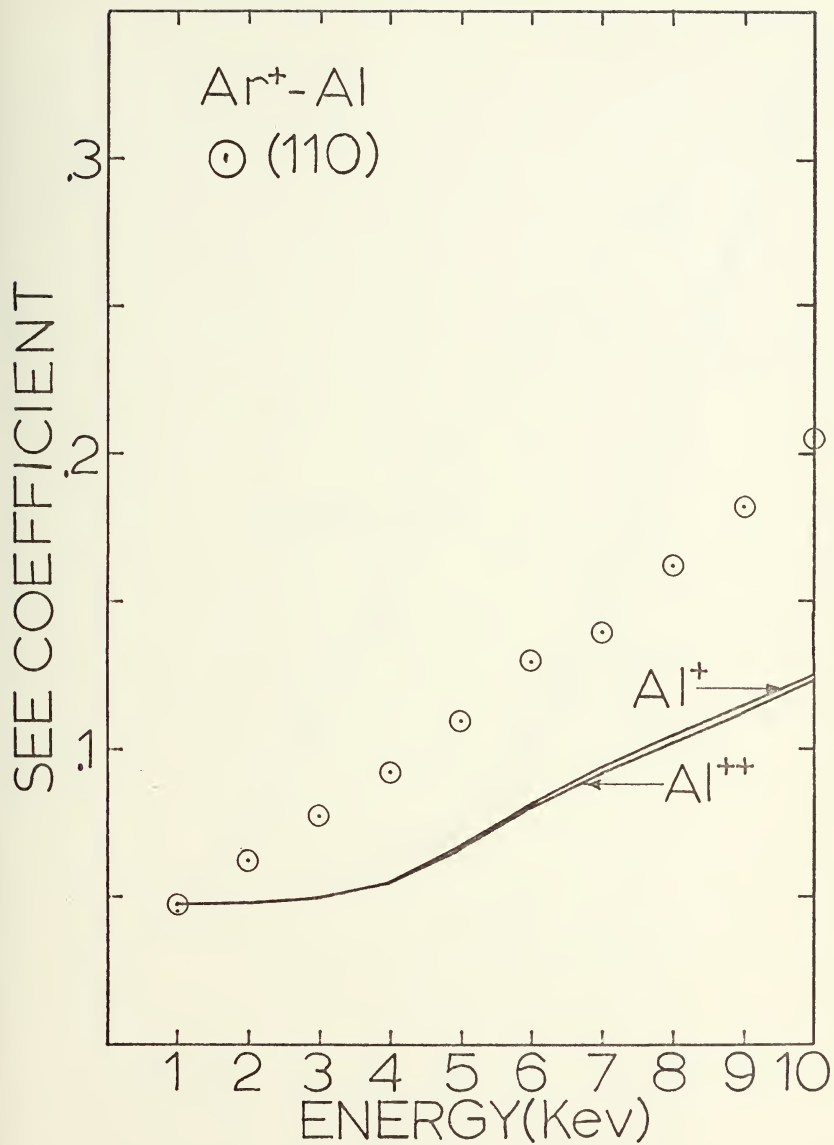


Figure 46. Effect of varying target atom ionization in the HCM model on secondary electron emission from the $\text{Ar}^- \text{Al}$ system.

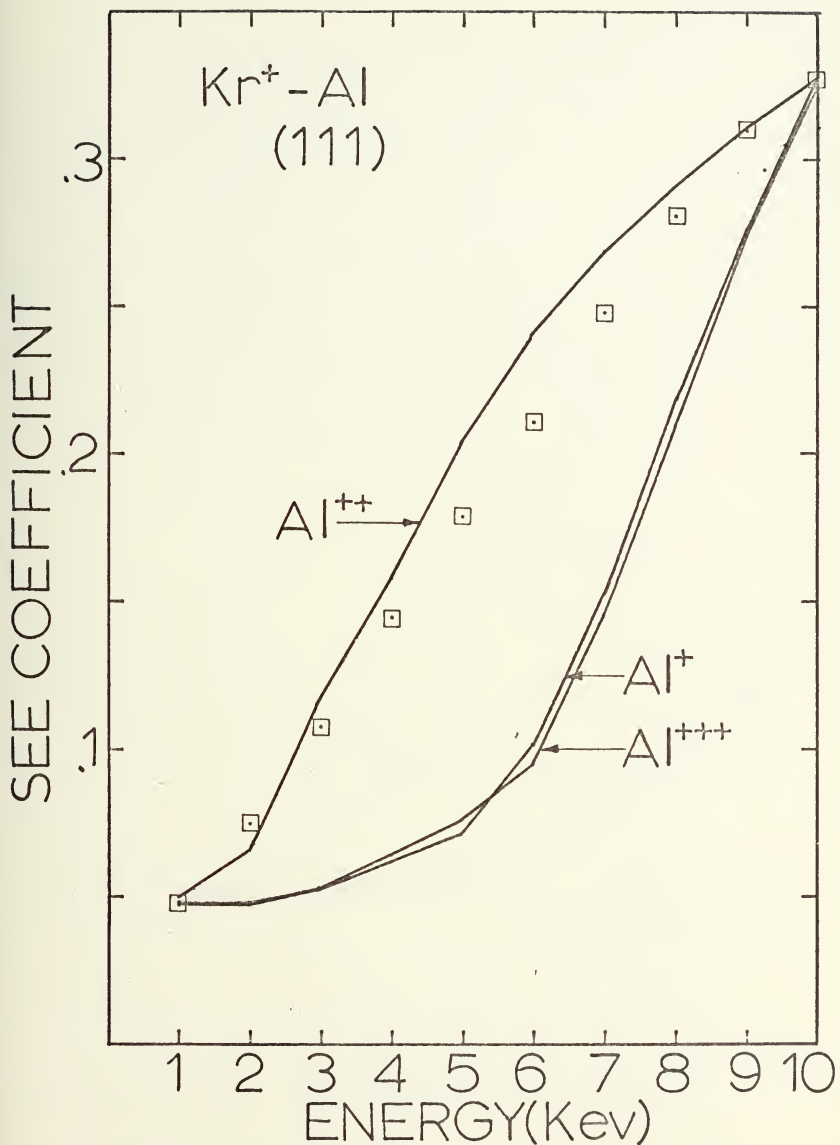


Figure 47. Effect of varying target atom ionization in the HCM model on secondary electron emission from the $\text{Kr}^+ - \text{Al}$ system.

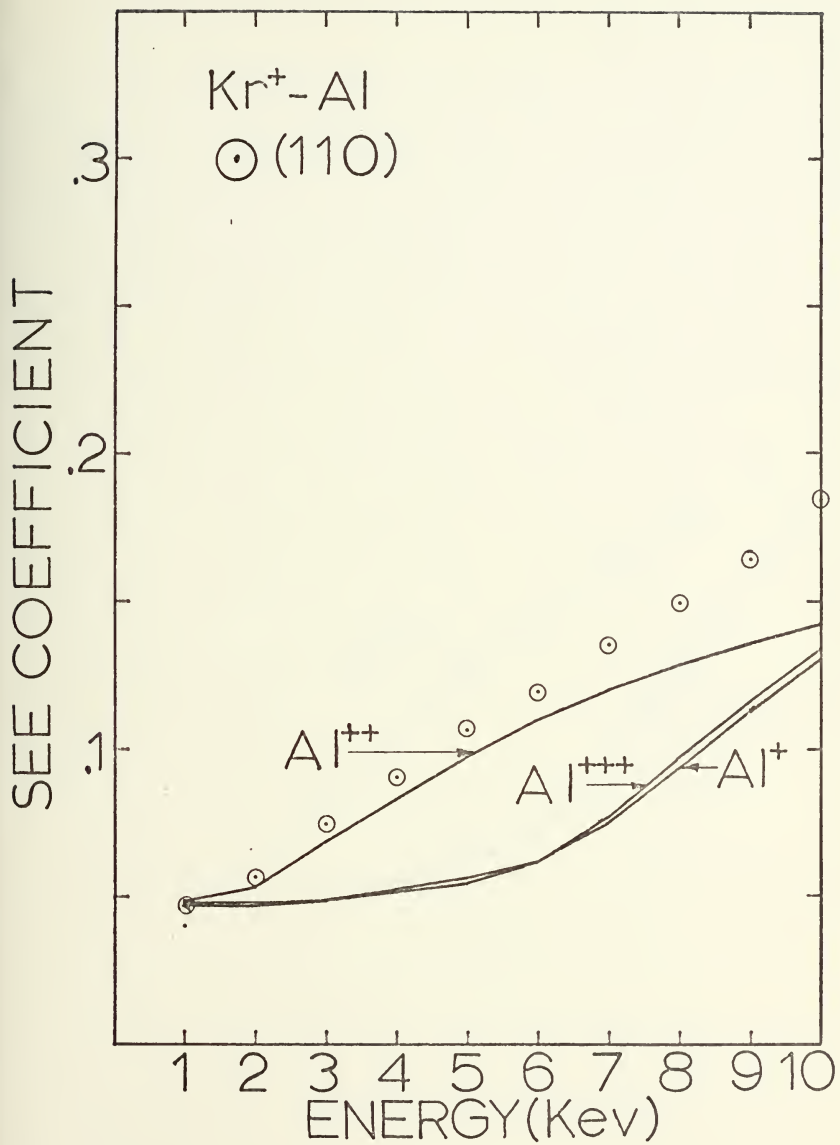


Figure 48. Effect of varying target atom ionization in the HCM model on secondary electron emission from the $\text{Kr}^+ - \text{Al}$ system.

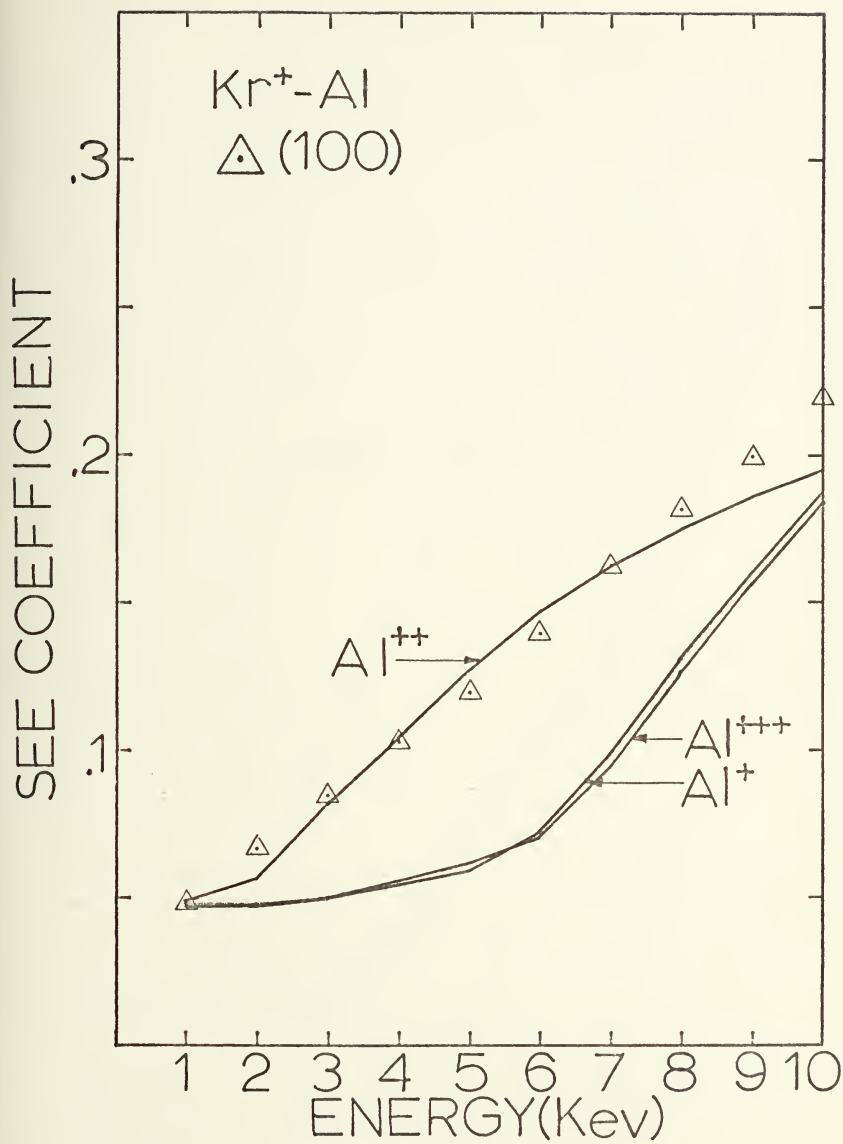


Figure 49. Effect of varying target atom ionization in the HCM model on secondary electron emission from the $\text{Kr}^+ - \text{Al}$ system.

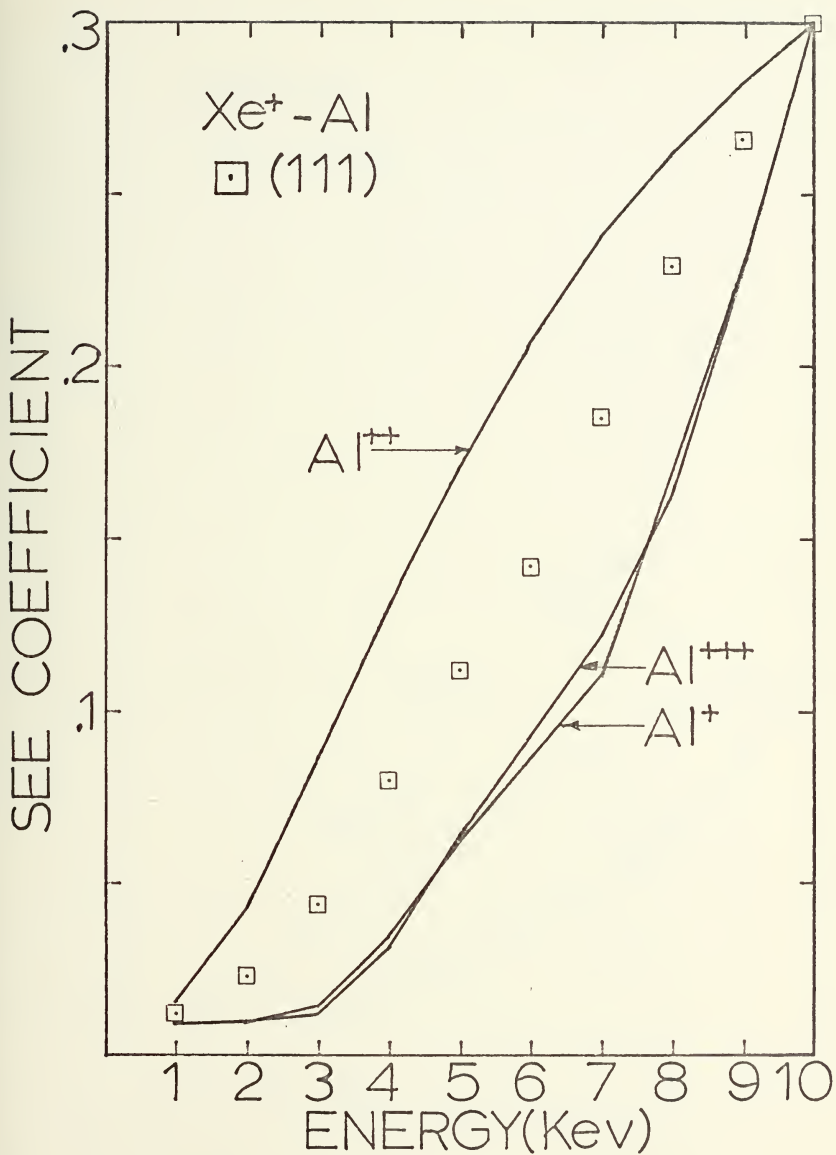


Figure 50. Effect of varying target atom ionization in the HCM model on secondary electron emission from the $\text{Xe}^+ - \text{Al}$ system.

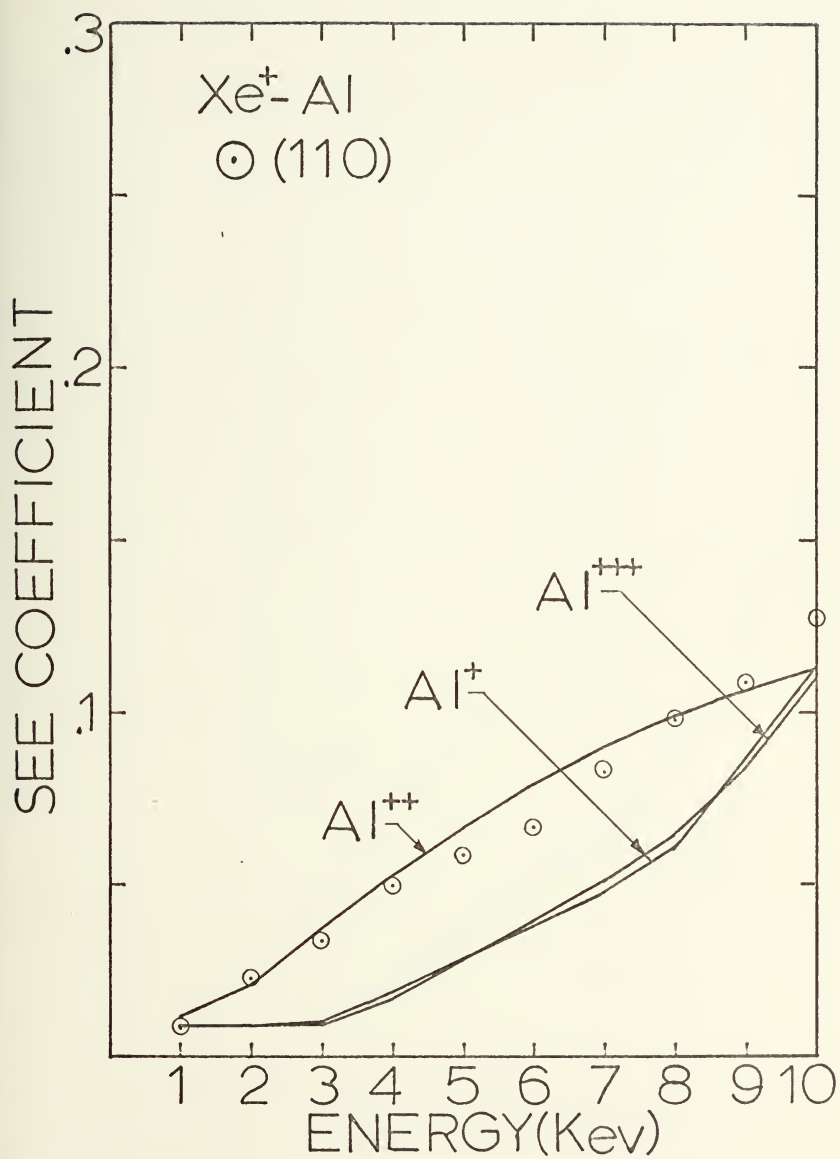


Figure 51. Effect of varying target atom ionization in the HCM model on secondary electron emission from the Xe^- - Al system.

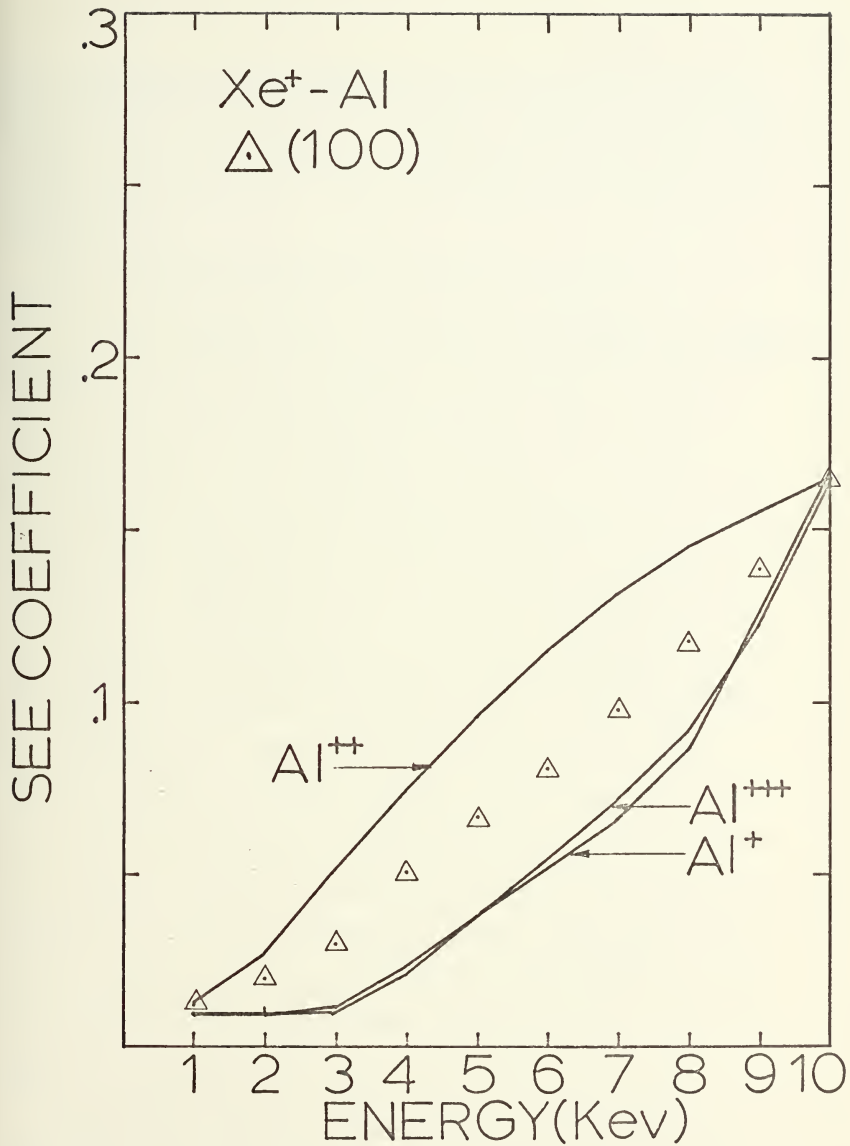


Figure 52. Effect of varying target atom ionization in the HCM model on secondary electron emission from the $\text{Xe}^+ - \text{Al}$ system.

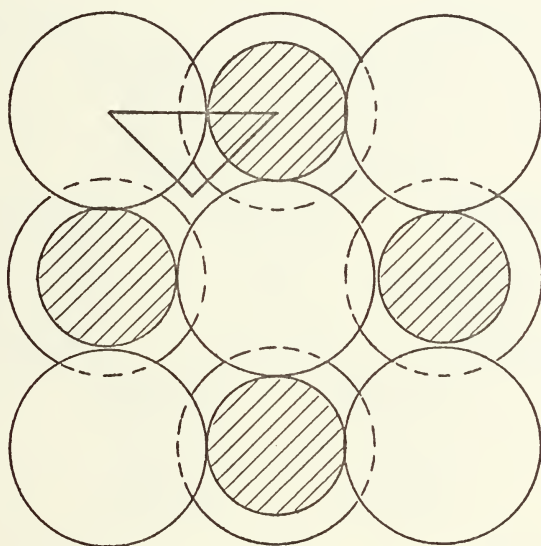
the bombardment of potassium chloride by argon and neon ions normally incident on the (100), (110) and (111) faces of the single crystal. These two cases are discussed in detail below.

1. Potassium-Chloride Bombarded by Ar Ions

The calculations of the SEE coefficient for alkali-halide single crystals present a theoretical problem that was not addressed when the metal target results were presented. Specifically, the alkali-halide crystals in question have lattice structures comprised of two different atoms arranged in a similar fashion, but displaced in space by a distance (1/2, 1/2, 1/2). Because of this, the standard FCC distribution of impact parameters does not work in the alkali-halide case and must be replaced by a distribution representative of the normal impact of an ion with the target surface. The representative areas and distribution of impact parameters are chosen in a manner similar to that for the metal case, but are weighted to include preferential impact with the larger of the two ion cores in the lattice. The representative areas and distribution of impact parameters are shown in Figures 53 through 57.

The results for KCl bombarded by Ar^+ are shown in Figure 58. Experimentally, it was found that the SEE

REPRESENTATIVE AREA KCl (100)

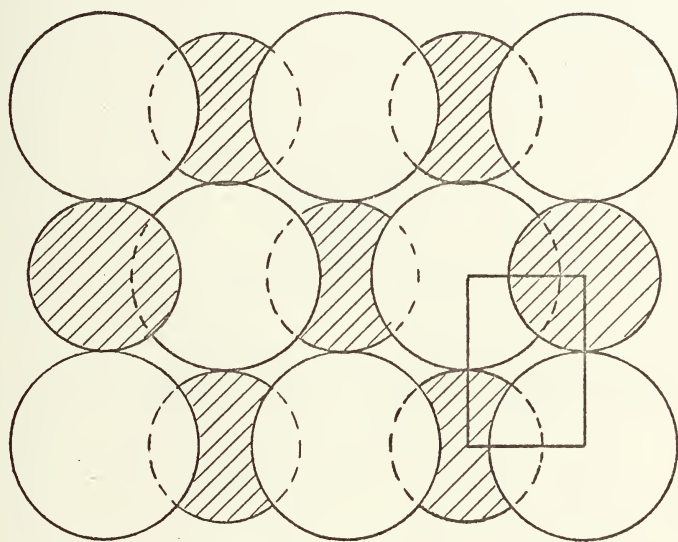


□ Cl atoms

▨ K atoms

Figure 53. Representative area KCl (100).

REPRESENTATIVE AREA KCl (110)



□ Cl atoms

■ K atoms

Figure 54. Representative area KCl (110).

REPRESENTATIVE AREA

KCl (111)

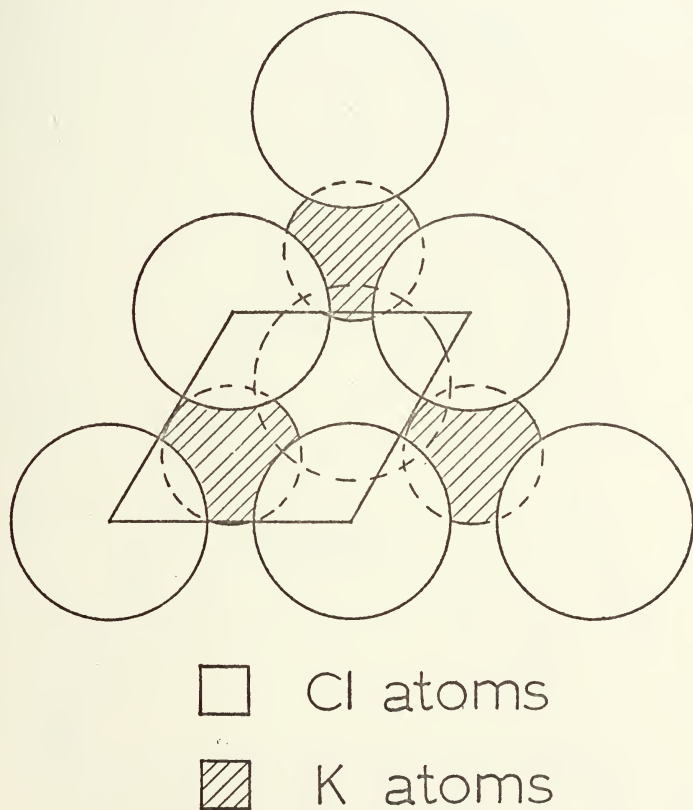


Figure 55. Representative area KCl (111).

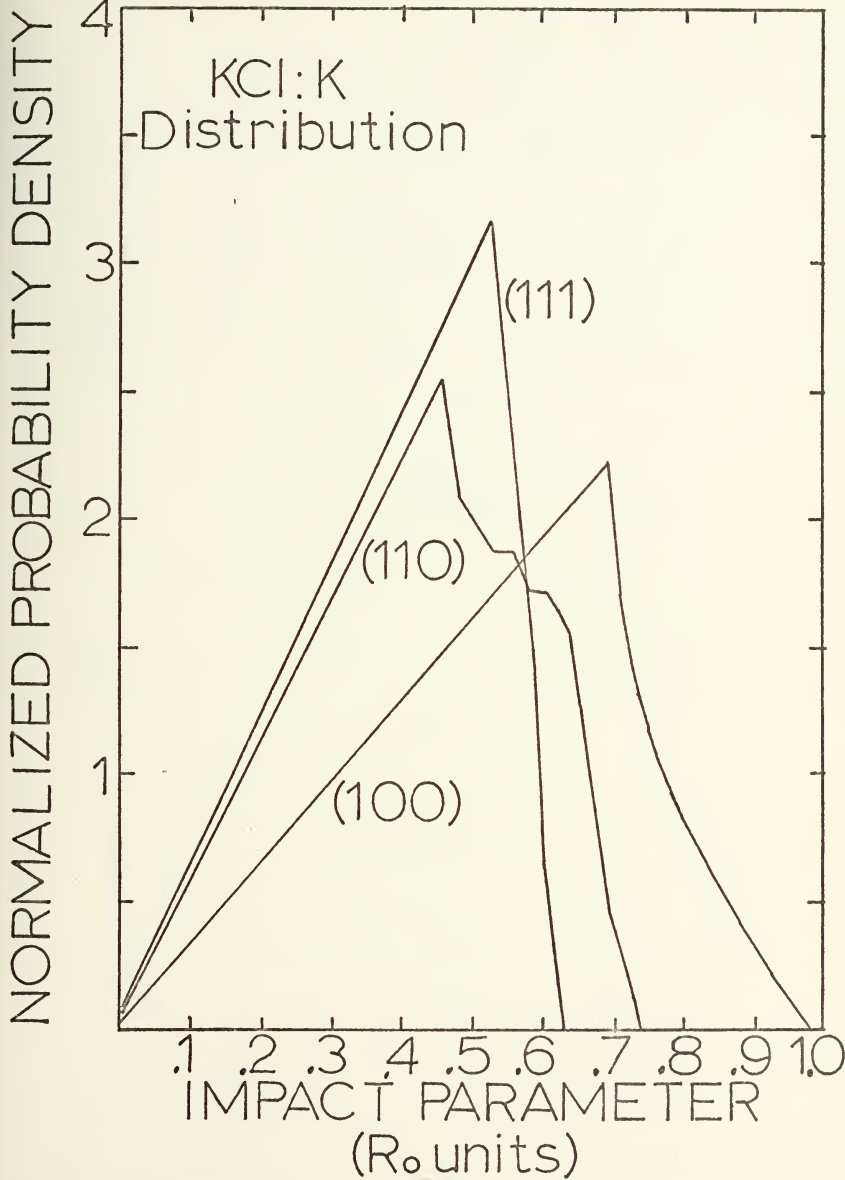


Figure 56. Potassium distribution of impact parameters in KCl.

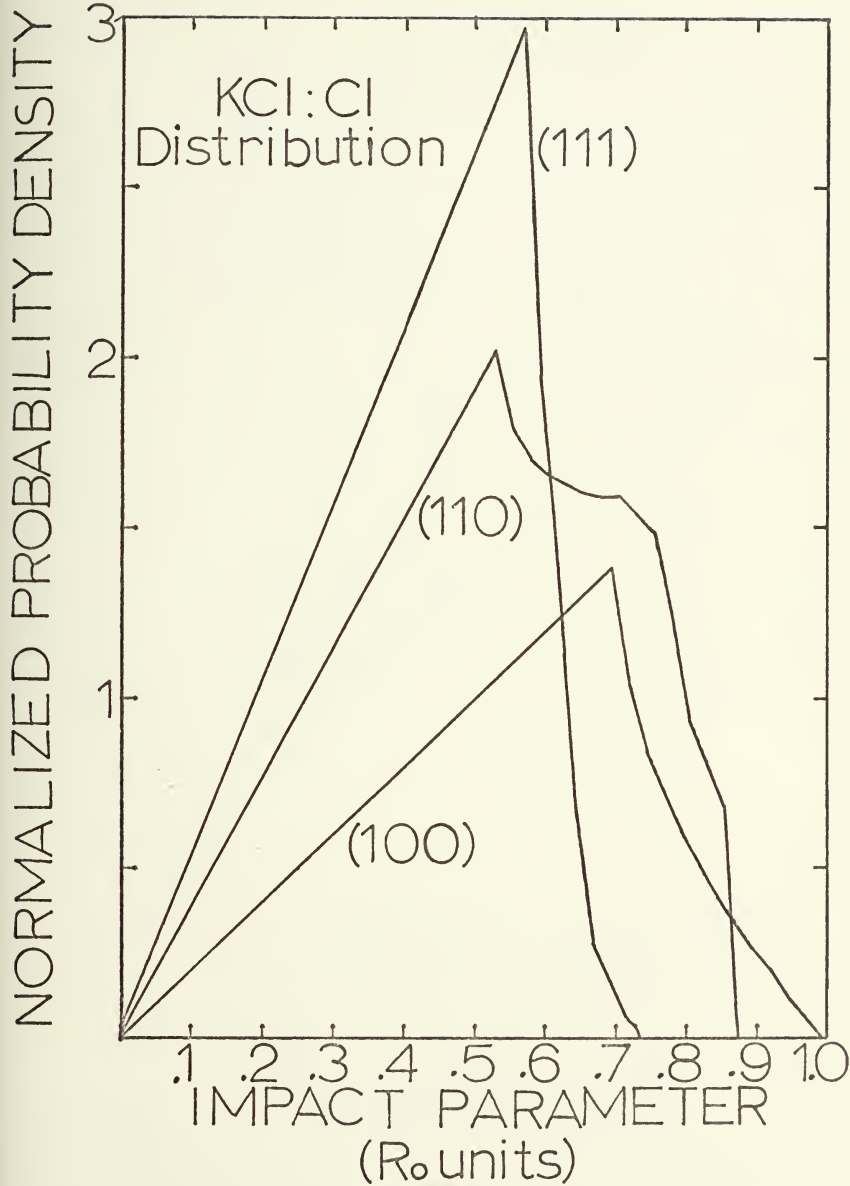


Figure 57. Chlorine distribution of impact parameters in KCl.

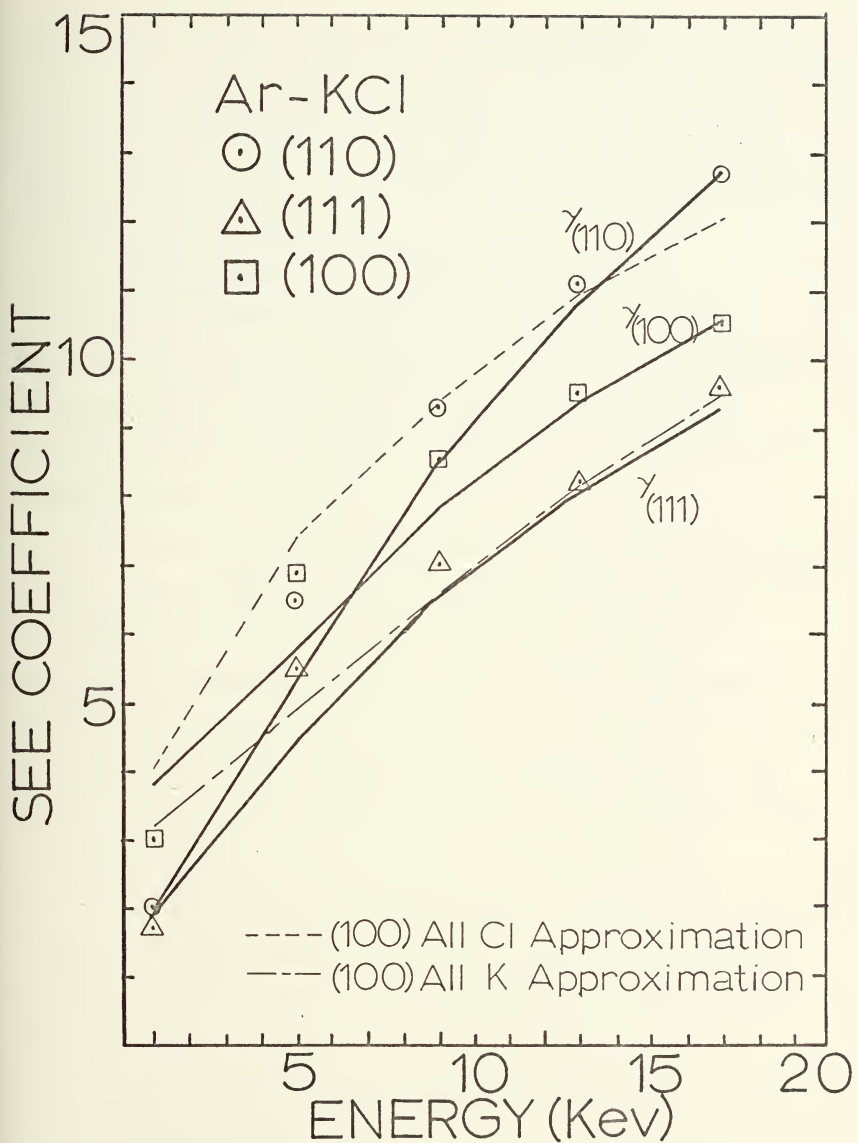


Figure 58. SEE coefficient as a function of energy for KCl bombarded by Ar ions.

coefficient for the (100) face crossed that of the (110) face in the five to six Kev region. This behavior, as well as that for the (111) and (110) faces, is predicted by the HCM modified model. A PSE contribution is evident but has not been investigated.

2. Potassium-Chloride Bombarded by Ne Ions

In the case of KC1 bombarded by Ne^+ , the HCM modified model predicts a crossing of the (100) and (110) surfaces' SEE coefficients as a function of energy at approximately five Kev. Such a behavior is not confirmed experimentally.

In an attempt to explain this anomaly, two theories arose. First, such a behavior can be explained, if the KC1 crystal tends to cleave on the (100) face with all the chlorine or potassium atoms up. Second, the crossing behavior might be due to preferential sputtering by the primary ion of one of the two types of atoms comprising the (100) face, leaving a surface that contains either all potassiums or all chlorines.

In the first case, the crystal structure of the (100) face should be the same for both Ar^+ and Ne^+ bombardment, as long as preferential sputtering does not occur. Hence, SEE from this face should be due to the bombardment of either pure chlorine or pure potassium, whichever is left in the "up" position.

In the second case, however, preferential sputtering of chlorine atoms by Ar^+ is the case most likely to occur,

since both the ion and target atom are of comparable mass. In this situation, preferential sputtering would affect the Ar^+ - KC1 system more than it would the Ne^+ - KC1 system. Since the Ar^+ - KC1 system's SEE coefficient as a function of energy is accurately predicted for all surfaces examined, it appears that sputtering is not directly responsible for the results that are obtained from either system.

The effect of an all-potassium or all-chlorine approximation to the KC1 (100) surface on the SEE coefficient as a function of energy and primary ion type is shown graphically in Figures 58 and 59.

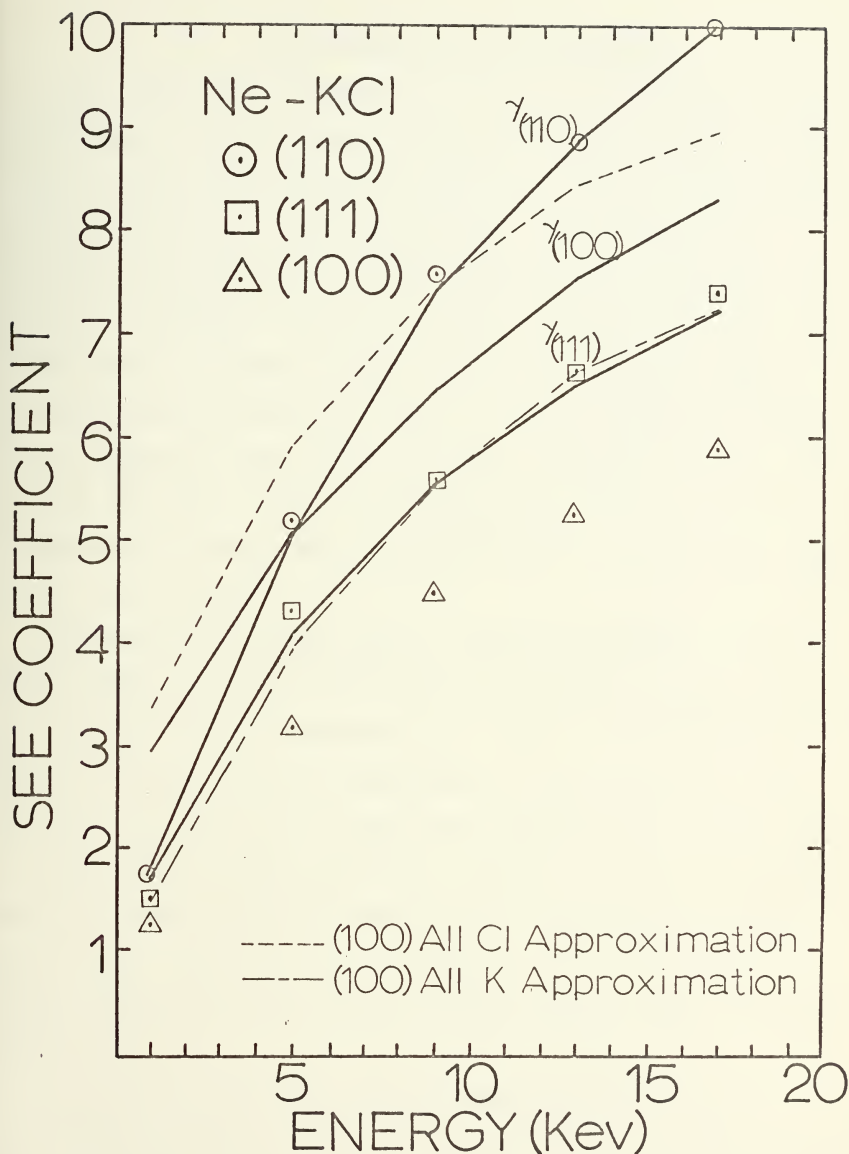


Figure 59. SEE coefficient as a function of energy for KCl bombarded by Ne^+ ions.

VIII. CONCLUSIONS AND RECOMMENDATIONS

This thesis has attempted to predict the behavior of the coefficient of ion electron emission for various primary ion-target combinations using the Harrison, Carlston and Magnuson theory of secondary electron emission. Three aspects of secondary electron emission were investigated, including angularly dependent secondary electron emission from the (100) face of a copper single crystal rotated about $\langle\bar{1}10\rangle$, secondary electron emission from Ar, Ne, Kr and Xe ions normally incident on the (100), (110) and (111) faces of Cu, Ag, Mo and Al single crystals, and secondary electron emission from Ar and Ne ions normally incident on the (100), (110) and (111) faces of KC1.

According to the HCM theory, angularly dependent results do not demonstrate the non-monotonic dependence on the angle of incidence found experimentally. Even so, the HCM theory does accurately model the dependence of the SEE coefficient of angle of incidence for inert gas ions normally incident on a polycrystalline metal surface. For this reason, it appears that the single collision model is not sophisticated enough and further modification must be made to it, if secondary electron emission from rotated, single-crystal faces is to be predicted.

In the case of metal targets bombarded by inert gas ions, it was found that the SEE coefficient as a function of energy, predicted by the modified HCM model, deviated from that experimentally obtained. This was contrasted with the results obtained using HCM's original model which yielded

reasonable results in almost all cases investigated. Since the modifications presented here were refinements to the original HCM model, it was hoped the results obtained would more accurately represent the secondary electron mechanism. For this reason, the difference between the SEE coefficient obtained here and the experimental result was identified as the potential secondary electron emission component operating at higher energies. Such a hypothesis is substantiated by experiment [1]. Analysis showed that the potential component in general rose to a peak and then decreased at higher energies. Furthermore, this component of secondary emission seemed to demonstrate behavior that could possibly be attributed to primary ion type as well as the face of the crystal being bombarded. The reason for this behavior was not positively identified, but the PSE process appears to be more complicated than was originally thought.

In the case of potassium-chloride bombarded by Ar ions, the HCM model fairly accurately predicted the SEE coefficient in the zero to 20 Kev energy range for all faces examined. On the other hand, potassium-chloride bombarded by Ne ions demonstrated a crossing of the SEE coefficient for the (100) and (110) faces as a function of energy which was not predicted experimentally. Two hypotheses were proposed that might possibly explain this behavior. The first hypothesis proposes that KCl cleaves with either all the potassium atoms or all the chlorine atoms up, essentially presenting a uniform layer of pure potassium or chlorine to the bombarding ion

beam. This hypothesis slightly improved the SEE coefficient for the Ne^+ KCl (100) surface, but adversely affected the results obtained for the Ar^+ - KCl system. The second hypothesis assumes that the (100) surface of KCl might demonstrate preferential sputtering. However, if this were the case, preferential sputtering should have been most evident in the Ar^+ - KCl system, because of the comparable mass of Ar and Cl. Since this system demonstrated the correct behavior without invoking the preferential sputtering assumption, it was surmised that preferential sputtering did not play an important role in the SEE process from the KCl (100) surface.

In all cases tested in the present investigation, the SEE coefficient as a function of energy tended to become a better approximation to the experimental results at higher energies. For this reason, it is recommended that primary ion-target atom combinations be run for primary ion energies between ten and 20 Kev. If in fact the potential component of secondary electron emission is real in this energy range, it should reach some constant value as primary ion energy is increased. Furthermore, because results obtained using the modified HCM model are dependent on the ion core configuration of the target atoms, it is recommended that more work be done in testing the influence of ion-target atom core ionization on secondary electron emission. Typically, for secondary electron emission from elements such as Cu and Ag, which appear in column I of the periodic table, the

ion core electron configuration is uniquely determined by considerations of the atomic valence, but the effect of the electronic structure of the ion core upon KSE for Mo and Al needs more investigation.

APPENDIX A
COMPUTER PROGRAMS

In this appendix, the parameters that appear in the computer programs are presented and explained. Variables that appear in the data input as constants are stated as such. A pictorial representation of how these data are entered into the programs is shown in Figures 12 - 16.

A. HERMAN SKILLMAN RADIAL ELECTRON DENSITY PROGRAM

CARD #	NAME	FORMAT	DESCRIPTION
1	HEADER CARD	- CONTAINS 80 CHARACTERS OF INFORMATION DESCRIBING THE CASE TO BE RUN	
2	KEY	(I4)	SEE Reference (), 0
2	TOL	(F8.6)	" , 000001
2	THRESH	(I4)	" , 521
2	MESH	(I4)	" , 1
2	IPRATT	(I4)	" , 40
2	MAXIT	(I4)	" , 0
2	NOCOPY	(I4)	" , 0
2	KUT	(I4)	" , 0
3-A*	RU2(I)	(IPE15.7, IP4E14.7)	Normalized self-consistent potential as a function of X. Taken directly from Reference 16. This is a "starter" for generating the wavefunctions for the atom under investigation.
B	Z	(F4.0)	Atomic number of atom in question
B	NCORES	(I4)	No. of shells of atom in question
B	NVALES	(I4)	0
B	ION	(I4)	Degree of ionization of atom in question
C	NNLZ(I)	(I4)	n,l,m quantum no. for shells
C	WWNL(I)	(F4.0)	No. electrons in shell
C	EE(I)	(F8.4)	Trial eigenvalue for each shell, taken from Reference 16.

B. POTENTIAL PROGRAM

CARD #	NAME	FORMAT	DESCRIPTION
1	INUC	(I2)	0
1	KSTEP	(I3)	10
1	AZ	(F3.0)	Atomic no. of the first atom following the header card below.
1	AI	(F2.0)	Ionization of the first atom following the header card.
1	BZ	(F3.0)	Atomic no. of the second atom following the header card.
1	BI	(F2.0)	Ionization of the second atom following the header card.
1	DM	(F2.0)	5
1	RM	(F2.0)	5
1	RTEST	(F2.0)	5
1	DD	(F5.1)	.020
1	FRR	(F5.1)	1.20
1	DRS	(F5.1)	.010
1	IPN	(I4)	1
2	HEADER CARD - CONTAINS 30 CHARACTERS OF INFORMATION DESCRIBING THE CASE TO BE RUN		
3	OUTPUT FROM ELECTRON DENSITY PROGRAM WITH FIRST CARD REMOVED CORRESPONDING TO THE ATOM DESCRIBED BY AZ AND AI ABOVE		
4	OUTPUT FROM ELECTRON DENSITY PROGRAM WITH FIRST CARD REMOVED CORRESPONDING TO THE ATOM DESCRIBED BY BZ AND BI ABOVE		

C. DISTRIBUTION OF IMPACT PARAMETERS PROGRAM

CARD #	NAME	FORMAT	DESCRIPTION
1	HEADER CARD -	80 CHARACTERS OF INFORMATION DESCRIBING THE CASE TO BE RUN	
2	ICODE	(I3)	1, if representative area is a rectangle 2, if representative area is a triangle
2	A	(F10.4)	Height of representative area in Ro units.
2	B	(F10.4)	Length of representative area in Ro units.
2	INUMBER	(I3)	No. of atoms in representative area.

C. DISTRIBUTION OF IMPACT PARAMETERS PROGRAM (Continued)

CARD #	NAME	FORMAT	DESCRIPTION
3	LARGE(I)	(I2)	Logical array that indicates if any particular atom is larger than the other, i.e., Cl in KC1. 1, yes. 2, no. If yes the distribution is skewed to indicate preferential collision with the larger atom.
4	SCALEF	(F10.4)	1.0
4	RNA	(F10.4)	Ionic radius of smaller of two atoms.
4	RCL	(F10.4)	Ionic radius of larger of two atoms--Both RNA and RCL can be set to anything if atoms are both the same size.
5-7	A5(I,J)	(3F10.4)	An array that contains the (x,y) vertices of a triangular representative area in Ro units. If the area is not triangular, they can be set to anything.
8-11	A6(I,J)	(3F10.4)	An array that contains the (x,y,z) position of atoms in the representative area in Ro units. I runs from 1 to INUMBR, J runs from 1 to 3.
12	PHI	(F10.4)	Angle in radians x'-axis makes with x-axis.
12	XR	(F10.4)	(x) position of (x',y') origin.
12	YR	(F10.4)	(y) position of (x',y') origin.
12	ALPHA	(F10.4)	Angle in radians the representative area is rotated through.
12	RMAX	(F10.4)	Maximum impact parameter expected. The no. 250 is usually sufficient.

D. NUMERICAL INTERPOLATION PROGRAM

CARD #	NAME	FORMAT	DESCRIPTION
1	NPOINT	(I4)	No. points from the distribution of impact parameters program to be smoothed.
1	IFLAG	(I4)	1, indicates written output only. 2, indicates written output, card output and graphical output desired.
2	HEADER CARD - 46 CHARACTERS TO BE OUTPUT WITH GRAPHS		
3	HEADER CARD - 46 CHARACTERS TO BE OUTPUT WITH GRAPHS		
4	OUTPUT FROM DISTRIBUTION OF IMPACT PARAMETERS PROGRAM WITH ALL "NEW ATOM" CARDS REMOVED		

E. KSE PROGRAM

CARD #	NAME	FORMAT	DESCRIPTION
1	LCRYST	(A4)	Crystal type "FCC"/"BCC"
1	LTPE	(I2)	1
1	BMAX(I)	(3F6.4)	Maximum impact parameter in Ro units for each face.
1	PUD(I)	(3F6.4)	R _A for each face in Ro units.
1	ARO(I)	(3F6.4)	No. atoms per representative area in Ro units, for each face.
1	LM(I)	(313)	Total number of points in each distribution.
1	KM	(I4)	250
1	FACL	(F7.4)	(2) ^{1/2} /4 for FCC, (3) ^{1/2} /4 for BCC.
2-A	FLP(I)	(20I4)	Distribution of impact parameters from Interpolation Program.
B	IH1	80A1	80 characters of information.
C	IH3	19A4	76 characters of information from first card of output from Potential Program.
C	KMR	(I4)	250
D	APSI(I)	10F8.5	Wave functions from the Potential program, Atom A.
D	BPSI(I)	10F8.5	Wave functions from the Potential program, Atom B.

E. KSE PROGRAM (Continued)

CARD #	NAME	FORMAT	DESCRIPTION
E	V(I)	5F12.5	Potential between atoms A and B from the Potential Program.
F	EA(I)	8F8.4	Spectroscopic ionization potentials, numbers 11 to 18.
F+1	IAH	4A4	16 characters of accounting information.
F+1	EA(I)	10F8.4	Spectroscopic ionization potentials, numbers 1 to 10.
F+2	JFIT	I10	No. of values to which results are fit.
G	PSE(I)	(F5.3)	γ_{PSE} experimental for curve being fit.
G	FIT(J)	(F5.4)	γ experimental for (111) face at 10 Kev.
H	ZB	F4.0	Atomic no. for atom A.
H	ZT	F4.0	Atomic No. for atom B.
H	BMAS	F8.4	Atomic weight for atom A.
H	TMAS	F8.4	Atomic weight for atom B.
H	EOS	F8.0	Energy in Kev at which results are to start.
H	DEO	F3.0	Energy step in Kev.
H	KEOM	F3.0	Energy in Kev at which results are to end.
H	AO	F7.3	Lattice constant in angstroms.
H	LSKIP	I3	1
H	NM	I3	15
H	RES	F3.0	50
H	DRE	F3.0	50
H	REM	F5.0	5000
H	IH2	4A4	Accounting data.

*indicates that the actual card number varies from run to run and has been replaced by a letter to indicate the order in which the cards are arranged.

/// EXEC.FORTCLG REGION .GO=150K

CC HARTREE-FOCK-SLATER SELF-CONSISTENT ATOMIC FIELD PROGRAM
CC ORIGINALLY WRITTEN BY SHERWOOD SKILLMAN
CC RCA LABORATORIES, PRINCETON NEW JERSEY, SPRING 1961
CC MODIFIED BY FRANK HERMAN, SUMMER 1961
CC FURTHER MODIFIED BY RICHARD KORTUM, LOCKHEED RESEARCH
CC LABORATORIES, PALO ALTO, CALIFORNIA, SUMMER 1962
CC THE PRESENT FORM WAS WRITTEN BY D.E. HARRISON, JR. FOR
CC USE ON THE IBM/360 AT THE NAVAL POSTGRADUATE SCHOOL,
CC MONTEREY, CA. 93940

COMMON/COM1/V(521),R(521),RU(521),RU2(521),RU3(521),X(521),
2 XI(521),XJ(521),RSCORE(521),RSATCM(521),RSVAL(521),
3 XJNL(521),XJNL2(521),RUFNL(521),RUFNL2(521),RLEXCH(521),
4 XNUM(521),DENM(521),SNLD(521),GG(521),RR(521),
5 NNLZ(24),NNNL(24),NKKK(24),EE(24),A(4,5),SNL(24,521)
START=0.01*ITIME(XX),
DC 5500 1=1,521
V(1)=0.0
R(1)=0.0
RU(1)=0.0
RU2(1)=0.0
RU3(1)=0.0
X(1)=0.0
RR(1)=0.0
XJ(1)=0.0
RSCLCR(1)=0.0
RSATUM(1)=0.0
RSVAL(1)=0.0
XJNL(1)=0.0
XJNL2(1)=0.0
RUFNL(1)=0.0
RUFNL2(1)=0.0
RLEXCH(1)=0.0
XNUM(1)=0.0
DENM(1)=0.0
SNLD(1)=0.0
GG(1)=0.0
DC 9510 1=1,24
NNLZ(1)=0.0
NNNL(1)=0.0
NKKK(1)=0.0
EE(1)=0.0
9510 FFORMAT(72H
9000 1)


```

901C F C R M A T ( F 8 . 5 , 9 F 7 . 5 )
902C F C R M A T ( I 4 , 1 P 3 E 1 4 . 7 , I 4 , 1 P E 1 4 . 7 )
903C F C R M A T ( F 4 . 0 , 3 1 4 )
904C F C R M A T ( F 8 . 8 )
905C F C R M A T ( 6 H , N W W = F 4 . 0 , 6 H , Z Z Z = F 4 . 0 , 6 H , N C O R E S = I 4 ,
11H , N C S P V S = I 4 / 2 5 H , C O N T R O L C A R D S I N C O R R E C T . ) )
906C F C R M A T ( I 4 , N F 5 . 2 , F 1 0 . 3 )
907C F C R M A T ( I 4 , F 4 . 0 , F 3 . 4 )
908C F C R M A T ( I 7 , F 7 . 0 , 1 P E 1 4 . 7 , O P 2 ( I 6 , F 9 . 3 ) )
909C F C R M A T ( C , I 5 5 , 1 P E 1 4 . 7 )
910C F C R M A T ( 1 P E 1 5 . 7 , 1 P 4 E 1 4 . 7 )
911C F C R M A T ( I 0 H , N C A R D S = I 4 , 1 0 H , M C A R C S = I 4 . )
912C F C R M A T ( I 4 , 2 F 8 . 6 , 5 1 4 )
913C F C R M A T ( 2 F 4 . 0 , 2 F 7 . 3 )
914C F C R M A T ( 6 H , Z Z I = F 4 . 0 , 3 H , Z Z Z = F 4 . 0 , 1 0 H , B E T A I = F 7 . 3 ,
1 1 0 H , B E T A Z = F 7 . 3 )
915C F C R M A T ( 7 H , K E Y = I 4 )
916C F C R M A T ( 6 H , I T E R , 7 X , 1 H Z , 4 X 5 H D E L A , 7 X , 3 0 H I ( C E L ) I ( C U T ) X
1 ( C U T ) )
917C F C R M A T ( I 4 , 1 P 3 E 1 4 . 7 , I 4 , 1 P E 1 4 . 7 , 8 X , 1 H Z , I 3 , I 4 )
918C F C R M A T ( F 4 . C , 3 1 4 , 5 6 X , 1 H Z , I 3 , I 4 )
919C F C R M A T ( 1 P E 1 5 . 7 , 1 P 4 E 1 4 . 7 , 1 X , 1 H Z , I 3 , I 4 )
920C F C R M A T ( 1 P E 1 5 . 7 , 1 P 4 E 1 4 . 7 , 1 X , 1 H Z , I 3 , I 4 )
921C F C R M A T ( 7 H , S T A R T I N G P O I N T I N S A N D Z = F 4 . 0 , 9 H , I N E R R O R ) { 2 F 4 . 0 )
922C F C R M A T ( 4 0 H L I , X , R U 3 , R U I N 1 , R U F N L 1 , R U I N L 2 , R U F N L 2 , R U
923C F C R M A T ( I 8 , F 1 0 . 4 , 1 P 6 E 1 6 . 7 )
N F I L E S = 0
10 R E A D ( 5 , 9 0 0 0 0 )
R E A D ( 5 , 9 1 2 0 ) K E Y , T O L , T H R E S H , M E S H , I P R A T T , M A X I T , N O C O P Y , K U T
N C A R D S = 9 0
W R I T E ( 6 , 9 1 5 0 ) K E Y
I F ( M A X I T ) 2 0 , 2 0 , 3 0
M A X I T = 2 0
3 C N B L C C K = M E S H / 4 0
I X ( I ) = 1
I X ( I ) = 0 . 0
R ( I ) = 0 . 0
D E L T A X = 0 . 0 0 2 5
T H I R D = 1 . 0 / 3 . 0
R 6 = 1 . C / E . 0
R 2 4 = 1 . 0 / 2 4 . 0
R 3 2 = 1 . 0 / 3 2 . 0
R 2 1 5 = 1 . C / 3 1 5 . 8 2 2 7 3 4
C C 4 0 J = 1 , N B L C C K
C C 3 5 K = 1 , 4 0
I = 1 + 1
3 5 X ( I ) = X ( I - 1 ) + D E L T A X

```



```

40  DELTAX=DELTAX+DELTAX
41  IF(KEY=1) 60,70,50
50  READ(5,9100) (RU2(M),M=1,441)
51  READ(5,9100) (RU3(M),M=1,441)
52  ZE2=-0.5*RU2(1)
53  ZE3=-0.5*RU3(1)
54  GC TO 100 (RU2(M),M=1,437,4)
55  GC TO 100 (RU3(M),M=1,437)
56  READ(5,9100) (RU2(M),M=1,441)
57  READ(5,9100) (RU3(M),M=1,441)
58  ZE2=-0.5*RU2(1)
59  ZE3=-0.5*RU3(1)
60  READ(5,9030) Z,NCORES,NVALES,ION
61  IF(Z) 999910,110
62  NFILES=NFILES+1
63  IZ=2
64  TZ=Z+Z
65  NCSPVS=NCORES+NVALES
66  C=0.8853438/Z**THIRD
67  TWCICN=ICN+ICN
68  ZZ=10N+1
69  TWCIZZ=ZZZ+ZZZ
70  DC 140 I=2,MESH
71  K(1)=C*X(1)
72  K(1)=1.0/R(1)
73  READ(5,9070) (NNLZ(I),WNLN(I),EE(I),I=1,NCSPVS)
74  WNWDO
75  DC 120 I=1,NCSPVS
76  DC 120 I=1,NCSPVS
77  WNW=WNW+WNLN(I)
78  IF(ABS(Z+1.0-WNW-ZZZ)-0.001) 150,140,140
79  GC TO 9595 WRITE(6,9050) WNW,ZZZ,Z,NCORES,NVALES,NCSPVS
80  GC TO 9595 IF(KEY=1) 300,400,200
81  GC TO 9999 IF(ABS(ZE2-ZE3)-0.001) 220,220,210
82  GC TO 9999 WRITE(6,9210) Z,ZE2,ZE3
83  DC 250 I=1,441
84  DC 250 I=RU3(1)+RU3(1)-RU2(1)
85  GC TO 500
86  TWCIZ=TZ
87  DC 340 I=1,437,4
88  RU(1)=-RU2(1)*TWCZ
89  RU(441)=RU(437)
90  RU(445)=RU(437)
91  M=5
92  DC 350 I=1,437,4
93  M=M-1
94  IF(M) 320,330,330
95  RU(I+1)=(22.0*RU(I)+11.0*RU(I+4))-RU(I+8))*R32

```



```

RL(I+2)={10.0*RU(I)+15.0*RU(I+4)-RU(I+8)}*R24
RL(I+3)={ 6.0*RU(I)+27.0*RU(I+4)-RU(I+8)}*R32
N=9
GC TO 350
GC TO 350
330 RU(I+1)={(2.1-0*RU(I)+14.0*RU(I+4)-3.0*RU(I+8))*R32
RU(I+2)={( 3.0*RU(I)+ 6.0*RU(I+4)-RU(I+8))*R8
RU(I+3)={( 5.0*RU(I)+30.0*RU(I+4)-3.0*RU(I+8))*R32
350 CONTINUE
GL TO 500
400 IF(ABS(ZE3-Z)-0.001) 410,410,430
410 DC 420 I=1,441
420 RL(I)=RU3(I)
421 GC TO 500
422 2CZ=Z/ZE3
423 CC 440 I=1,441
440 RU(I)=RU3(I)*Z0Z
441 V(I)=-5.9E35
N=FINO(441,MESH)
IF(KUT) 600,700,600
600 UC 610 I=1,M
610 V(I)=RU(I)*KR(I)
611 LF(NESH-M) 620,620
620 DC 620 C=442,MESH
621 V(I)=-TWO1CN*RK(I)
622 C LIMIT=M
ICLU=MESH
ICL=MESH
GC TO 900
700 ICUT=0
GC 750 I=2,M
710 IF((ICUT=710,710,730
720 ICL=1
721 V(I)=-TWOZZZ*RR(I)
730 V(I)=750
740 V(I)=RU(I)*RR(I)
750 CONTINUE
751 IF((ICUT) 790,790,800
752 ICL=1
753 LIMIT=ICUT
754 IF(NESH-M) 800,900,810
810 DC 850 I=442,MESH
850 V(I)=-TWOZZZ*RK(I)
851 CELTA=10000000.
852 NITER=0
NINM=2
IFRSW=0
WRITE(6,9160)

```



```

100C NCARDS=SC
110C IF(MAXIT-NITER) 110C,200C,2000
110C WRITE(6,9220)
110C CC15C0 I=1,5,WE$H,5
110C WRITE(6,9230) I,X(I),RU3(I),RU1NL(I),RUFNL(I),
110C 1,RUINL(I),RU(I),
110C CCNTINUE
110C CC TO 100
120C DC 2010 I=1,MESH
120C R$C$CRE(I)=C*0
120C R$VAL(E(I))=0.0
120C DC 2500 I=1,NCSPV$S
120C E=EE(M)
120C NN NN Z(M)/100
120C LAW =NNLZ(M)/10 -10*NN
120C XL= LAW
120C CALL LS$CSEQ(Z,E,LAM,NN,KKK,MESH,C,THRESH)
120C IF(M-NC$CRES) 210C,210C,220C
120C DC 2150 I=1,KKK
120C SNL(N,I)=SNL(I)
120C R$C$CRE(I)=R$C$CRE(I)+W$NL(M)*SNL(I)*SNL(I)
120C CC TO 2300
120C DC 2450 I=1,KKK
120C SNL(M,I)=SNL(I)
120C R$VAL(E(I))=RSVAL(E(I)+W$NL(M)*SNL(I)*SNL(I)
120C KKKK(M)=KKK
120C NCARDS=NCARDS+2*((KKK-1)/40)*8
120C EE(E)=E
120C CC 2600 I=1,WE$H
120C RSATOM(I)=R$C$CRE(I)+RSVAL(E(I)
120C RUEACH(I)= -6.0*(3.0*R(I)*RSATOM(I)*R315)*THIRD
120C 2600 AL=C*0
120C ASUM=0. C
120C E1=0.0
120C B$UM=0. C
120C F=C*0.025*C
120C I=1
120C XI(I)=0.0
120C XJ(I)=0.0
120C CC 2620 J=1,NBLOCK
120C DC 2610 K=1,40
120C I=I+1
120C A2=RSATC(I)*0.5
120C A1=A1+A2
120C E2=A2**RR(I)
120C E1=E1+B2
120C X1(I)=ASUM+A1*H
120C XJ(I)=B$UM+B1*H

```



```

A1=A1+A2
B1=B1+B2
A1=A2
B1=0
2610 F=F+H
DC 2650 I=1,MESH
XJ(I)=XJ(I)+R(I)*(XJ(MESH)-XJ(I))
XJ(I)=XJ(I)+RUEXCH(I)
2650 GCONTINUE
DC 2700 I=1,MESH
RUINL1(I)=RUINL2(I)
RUFNL1(I)=RUFNL2(I)
RUINL2(I)=RU(I)
RUFNL2(I)=XJ(I)
NCFEKN=NCFEKT+1
PCELTA=PCELTA
PCELTA=0
DC 2800 I=1,LIMIT
SNL(I)=BS(SNL(I)-XJ(I))
XJ(I)=ABS(SNL(I))
IF((XJ(I)-DELT A)>2800,2800,2750
2750 DELTA=XJ(I)
IDELTA=I
2800 GCONTINUE
WHITE(9,9080) NITER,Z,DELTA,X(IDELTA),ICUT,X(ICUT)
IF(DELTA-TCL)<0.0003000
3000 DC 3110 I=2,LIMIT
3110 R(I)=0.5*(RU(I)+XJ(I))
IF((MESH-LIMIT)<3140,3140,3120
3120 RUZM=XJ(MESH)
RATIO=(RUZM-RU(LIMIT))/(RUZM-XJ(LIMIT))
3130 DC 3130 I=LIMIT,MESH
RU(I)=RUZM-RATIO*(RUZM-XJ(I))
LIMIT=MESH
3140 PRSW=IPRATT
GC TO 3500
3150 IF(NGNM(N)=3100,3100,3160
3160 IF(PDELTA-DELTA)<3170,3170,3200
3170 NENM(N)=NENM(N-1)
IF(NENM(N)=3100,3100,3200
3200 ALPH=0.5
DC 3200 I=2,ICUT
XNUM(I)=RUINL1(I)*RUFNL2(I)-RUINL2(I)*RUFNL1(I)
DENM(I)=RUFNL2(I)-RUFNL1(I)-RUINL2(I)+RUINL1(I)
IF(ABS(DENM(I)/RUFNL2(I))<0.0001) 3210,3210,3220

```



```

321C ALPH=0.5
322C GC TU 3260
3220 ALPH=(XNUM(I)/DENNM(I)-RUFNL2(I))/SNL0(I)
3230 IF(ALPH) 3230,3260,324C
3230 ALPH=0.0
324C GC TU 3260
3240 IF(0.5-ALPH) 3250,3260,3260
3250 ALPH=0.5
325C X1(I)=ALPH
326C X1(I)=ALPH
327C IFRSN=IFRSW-1
3270 IFFKUT,3340,3310,3340
328C IC=ICUT+20
329C ADEL=0. C5*X1(ICUT)
3290 IC=IC1,IC
330C X1(I)=X1(I-1)-ADEL
331C XJ(I)=U5
332C XJ(I)=U2
333C ASUM=X1(2)+X1(3)+X1(4)+X1(5)
334C DC 3350 U=3,ICUT
3350 ASUM=ASUM*0.2
3350 ASUM=ASUM-X1(I-2)+X1(I+3)
336C IFFKUT,3360,3360,3380
3360 IC=IC1+1
337C DC 3370 I=IC1, MESH
3370 XJ(I)=U0
338C RL(I)=RUFNL2(I)
3380 DC 3390 I=2,IC
339C RL(I)=RUFNL2(I)+XJ(I)*SNL0(I)
3390 DC 3600,3700,3600
340C LIMIT=MESH
3400 DC 3650 I=2, MESH
341C VLAST=V(I)
342C V(I)=RU(I)*RR(I)
343C X1(I)=V(I)-VLAST
344C GC TU 3500
345C ICUT=0
346C DC 3550 I=2, MESH
347C VLAST=V(I)
348C IF(ICUT) 3840,3860,3860
3480 IF(TwoZ2+RU(I)) 3880,3880,3880
349C ICUT=1
350C V(I)=-TWOZ2/R(I)
351C GC TU 3890
352C V(I)=RU(I)*RK(I)

```



```

3890 X1(I)=V(I)-VLAST
3900 X1(I)=0.0
NCARDS=50
CC 3990 P=1,NCSPVS
K=6NKKK(M)-1)/40
L=OC*U02L*C
PH=0.5*H
ASUM=0.0
A1=0.0
I=1
DC 3960 J=1,K
DC 3940 L=1,40
I=I+1
A2=X1(I)*SNL(M,I)*SNL(M,I)
A2=A1+A2*H
ASUM=ASUM+A1-A2*HH
F=F+F
F=F+F
F=F+F
A1=HH*A2
EE(M)=EE(M)+ASUM
NCARDS=NCARDS+G*K+2
GOTO 1G0D10 NCARDS,MCARDS
4000 WRITE(9,9110) NCARDS,MCARDS
NCAL=1
WRITE(6,5180) Z, NCERES, NVALES, ICN, IZ, NC
CC 4190 I=1,441
1F(7,9101) 4190, 4190, 4120
DC 4140 M=1,441
RUINL2(M)=TWOION
4140 CCNTU4200
419C CCNTINUE
4200 DC 422U MIN=1,440,5
MAX=MN+4
NC=NC+1
WRITE(6,9190)(RUINL2(M),M=MIN,MAX),IZ,NC
4220 WRITE(7,5910) Z, ICN
FORMAT(F10.1) 15
4230 WRITE(6,9960) RSATCM(I), I=1,441
FLRAT(5E15.7)
4240 NC=NC+1
WRITE(6,9200) RUINL2(441),IZ,NC
CC 4400 N=1,NCSPVS
NL2=NNL2(M)
KKK=NKKK(M)
XL=NLZ/10-10*(NLZ/100)
XL=XL+1.0
CC 4450 I=1,44

```



```

DE=0.0
APRINT=C
LAMY=LAM-1
LAMP=LAM+1
XLP=LAMP
ACCR=NN-LAMP
E=LAM*(2)
CC=CC
H=CC
HSC=H*H
B3=(V(3)-V(2))/H-Z/HSQ
Y=I+H
FLES=4*LAM+6
SLPT=6*LAM+12
ELPT=8*LAM+20
A1=-Z/XLP
YSG=Y*Y
E1=-Z-Z
E2=A1*E1
E3=A1*E2
C
RAISE H AND Y TO LAM+1
FTL=H
YTL=Y
IF(LAM) 105,120,100
105
NSTCP=105
GCC10 9900
1CC
DC 110 I=1,LAM
FTL=FTL*H
110 YTL=YTL*Y
120 H1=HSQ
ECS=B1/HSQ
ECP=B1/P
BTH=b2*B
B63=BOK*S+BTH
B64=0.25*BCHS+0.50*BOH+BTH+BTH
BPL=8*LAM
FPL=5*LAM
XIFC=C*21701389E-4
C
START OUTWARD INTEGRATION
SEGMENT
200 APRINT=NPRINT+1
EPS=E-EG
EC=E
IF(MANY-APRINT) 9920,210,210
DC 220 I=1,MESH
220 SNL(I)=0.0
225 IF(APRINT=225) 225,300,400
225 NSTCP=225

```



```

GC TO 9900
DC 310 1=4,MESH
311 C(1)=V(1)+B*RR(1)*RR(1)-E
N=MESH
DC 330 1=4,MESH
1F(GQ(M)) 320,330,330
1K=N+1
GL TC 350
N=N-1
C IS EVERYWHERE POSITIVE
AS TCP=350
GC TO 9900
350 IF(MESH-IK) 360,360,430
EFS = G(MESH-40)
EE = E+EPS
DC 420 1=4,MESH
420 GC(1) = GQ(1)-EPS
GC TO 315
ACROSS=0
SIGN=1.0
F=CC
Y=F+H
B2=5.0*Z/H-E+2.0*v(2)-V(3)
A2=(AB1+B2)/FLPS
A3=(A2*B1+A1*B2+B3)/SLPT
A4=(A3*B1+A2*B2+B4)/ELPT
P(2)=(1.0+Y*(AI+H*(A2+H*(A3+H*A4))))*HTL
P(4)=(1.0+Y*(AI+Y*(A2+Y*(A3+Y*A4))))*YTL
G(3)=BQ3+B2
G(4)=BQ4+B2
SLU(2)=P(2)
SLU(3)=P(4)
I=3
DCX=0C
H4=H**2
T<=T1/12*C
T(3)=P(3)*(1.0-H2*G(3))
T(4)=P(4)*(1.0-H2*Q(4))
L((4)=T(4)-T(3)
NCOUNT=3
NIN=2
440 I=1+1
C 1F END CF MESH IS REACHED, MODIFY TRIAL EIGENVALUE
450 1F(1-MESH) 460,450,400
C RETURN TO BEGINNING CF CUTWARD INTEGRATION IF NECESSARY
460 G(5)=Q(1) 700,700,500
1F(IK-1) 700,700,500

```



```

5CC D(5)=D(4)+H1*Q(4)*P(4)
T(5)=D(5)+T(4)
IF(1.0-ABS(H2*Q(5)))>450,450,540
54C P(5)=T(5)/(1.0-H2*Q(5))
SNLC(I)=P(5)
IF(SIGN)=P(5)
NSTCP=545
GCC TO 9900
IF(P(5))580,580,570
IF(P(5))570,580,580
57C NCROSS=NCROSS+1
C COUNT CHANGES IN SIGN
SIGN=SIGN
ACCOUNT=ACCOUNT+1
IF(7-ACCOUNT)535,590,600
585 NSTCP=585
GCC TO 9900
59C ACCOUNT=2
NINT=NINT+1
6CC NINT=40-NINT
IF(40-NINT)605,610,620
6C5 NSTCP=65
GCC TO 9900
DX=DX+DX
61C DX=DX
h=DX
r1=r/*2
r2=h1/12.0
NINT=0
T(5)=P(5)*(1.0-H2*Q(5))
T(3)=P(3)*(1.0-H2*Q(3))
D(5)=T(5)-T(3)
620 D(5)=P(5)-T(4)
P(K)=P(K+1)
T(K)=T(K+1)
D(K)=D(K+1)
65C Q(K)=Q(K+1)
GL TO 44C
70C IF(ACCOUNT>2)705,710,500
7C5 NSTOP=7C5
GCC TO 9900
IF(NINT=4)500,500,720
C WATCHING RADIUS HAS BEEN REACHED GCING CUT
C IF INDIR NOT EQUAL TO NCROSS, MODIFY TRIAL EIGENVALUE
72C EIGENVE
IF(INDIR-NCROSS)800,1000,900
800 NCROSS=1
C TCC MANY CROSSINGS, INCREASE ABS(F(E))
IF(MOREV>1)805,830,820

```



```

805 NSTCP=805
820 GC TO 9900
820 1F( E - E*CRE ) 830,840,840
820 ENCRE= E
820 IF (LESS) 845,860,990
845 NSTCP=845
845 GC TO 9900
860 E=1.*25*EG
860 GC TO 200
900 LESS=1
900 TCCS FEW CROSSINGS, DECREASE ABSF(E)
900 LESSV=LESSV+1
900 IF(LESSV-1) 905,920,910
925 NSTCP=925
925 GC TO 3500
925 1F(LESS- E) 920,930,930
930 1F(MORE) 935,950,950
935 NSTCP=935
935 GC TO 9500
950 E=0.75*EG
950 GC TO 200
990 E=C.5*(EMORE+ELLESS)
990 GC TO 4000
990 IF(ABS(SNL((I-1))-AES(SNL((I-2))) 1010,1040,1040
C CHECK THAT SEE THAT WAVE IS IN THE DAMPED REGION (ABSOLUTE VALUE
C INCREASING AND SIGNS ALIKE)
1010 1F(P((5)) 1020,1000,1C30
1020 1F(SNL((I-2)) 1020,1000,1C30
1030 1F(SNL((I-2)) 1030,1000,1C30
1040 IF((1.0E+25 -ABS(P((5))) 1900,900,500
C LARGE ABSOLUTE VALUE OF P IN WHAT SHOULD BE THE DAMPED REGION
C INDICATES TWO FEW PEAKS, DECREASE ABSF(E)
C NEWNDCK = NCROSS AND MATCHING RADIUS LIES IN DAMPED REGION
110C NEWATCH=I-2
110C XWATCH=R((I-2))
110C PFCUT=(T((4)-T((2))-0.5*(P(4)-P(2)))/H
110C S2=PPCUT/P(3)
C INTEGRATION IS BY 8 APPLICATIONS OF NEWTON-COTES CLOSED
C QUADRATURE FOR FIVE INTERVALS IN EACH BLOCK
C XIFC=(5*H(BLOCK 1)/288)/2 ,H(1)=0.0025*SCALE FACTOR
C SUMI=0.0
C XIF=XIFC
1=1
1 VALUE=0.0
1 NY=6
1 SUM2=0.0
1 XIF=XIF+XIF
111C

```



```

112C Y=VALUE
      VALUE=SNL0(I+5)*2
      SNL2=SUM2+19.0*(SNL0(I+2)**2+SNL0(I+3)**2)
      1 +50.0*(SNL0(I+2)**2+SNL0(I+3)**2)
      I=I+5
      IF(1MATCHb-1) 1125,1150,1130
      NSTOP=1125
      GC TO 9900
      NY=NM-1
      IF(NM)1135,1140,1120
      NSTOP=1135
      GC TO 9900
      SY=SUM2*XIF+SUM1
      GL TO 1110
      SUM1=SUM1+SUM2*XIF
      SI=SUM1/P(2)**2
      PWT=PATCH=P(3)
      IF(NN-1)1165,1170,1180
      NSTOP=1165
      GL TO 9900
      XINW=EP1*XMATCH
      C FLRN=1, START INWARD INTEGRATION AT(8+LAM)*XMATCH CR X MAX
      GC TC 1200
      XINW=EP1*XMATCH
      C FLRN,NLT=1, START AT (5+LAM)*XMATCH OR X MAX (END CF MESH
      CC 1220,I=41, MESH,40
      IF(XINW-(I-1))121C,1210,1220
      KKK=I
      121C
      GC TO 1250
      KKK=MESH
      I=KKK
      DX =K(I-1)-K(I)
      F =DX
      XIF=U*1.7361111E-1*Dx
      FSC=H*H
      FSC12=HSQ/12.0
      G(3)=Q(1)
      P(3)=EXP(-R(1)*SQRT(Q(3)))
      126C
      1=1-1
      G(4)=GC(1)
      P(4)=EXP(-R(1)*SQRT(Q(4)))
      127C
      1F(ABS(P(4))-1.0E-35)1280,1280,1300
      KKK=KKK-4C
      1F(KKK-IMATCH)1290,1290,1250
      128C
      WRITE(6,5030)Z,NN,LAM,KKK
      P(3)=1.0E-35
      KKK=KKK+40

```


$P(4) = 1.5E-35$
 $1300 \text{ IF}(PMATCH) 1310, 1305, 1320$
 $1305 \text{ NSCP}=1355$
 $GC\ TO\ 9500$
 $1310 \text{ F}(3)=-P(3)$
 $P(4)=-P(4)$
 $1320 \text{ SNL}(1+1)=P(3)$
 $SNL(1)=P(4)$
 $T(3)=P(3)*\{1.0-HSQ12*\zeta(3)\}$
 $T(4)=P(4)*\{1.0-HSQ12*Q(4)\}$
 $DL(4)=T(4)-T(3)$
 $DL(1350)=T(3)$
 $M=2,40$
 $I=I-1$
 $\zeta(5)=\zeta(1)$
 $\zeta(5)=HSQ*\zeta(4)*P(4)+D(4)$
 $T(5)=D(5)+T(4)$
 $P(5)=T(5)/(1.0-HSQ12*\zeta(5))$
 $IF(1-IMATCH+1) 1335, 1400, 1340$
 $NST(P)=1335$
 $GC\ TO\ 9500$
 $SNL(1)=P(5)$
 $GC(1350)=K=1,4$
 $P(K)=P(K+1)$
 $T(K)=T(K+1)$
 $D(K)=D(K+1)$
 $Q(K)=Q(K+1)$
 $1340 \text{ SNL}(1)=\zeta(1-2)$
 $D(5)=HS*\zeta(4)*P(4)+D(4)$
 $T(5)=D(5)+T(4)$
 $F(5)=T(5)/(1.0-HSQ12*\zeta(5))$
 $P(5)=1.09375*P(4)+0.2734375*P(5)-0.546875*P(3)+0.21875*P(2)-$
 $1.0390625*P(1)$
 $I=1-1$
 $DX=DX/2^0$
 $Q(5)=\zeta(1)$
 FE_X
 $F(G)=H*H$
 $HSQ12=HS\zeta(12.0)$
 $T(5)=P(5)*\{1.0-HSQ12*\zeta(5)\}$
 $SNL(1)=P(5)$
 $T(4)=P(4)*\{1.0-HSQ12*Q(4)\}$
 $GC\ 1380$
 $P(L)=P(L+1)$
 $T(L)=T(L+1)$
 $D(L)=D(L+1)$
 $G(L)=G(L+1)$
 $GC\ TO\ 1230$

C WATCHING RADIUS HAS BEEN REACHED CCOMING IN

1400 K=KKK
VALUE=SNLC(K)*SNLC(K)

GC TO 1420
SUM3=SUM3+XIF*SUM4
XIF=XIF+0.5

1420 N=N-
SUM4=0.0
Y=VALUE

1430 VALUE=SNLO(K-5)*SNLO(K-5)
SUM4=SUM4+19.0*(VALUE+Y)+75.0*(SNLO(K-1)**2+SNLO(K-4)**2)
K=K-5
IF (K-1)MATCH 1435,1450,1440
NSTCP=1435
GC TO 9500

1440 N=N-1
IF (N) 1445,1410,1430

1445 NSTCP=1445
GC TO 9900

1450 SUM3=SUM3+XIF*SUM4
S3=SUM3/P(4)**2

S4=PPIN/P(4)
P(5)=T(3)-0.5*(P(5)-P(3))/h

CE=(S2-S4)/(S1-S3)
DEPPEUE/E

1460 IF (ABS(CE/E)-THRESH) 2000,1460,1460
EE+E/DE

1460 IF (EE) 200,1480,1480

EE-E/DE
WRITE(6,9670) E,DE

9670 FORWARD(2E1C.5)
EE=0.50*DE

GC TO 1460
IMPROVE TRIAL EIGENVALUE BY PERTURBATION THEORY IF NECESSARY

C CALCULATE THE NORMALIZED WAVE FUNCTIONS

2000 PCP=PMATCH/P(4)
DC=2000
SNLC(J)=SNLC(J)*PCP
SNL1=0.0
J=1

XIF=XIF/C
VALUE=0.0
N=N-3

2020 XIF=XIF+XIF
SUM2=0.0
Y=VALUE
VALUE=SNLC(J+5)*SNLC(J+5)


```

1 SUM2=SUM2+19.0*(VALUE+Y)+75.0*(SNL0(J+4)*#2+SNL0(J+1)*#2)
1 J=J+5
1 M=M-1
1 IF(MM)=0*(SNL0(J+2)*#2+SNL0(J+3)*#2)

```

```

2035 NSTCP=2035
GC TO 9900

```

```

2040 SUM1=XIF*SUM2
IF(KKK-J)=2045,205C,2020

```

```

2045 NSTLP=2045
GC TO 9900

```

```

2050 C1=6RT(SUM1)
IF(SNL0(J3)) 2060,2055,2070

```

```

2055 NSTOP=2055
GC TO 9900

```

```

2060 C1=-C1
GC 2080 I=1,KKK

```

```

2080 SNL0(I)=SNL0(I)/C1
RETURN

```

```

9900 WRITE(6,9020) NSTOP

```

```

9920 STCP

```

```

9010 FORMAT(20H NO CONVERGENCE ON,14,11,F4.0)

```

```

9C2C FCRNT(5HCSTOP,14,8HIN SCHEQ)

```

```

9U30 FCRNT(6HOAT,Z,F6.0,6H

```

```

IN MATCH =15,43H INWARD INTEGRATION WILL BE TRIED AT KKK+40)

```

```

96CC FORMAT(14,2F12.5)
END

```

```

SUBROUTINE CROSYM(M)
C SINULTANEOUS EQUATION SOLVER
C WRITTEN BY L.C. HANSON, SCIENTIFIC COMPUTATION DEPARTMENT,
C ROCKHEED MISSILES AND SPACE COMPANY, SUNNYVALE, CALIFORNIA
C COMMUN/COM1/V(521),R(521),RU(521),RU3(521),X(521),
2 XI(521),XJ(521),RSCORE(521),RSATC(521),RSVALE(521),
3 RUINL(521),RUJNL(521),RUFL(521),RUFL1(521),RUFL2(521),
4 XNUM(521),DENM(521),SNL0(521),SNL1(521),RR(521),
5 NNZ(24),NNNL(24),NNKK(24),EE(24),A(4,5),SNL(24,521)
N=N+1
11=1
12=11
SUM=2BS(A(11,11))
DC=120 I=1,M
1 IF(SUM-ABS(A(1,11))) 110,120,120
11C I=1

```



```

SUN=ABS(A(I,II))
12C CNTINUE
1F (I2-I1) 130,150,130
13C DC 14C J=1,N
SUN=-A(I1,J)
A(I1,J)=A(I2,J)
14C A(I2,J)=SUM
15C I=I+1
DC 160 I=I3,M
A(I1,I1)=A(I2,I1)/A(I1,I1)
16C J=I-1
J2=I+1
1F (J2) 180,200,180
DC 190 J=I3,N
DC 190 I=I2,J2
180 A(I1,J)=A(I1,J)-A(I1,I2)*A(I1,I1)
19C A(I1,J)=A(I1,J)-A(I1,I2)*A(I1,I1)
200,220,200
200 J2=I+1
I1=I+1
DC 210 I=I1,M
DC 210 J=I2,N
A(I1,I1)=A(I1,I1)-A(I1,J)*A(I1,I1)
DC 224 U2 I=1,M
DC 224 U2 I=100,170,100
22C DC 224 U2 I=1,M
J2=I+1
J2=I+1
A(I2,N)=A(I3,N)/A(I3,I3)
1F (J2) 230,250,230
DC 24U J=1,J2
A(J,N)=A(J,N)-A(I3,N)*A(J,I3)
24C RETURN
250 END
*GC.SYSIN DD

```



```

10 CONTINUE
15 READ(5,1502C) (RU(I), I=1,441)
 9020 FCKMAT(5E15.7)
 9500 WRITE(6,9500)
 9501 FCKMAT(1H1)
 9502 WRITE(9,9510) (RU(I), I=1,441)
 9510 FCKMAT(1OF10.5)
 9520 FCKMAT(5X,1CF10.5)
N=1
DC 19 J=1,11
DC 18 I=1,40
TX(I,J)=X(M)*C(N)
 18 M=M+1
 19 CONTINUE
 20 GC TO 150
 21 IF Z=2 (21,22,23), IP2
 22 CALL FILL(1,1)
 23 GC TO 200
 24 IF Z=3 (24,25,26), IP3
 25 CALL FILL(1,21)
 26 GC TO 200
 27 IF Z=1 (27,28,29), IP4
 28 GC TO 31
 29 IF Z=2 (31,32,33), IP3
 30 CALL FILL(2,1)
 31 GC TO 21
 32 IF Z=3 (32,33,34), IP5
 33 GC TO 21
 34 IF Z=1 (34,35,36), IP4
 35 GC TO 31
 36 IF Z=2 (36,37,38), IP4
 37 GC TO 31
 38 IF Z=3 (38,39,40), IP5
 39 GC TO 41
 40 IF Z=2 (40,41,42), IP4
 41 GC TO 31
 42 IF Z=3 (42,43,44), IP4
 43 GC TO 31
 44 IF Z=1 (44,45,46), IP5
 45 GC TO 41
 46 IF Z=2 (46,47,48), IP4
 47 GC TO 41
 48 IF Z=3 (48,49,50), IP5
 49 GC TO 41
 50 IF Z=1 (50,51,52), IP5
 51 IF Z=2 (51,52,53), IP5
 52 IF Z=3 (52,53,54), IP5
 53 GC TO 41

```



```

113 IF11=1          695
   GC TO 3CO          696
150 CNTINUE          697
   RCX=1.U/DX(1)      698
   RT=C.0             700
   K=0                701
   NFS=0              704
   J=4.1              705
   UU(41)=0.0          706
   XX(41)=1.0          707
160 RT=R+DD          708
   K=K+1              709
   IF(KMR.LT.K)      709
   IF(J-4) 230,180,700
   IF(K-1) 9999,200,20
220 XX(1)=XX(41)      9999
   UU(1)=UU(41)      200
   UC 210,I=2,41      20
   XX(1)=TX(I-1,1)    1
   UU(1)=TRU(I-1,1)   1
221 J=1               1
   IF(J+1,230,230,20
   IF(RT-XX(J))      230,240,220
230 RT=RT             220
   RR(K)=RT           221
   RR(K)=1.0/RT       221
   FPR2D(K)=FPD*RT*RT
   FFD(N-1) 99.99,245,345
245 ADC(K)=DD*UU(J)
   GC TO 260           245
   RR(K)=RT           260
   RR(K)=1.0/RT       260
   FPR2D(K)=FPD*RT*RT
   FFD(N-1) 99.99,255,355
255 ADC(K)=DUX((RT-XX(J-1))*RDX*(UU(J)-UU(J-1))+UU(J-1))
   ARHO(K)=AD(K)/FPR2D(K)
   APSI(K)=SQRT(ARHO(K))
   ARFT(K)=ARHO(K)**FCT
   AFOT(K)=ARHO(K)**FCT
   J=J-1               255
   IF(K-1) 9999,270,280
270 AG(K)=ADQ(K)      270
   GC TO 160           280
   AG(K)=AQ(K-1)+ADQ(K)
300 CNTINUE           280
   IF(N-1) 9999,310,320
310 WRITE(6,9550) A2,A1

```



```

9550 FCRMAT(1H1,20X,'NUCLEAR CHARGE WAS',F4.0,'', THE ATOM WAS',F4.0,'', T
21NESIGNIZED,'/')
9551 WRITE(6,9580),((R(I),ADQ(I),AQ(I)),I=1,KMR)
9552 FCRMAT(3,F8.3,2F10.5,E10.2)
9553 KRITE(6,9500)
9554 GCTO(39514)400,400, INUC
9555 WRITE(6,9555),B2B1
21NESIGNIZED,'/')
9556 FCRMAT(1H0,20X,'NUCLEAR CHARGE WAS',F4.0,'', THE ATOM WAS',F4.0,'', T
9557 WRITE(6,9580),((R(I),BDQ(I),BQ(I)),I=1,KMR)
9558 FCRMAT(1H0,20X,'NUCLEAR CHARGE WAS',F4.0,'', THE ATOM WAS',F4.0,'', T
21NESIGNIZED,'/')
9559 KRITE(6,9500)
9560 GCTO(400)
9561 BCC(K)=UU*UU(U(J)
9562 GC TO 360
9563 BDQ(K)=DD*((RT-XX(U-1))*RDX*(UU(J)-UU(J-1))+UU(J-1))
9564 BRHC(K)=BCC(K)/FPR2D(K)
9565 BPSI(K)=SQRT(BRHO(K))
9566 BRFT(K)=BRHU(K)**FT
9567 BFFT(K)=BRHO(K)**FFT
9568 J=J-1
9569 IF(K-1)=9999,370,380
9570 BQ(K)=BDQ(K)
9571 GC TO 160
9572 BQ(K)=BQ(K-1)+BDQ(K)
9573 GC TO 160
9574 DC 395 1=1,KM
9575 BQ(I)=AQ(I)
9576 BRHO(I)=ADQ(I)
9577 BPSI(I)=ARHO(I)
9578 BRFT(I)=APSI(I)
9579 BFFT(I)=ARFT(I)
9580 ARFT(I)=ARFOT(I)
9581 DC 399 K=1,KM
9582 AG(K)=BQ(K)
9583 ARHO(K)=BDQ(K)
9584 BPSI(K)=ARHO(I)
9585 ARFT(K)=BPSI(K)
9586 ARFOT(K)=BRFOT(K)
9587 CNTINUE(6,9520) 1H
9588 FCRMAT(1H1,20X,20A4,/,/,'HETEROЯUCLEAR MODEL, AUGUST 1969 FCRM'
9589 X
500 CNTINUE
9590 ARFT(K)=BRFT(K)
9591 ARFOT(K)=BRFOT(K)
9592 CNTINUE
9593 WRITE(6,9540),DZ,DRS,FRK,RTEST,KSTEP,RN
9594 FCRMAT(10X,DZ=1,F6.3,1,DRS=1,F6.3,1,FRK=1,F5.2,1,RTEST,WAS',2,13,1,STEPS,MAX=1,F5.2,1,MOD9
2 F5.2,1,DD WAS,1,F6.3,1,RUN EVERY,13,1,MOD9

```



```

VVA1=VBA1+BDC(J)*RR(J)
VVB1=VBB1+ADQ(J)*RR(J)
VVA2=VBA2+BDC(J)*RR(J)
VVB2=VBB2+ADQ(J)*RR(J)
VVA3=VBA3+BDC(J)*RR(J)
VVB3=VBB3+ADQ(J)*RR(J)
VVA=HRD*(CC1*VBA1+CC2*VBA2+CC3*VBA3)
VVB=HRD*(CC1*VBB1+CC2*VBB2+CC3*VBB3)
VAB=0.0
VAA=0.0
VAA=VAA+BDC(J)*RR(J)
VAB=VAB+ADQ(J)*RR(J)
VVAE=VVE+DVEE
VVE=VVE+DVEE
VVSZ=VVSZ+DVNN
VVSNC=VNN+VNE+VNE
VSN=VNN+0.5*VNE
CALL CLAP EDD,EXX, FT, FOT, KMR)
DXC=2.0*C*EDD-EXX}
VSNC=VSN+VDC
VSN=VSN+VDC
VFK=VVSZ+VDC
VDXA=R3*(EDD-2.0*EXX)
VA=VSNA+VDXA
FORMAT(F10.3,1F10.3)
IF(K-KSTEP) 9999,620,700
620 DIS=J.0
VSNC=D VSZ*D
DC 650 I=1,KSM
DIS=DIS+DD
650 VP(I)=VSNC/DIS+VDAC
650 VP(I)=VSNC/1000
750 KL=K-KSTEP
DC 750 I=1,KSM
VP(KL+1)=VP(KL+1-1)-DVP
1000 CONTINUE
1010 IF(IPN) 1010,2,1010
1010 CONTINUE
WHITE(7,9610), (IH(1),I=1,15),KM
9610 FORMAT(7, DIFFERENT,TRUE,15A4,I4)
WRITE(7,9630) (APSI(I),I=1,20)
9620 FORMAT(7,9634)
WRITE(7,9635) (APSI(I),I=21,KM)
9635 FORMAT(10F8.5)
WHITE(7,9635) (BPSI(I),I=1,20)

```



```

      WRITE(7,9635) (BPSI(I),I=21,KM)
      WRITE(7,9660) (IH(I),I=1,15),KM
      9660  FCRMAT(7,FCTENTIAL,FRCM,15A4,14)
      WRITE(7,9640) (VP(I),I=1,20)
      9640  FCRMAT(5FL2*4)
      WRITE(7,9645) (VP(I),I=21,KM)
      9645  FCRMAT(8FLIC,5)
      9995  GC_TOC 2
      STOP
      END

```

```

SUBROUTINE FILL(N,M)
COMMON/COM1/TX(40,11),TRU(40,11),DX(11),DR(11)
N=N+1
JJ=C
CC=100
I=1,37,2
N=N+JJ
NP=MM+1
TRU(I,N)=TRU(MM,NN)
TX(I,N)=TX(NM,NN)
IP=I+1
TX(I,P,N)=TX(I,N)+DR(N)
TRU(I,P,N)=0.5*(TRU(I,N)+TRU(MP,NN))
I=I+1
NP=N+19
PP=M+2C
TRU(39,N)=TRU(MP,NN)
TX(39,N)=TX(MP,NN)
TX(40,N)=TX(39,N)+DR(N)
TRU(40,N)=2.0*TRU(39,N)-TRU(38,N)
RETURN
END

```

```

      SUBROUTINE ULAP(LU,EXX,EXY,EXZ,EXR,EXI,EXJ,EXK,EXL)
      COMMON/CUM2/ADQ(1000),ARHO(1000),ARFT(1000),ARFOT(1000)
      COMMON/CUM3/D,DDR,DRS,FRR,DZ,ARTEST,RT2,RS,HDRS,HDD,ZMAX
      COMMON/CUM4/BQ(1000),BDQ(1000),BRHO(1000),BRFT(1000),BRFOT(1000)
      ELD=0.0
      EXX=0.0
      EXZ=C-RT*TEST
      EXS=0.0
      EXR=DRS
      EXI=R2+Z**2
      EXJ=IIF(RA-GT,RT2,GO TO 200)
      EXK=IIF(RA-GT,RT2,(L-Z)**2)

```



```

MOD9
IF(RB.GT.RT2) GO TO 200
RA=SCRT(RB)
RB=SCRT(RB)
I=KA*UD.RHCD
I=RB*DDK+HCD
RCR=R*FER
CR=DR*FER
IF((I.LT.1) .I=1
IF((J.LT.1) .J=1
IF((J.GT.KMR) GO TO 200
IF((J.GT.KMR) GO TO 200
IF((J.GT.KMR) GO TO 200
EDD+((ARHO(I)+BRHO(J))**FT-ARFT(I)-BRFT(J))**RDR
EXX=EXX+((ARHO(I)+BRHO(J))**FCUT-ARFOT(I)-BRFOT(J))*RDR
150
EXX=EXX+((ARHO(I)+BRHO(J))**FCUT-ARFOT(I)-BRFOT(J))*RDR
200
Z=Z+DZ
IF((Z.GT.ZMAX) GO TO 1000
IF((ABS(Z)-DD) 260) GO TO 260
250
IF((ABS(Z-D).GE.DD) GO TO 260
250
RS=RS
DR=DRS
GC TO 100
260
R=DD
CR=DRS
GC TO 100
1000
ELD=18.C39C2*DZ*EDD
IF(EDD.LT.C.0) EDD=0.0
EXX=4.64076*DZ*EXX
IF(EXX.LT.C.0) EXX=0.0
RETURN
END
//GO.FT6FC01 DD SYSSOUT=A,DCB=BLKSIZE=133
//GC.SYSIN DD

```



```

// EXEC FORTCLGP, REGION=100K
C THIS PROGRAM COMPUTES THE DISTRIBUTION OF IMPACT PARAMETERS
C
C   FX(R,THETA)=R*COS(THETA-PHI)-(YR*SIN(THETA-PHI)+XR*COS(THETA-PHI))
C   FY(R,THETA)=R*SIN(THETA-PHI)+(XR*SIN(THETA-PHI)-YR*COS(THETA-PHI))
C   DIMENSION IA(1500),A5(4,4),A6(6,3),E1(3),E2(3),E3(6),
C   K1(6),IS(6),S(6)
C   DIMENSION LARGE(6)
C   INTEGER R,TAU,ALFA,RN1
C   LOGICAL *1,CHAR(80)
C   READ(5,557,END=999) CHAR
C   READ(5,555) ICODE,A,B,INUMBR
C   READ(5,551) SCALEF,RNA,RCL
C   READ(5,501) (A5(I,J),J=1,2)
C   DC 3 I=1,INUMBR
C   READ(5,502) (A6(I,J),J=1,3)
C   READ(5,503) PHI,XR,YR,ALPHA,RMAX
C   WRITE(6,500) ICODE,A,B,INUMBR
C   WRITE(6,501) SCALEF,RNA,RCL
C   WRITE(6,501) (A5(I,J),J=1,2)
C   DC 990 I=1,INUMBR
C   WRITE(6,502) (A6(I,J),J=1,3)
C   WRITE(6,503) PHI,XR,YR,ALPHA,RMAX
C   990 FORMAT(13.2F10.4,I3)
C   991 FORMAT(3F10.4)
C   902 FORMAT(2F10.4)
C   903 FORMAT(5F10.4)
C   955 FORMAT(6I2)
C   950 FORMAT(1ZERO CHECK 10)
C   557 FORMAT(8I1)
C
C   ALFA=2**16+3
C   RN1=2*(2**30-2)+1
C   NN=1
C   TAU=1
C   SCALE2=RNA/RCL
C   THIS SECTION GIVES GRID ON WHICH TC WORK
C
C   IAA=A/.005
C   Id=B/.005
C
C   THIS STATEMENT INITIALIZES IAI(I) TC ZERO

```



```

PFR=CC5/SCALEEF
PFR1=SCALEEF/005
LA1(I)=0
5 C THIS SECTION CONVERTS ATOM POSITIONS TO SCALED COORDINATES
C DC 10 I=1,1, INUMBR
C DC 9 J=1,3
C AC(I,J)=AC(I,J)*PFR1
9 WRITE(6,950)
C CONTINUE
10 IF (ICODE-2) 51,2C,999
C THIS SECTION CONVERTS VERTICES INTO SCALED COORDINATES
C DC 25 I=1,3
20 DC 24 J=1,2
C AC(I,J)=AC(I,J)*PFR1
24
25 C CRITX IS THE X VALUE AT WHICH WE CHANGE THE CONDITIONS WHICH MUST BE
C MET IF THE GRIDDED COORDINATE IS TO FALL IN THE REPRESENTATIVE AREA.
C CRITX=A5(2,1)
C THIS SECTION CALCULATES THE EQUATIONS OF THE LINES BOUNDING THE TRIANGLE
C DC 35 I=1,2
C B1(I)=(A5(I+1,2)-A5(I,1))/(A5(I+1,1)-A5(I,1))
C WRITE(6,950)
C B2(I)=(A5(I,2)-B1(I)*A5(I,1)+A5(I+1,2)-B1(I)*A5(I+1,1))/2.0
35 B1(3)=0
B2(3)=A5(3,2)
C THIS SECTION CALCULATES THE NEW COORDINATES OF THE ATOMS IN THE
C REPRESENTATIVE AREA
C DC 50 I=1,1, INUMBR
C IF (A6(I,1)) 40,44,4C
40 THETA=ATAN(A6(I,2)/A6(I,1))
C WRITE(6,950)
4C GL TO 45
45 THETA=1.57C7963
R=SQRT(A6(I,2)**2+A6(I,1)**2)
A6(I,1)=FX(R,THETA)
A6(I,2)=FY(R,THETA)*COS(ALPHA)-A6(I,3)*SIN(ALPHA)
44 WRITE(6,950) ((A6(I,J),J=1,3),I=1,INUMBR)
45
50

```


650

FORMAT(3F10.3)

THIS SECTION CALCULATES THE ACTUAL DISTRIBUTION OF IMPACT PARAMETERS

```

C
C
1 X=IA+1
C X=IB+1
C C 75 I=1,IX
C C 74 J=1,IX
C ACK1=I-1
C ACK2=J-1
1 IF (ICODE=2) 54,53,54
1 IF (ACK2-CRITX) 100,100,150
1 IF (ACK1-(B1(1)*ACK2+B2(1)) 54,54,74
1 IF (ACK1-(B1(2)*ACK2+B2(2)) 54,54,74
1 IF (ACK2) 55,60,55
55 THETA = ATAN(ACK1/ACK2)
55 GOTO 65
60 THETA=1.707963
60 R=SQRT(ACK1**2+ACK2**2)
65 ACK1=FY(R,THETA)*CGS(ALPHA)
65 ACK2=FX(R,THETA)
C
C THIS SECTION CALCULATES THE SHORTEST IMPACT PARAMETER AND
C ASSIGNS IT TO THE CORRECT ATOM
C
C
RANGE=6.25E04
KEEP=0
DO 180 K=1,INUMDR
B2(K)=(A6(K,1)-ACK2)**2+(A6(K,2)-ACK1)**2
180 IF(LABE(K)-1) 79,178,999
178 B3(K)=B3(K)*SCALE2
179 IF(B3(K)-RANGE) 182,192,180
182 RANGE=B3(K)
KEEP=K
GOTO 180
192 CALL RANDOM(0.0,2.0,0.5,0,TAU,2.0,0,NN,ALFA,RN1,SN,SN1)
192 IF ((.5-SN) 180,555,555
555
180 COUNTINUE
180 IF (CLARE(KEEP)-1) 186,185,999
185 RANGE=SQR((RANGE)**2+1.0
186 ITALLY=(KEEP-1)*250+1 RANGE
186 ITALLY=IA(IITALLY)+1
74 COUNTINUE
74 COUNTINUE
DC 360 I=1,INUMDR

```



```

1 SUM=0
2 SUM(I)=0
3 JMAX=JMIN+249
4 SUM=ISUM+IA1(J)
5 CNTINUE(I)
6 WRITE(6,23X)60A1,///
7 550) CHAR
8 FORMAT(80A1)
9 34 1=1,INUMBR
10 JMIN=(I-1)*250+1
11 J1=JMIN+1
12 J2=J1+20
13 J3=J2+20
14 J4=J3+20
15 J5=J4+20
16 J6=J5+20
17 J7=J6+20
18 J8=J7+20
19 J9=J8+20
20 J10=J9+20
21 J11=J10+20
22 J12=J11+20
23 J13=J12+1C
24 WRITE(9,951)(IA1(J),J=JMIN,J1)
25 WRITE(7,951)(IA1(J),J=JMIN,J2)
26 WRITE(6,951)(IA1(J),J=JMIN,J3)
27 WRITE(7,951)(IA1(J),J=JMIN,J4)
28 WRITE(6,951)(IA1(J),J=JMIN,J5)
29 WRITE(7,951)(IA1(J),J=JMIN,J6)
30 WRITE(6,951)(IA1(J),J=JMIN,J7)
31 WRITE(7,951)(IA1(J),J=JMIN,J8)
32 WRITE(7,951)(IA1(J),J=JMIN,J9)
33 WRITE(6,951)(IA1(J),J=JMIN,J10)
34 WRITE(7,951)(IA1(J),J=JMIN,J11)
35 WRITE(6,951)(IA1(J),J=JMIN,J12)
36 WRITE(7,951)(IA1(J),J=JMIN,J13)
37 WRITE(6,951)(IA1(J),J=JMIN,J14)
38 WRITE(7,951)(IA1(J),J=JMIN,J15)
39 WRITE(6,951)(IA1(J),J=JMIN,J16)
40 WRITE(7,951)(IA1(J),J=JMIN,J17)
41 WRITE(6,951)(IA1(J),J=JMIN,J18)
42 WRITE(7,951)(IA1(J),J=JMIN,J19)
43 WRITE(6,951)(IA1(J),J=JMIN,J20)
44 JN=J7+1

```



```

      WRITE(6,951)(IA1(J),J=JMIN,J8)
      WRITE(7,951)(IA1(J),J=JMIN,J8)
      JMIN=J8+1
      WRITE(6,951)(IA1(J),J=JMIN,J9)
      WRITE(7,951)(IA1(J),J=JMIN,J9)
      JMIN=J9+1
      WRITE(6,951)(IA1(J),J=JMIN,JO)
      WRITE(7,951)(IA1(J),J=JMIN,JO)
      JMIN=JO+1
      WRITE(6,951)(IA1(J),J=JMIN,JJ1)
      WRITE(7,951)(IA1(J),J=JMIN,JJ1)
      JMIN=JJ1+1
      WRITE(6,951)(IA1(J),J=JMIN,JJ2)
      WRITE(7,951)(IA1(J),J=JMIN,JJ2)
      JMIN=JJ2+1
      WRITE(6,951)(IA1(J),J=JMIN,JJ3)
      WRITE(7,951)(IA1(J),J=JMIN,JJ3)
      FORMAT(2014)
      WRITE(7,914)
      FCRNAT(1,NEW_ATOM)
      WRITE(6,915)
      FCRNAT(1,20X,'TOTAL NUMBER OF IMPACT POINTS TALLIED',//)
      WRITE(6,913) LIS(I)
      FORMAT(28X,'ATOM',I1,'=',15,' POINTS',//)
      WRITE(6,958)
      FORMAT(1)
      GOTO 1
      STOP
      END

```

```

      SUBROUTINE RANDOM(A,B,SIGMA,MU,TAU,LAMBDA,G,NN,ALFA,
     1 RNL,SN,SN1)

```

```

      SUBROUTINE RANDOM GENERATES THREE PSEUDORANDOM NUMBER DISTRIBUTIONS:
      1) UNIFORM, 2) NORMAL, 3) EXPONENTIAL. IF TAU=1,2,3, ONE GETS A UNIFORM, NORMAL, EXPONENTIAL DIST. RESP. A DEFINITION OF THE OTHER TERMS USED IN THIS ROUTINE MAY BE FOUND IN THESSIS BOOK 1, K.L. ALLEN. THE ROUTINE WAS TAKEN FROM RALSTON AND WILF NUMERICAL METHODS FOR DIGITAL COMPUTERS.

```

```

      INTEGER TAU,ALFA,G,RN,RNL
      REAL MU,LAMBDA
      RNL=RN
      SN1=ALFA
      1
      RSTN=RN**2.0**(-31)
      IF ((TAU-2)**3/4 < C
      EXPONENTIAL DISTRIBUTION

```



```

2 IF(RSTN) S*S*8
3 RSTN=ABS(RSTN)
4 SN=-((1+C/LAMBDA)*ALCG(RSTN))
5 SN=ABS(SN)
6 SN=(B-A)*RSTN+A
7 SN=ABS(SN)
8 CC TO 5 DISTRIBUTION
9 UNIFORM DISTRIBUTION
10 CC TO 5 DISTRIBUTION
11 IF (G-1) 7,6,7
12 NN=NN+1
13 G=C+1
14 RN1=RN
15 RSTN1=KSTN
16 CC TO 1
17 IF (RSTN1) 11,11,10
18 KSTN1=ABS(RSTN1)
19 Z=SQRT((+2*0*ALCG(RSTN1))*SIGMA
20 SN1=Z*UCS((6.28318*RSTN)+MU
21 SN=Z*SIN((6.28318*RSTN)+MU
22 G=C
23 NN=NN+1
24 RN1=RN
25 RETURN
26 END
27 //CC•SYSIN DU *

```


// EXEC FCRTCLGP, REGION, GC=150K
//FCRT.SYSIN DD*

C THIS PROGRAM TAKES THE RAW DATA FROM THE IMPACT PARAMETER PROGRAM
C AND GENERATES A LEAST SQUARES POLYNOMIAL FIT THROUGH THE POINTS.
C SPECIFICALLY, THE PROGRAM SELECTS THE POINT AT WHICH THE
C DISTRIBUTION IS A MAXIMUM AND FITS A STRAIGHT LINE THROUGH ALL
C POINTS PRECEDING THIS POINT AND A TENTH DEGREE POLYNOMIAL TO ALL
C POINTS FOLLOWING THIS POINT. THE FIT IS ACCOMPLISHED BY
C GENERATING THE ORTHOGONAL POLYNOMIALS (LEGENDRE) ASSOCIATED WITH
C THE FUNCTION.

C DATA INPUT: CARD 1; NUMBER OF POINTS TO BE FITTED, IC NUMBER
C INDICATING IF CARD AND GRAPHICAL OUTPUT IS WANTED (1=NO, 2=YES);
C CARD 2,3: TWO CARDS WITH INFORMATION TO BE OUTPUTTED WITH GRAPHIFICATION
C MUST BE INSERTED FOR EVERY RUN; CARD4-N: DATA FROM THE DISTRIBUTION
C OF IMPACT PARAMETER PROGRAM

COMMON/POLY/ NTERMS,B(300),C(300),D(300)
DIMENSION X(300),F(300),W(300),ERRCR(300),PJ(300),PJ(300)
DIMENSION XX(300),YY(300),XX1(300),YY1(300),
DIMENSION IIF(300),
REAL*8 TITLE(12)
REAL LABEL1,'F(X)'/
REAL LABEL2,'E(X)'/
READ(5,999) NPOINT,IFLAG
1 899
FCRMA(2,14) TITLE E
950
FCRMA(6,8)
READ(5,900) (IIF(I),I=1,NPOINT)
900
FCRMA(2,14)
WRITE(6,907)
907
FCRMA(1,1)
NTERMS=2
ICOUNT=0
NFT=NPOINT
KEEP=0

C
C NTERMS=DEGREE OF FIT+1; ICOUNT=A COUNTER; KEEP= VALUE AT WHICH
C THE IMPACT PARAMETER DISTRIBUTION IS A MAXIMUM; IRANGE= THE RANGE
C CORRESPONDING TO THE MAXIMUM IMPACT PARAMETER;
C
C IRANGE=C
C 777 I=1,NPCINT
C IF (IRANGE-IIF(I)) 778,778,777
C
KEEP=1


```

IRANGE=11IF(I)
CCONTINUE
9000  WRITE(6,9000) KEEP
      FORMAT(1,25X,KEEP= '15,///)
      NPOINT=KEEP
      NCOUNT=ICOUNT+1
      IF (ICOUNT.EQ.2) GO TO 779
      GC TO 102
      GC 781 1=1,NPCINT
      11IF(I)=P(J(I))
      NTERMS=11
      NPCINT=NPT-NPCINT
      GC 781 1=1,NPOINT
      11IF(I)=11IF(KEEP+1)
      X(I)= X VALUES OF DISTRIBUTION TO BE FITTED; F(I)= VALUES OF THE
      C FUNCTION CORRESPONDING TO X;W(I)= WEIGHTING FACTORS FOR THE
      C TRIGONAL POLYNOMIALS;
      CC 5 I=1,NPCINT
      ACK=1
      X(I)=ACK*.005
      F(I)=11IF(I)
      W(I)=1.
5      CCONTINUE
      CALL CKTPCL(NPCINT,X,F,W,ERROR,PJW1,PJ)
      WRITE(6,6C1)(J,B(J),C(J),D(J),J=1,NTERMS)
      FCRWA(6:,25X,14,3D16.8)
      CC 60 I=1,NPCINT
      11IF(I)=F(I)
      P(J)=CKTVAL(X(I))
      WRITE(6,6OC)(X(I),11IF(I),PJ(I),ERRCR(I),I=1,NPCINT)
      FCRWA(6:,10X,F5.3,14,F10.5,EL3.3,//)
      IF (11FLAG.EQ.1) GC TO 72
      IF (11FLAG.EQ.2) GC TO 73
      1 CALL DRAW(NPOINT,X,F,1,0,LABEL,TITLE,.1, 4C.C,1,0,2,2,8,12,0,
      1 LAST)
      1 CALL DRAW(NPOINT,X,PJ,2,0,LABEL,TITLE,.1, 4C.0,1,0,2,2,8,12,0,
      1 LAST)
      1 CALL DRAW(NPCINT,X,ERRCR,3,0,LABEL2,TITLE,.1, 40.0,1,0,2,2,8,12,
      1 C,LAST)
      1 IF (ICOUNT.EQ.2) GO TO 888
      GC TO 1
      11IF(I+1,KEEP)=PJ(I)
      888  DC 889 1=1,NPOINT
      889 11IF(I+1,KEEP)=PJ(I)
      74  WRITE(7,90C) (11IF(I),I=1,NPT)
      GC TO 1
      999

```


END

```
FUNCTION ORTVAL(X)
C SUBROUTINE ORTVAL EVALUATES THE ORTHOGONAL POLYNOMIALS AT A
C SPECIFIED VALUE CF X
C COMMON/PCLY/NTERMS, E(300),C(300),D(300)
C NTERMS
C ORTVAL=D(K)
C PREV=0
C K=K-1
10 IF (K.EQ.0)
     PREV2=PREV
     PREV=ORTVAL
     ORTVAL=D(K)+(X-B(K))*PREV-C(K+1)*PREV2
     CC TO 10
     END

SUBROUTINE CTPOL (INPOINT,X,F,W,ERRCR,PJML,PJ)
C SUBROUTINE CTPOL CALCULATES THE COEFFICIENTS OF THE TERMS IN
C THE ORTHOGONAL POLYNOMIAL USED IN THE LEAST SQUARES FIT
C COMMON/POLY/INTERMS,B(300),C(300),D(300)
C DIMENSION X(300),F(300),W(300),ERRCR(300),PJML(300),PJ(300)
C DIMENSION S(300)
C CC 9 J=1,NTERMS
C C(J)=0.
C S(J)=0.
9  CC(J)=0.
C C 10 I=1,NPOINT
D(I)=D(I)+F(I)*W(I)
B(I)=B(I)+X(I)*W(I)
S(I)=S(I)+W(I)
U(I)=D(I)/S(I)
D(I)=I=1,NPOINT
B(I)=B(I)/S(I)
U(I)=B(I)-D(I)
11 IF (INTERMS.EQ.1)
     E(I)=B(I)/S(I)
     CC 12 I=1,NPOINT
     PJW(I)=X(I)-B(I)
     PJ(I)=X(I)-B(I)
     CC 12 I=1,NPOINT
     PJW(I)=0.
     S(I)=0.
     U(I)=0.
     D(I)=0.
     B(I)=0.
     CC 13 I=1,NPOINT
     E(I)=F(I)-D(I)
     RETURN
11 IF (INTERMS.EQ.1)
     E(I)=B(I)/S(I)
     CC 12 I=1,NPOINT
     PJW(I)=X(I)-B(I)
     PJ(I)=X(I)-B(I)
     CC 12 I=1,NPOINT
     PJW(I)=0.
     S(I)=0.
     U(I)=0.
     D(I)=0.
     B(I)=0.
     CC 13 I=1,NPOINT
     E(I)=F(I)-D(I)
     RETURN
```


20

```


$$\begin{aligned}
& J = J + 1 \\
& D C = P J(I) * W(I) \\
& P = P * P J(I) \\
& D(J) = D(J) + E R R C K(I) * P \\
& E(J) = B(J) + X(I) * P \\
& S(J) = S(J) + P \\
& D(J) = D(J) / S(J) \\
& C(J) = C(J) * N P O I N T \\
& E R R C K(I) = E R R C K(I) - D(J) * P J(I) \\
& I F (J . E C . N I E R M S) - D(J) * P J(I) \\
& B(J) = B(J) / S(J) \\
& S(J) = S(J) / S(J-1) \\
& D C = P J(I) * (X(I) - B(J)) * P J(I) - C(J) * P J M 1(I) \\
& P = P J(I) \\
& P J M 1(I) = P \\
& G L T O 20 \\
& E N D \\
& // G C . S Y S I N D D \\
& // G C . S Y S O U T A , S P A C E = ( C Y L , ( 3 , 1 ) )
\end{aligned}$$


```


1 // EXEC FORTCLG, REGION. GC=150K
2 // FCRT*SYSIN DD*

3 FRCGRAM INLSS
4 DIMENSION BMAX(3), PUD(3), ARC(3), LM(3), TFL(3), XM(3), KXM(3)
5 FLPD(750), BCNI(20,20), BCZZ(400)
6 IH(20), IH(4), IAH(4), PSE(8), FIT(8), EAV(3)
7 EN(20), BC(40), LCLT(40), IH(3,19), IH4(19)
8 ER(100), ERN(100), DREL(100), PP(100), EL(100), ET(100)
9 RHC(1000), EINC(1000), ELEC(1000), FN(1000), RX(1000), E(1000)
10 RX2(1000), RXZR(1000), RMIN(1000), E(1000)
11 SIG(1000), APS(1000), BPSI(1000)
12 ECUT(30,3), PEL(30,3), ECUT(30)
13 EQUIVALENCE(BCNI,BCZZ)
14 START=0.01*ITIME(XX)
15 CALL EP
16 CC 1 1=1,100
17 ER(1)=0.0
18 EL(1)=0.0
19 ET(1)=0.0
20 EA(1)=0.0
21 ECCLT(1)=0.0
22 UREL(1)=0.0
23 DC(2)=1,1000
24 RFC(1)=0.0
25 EIN(1)=0.0
26 ELEC(1)=0.0
27 FN(1)=0.0
28 RX(1)=0.0
29 RX2R(1)=0.
30 RMIN(1)=0.
31 E(1)=0.0
32 V(1)=0.0
33 SIG(1)=0.0
34 AFSI(1)=0.
35 BFSI(1)=0.
36 FPAR=1.0443E-27
37 PI=3.14159265
38 ECHRG=4.80286E-10
39 CVD=0.529172E-8
40 CVE=1.62021E-12
41 CVM=1.67239E-24
42 CAH=1.0E-8/CVD
43 ECT=0.0/C/3.0
44 FCT=4.0/C/3.0
45 KSTEP=5

1

159

7JCB, 722
7JCB, 723
7JCB, 724
7JCB, 725
7JCB, 726
7JCB, 727
7JCB, 728
7JCB, 729
7JCB, 730
7JCB, 731
7JCB, 733
7JCB, 734
7JCB, 735
7JCB, 736
7JCB, 737
7JCB, 738
7JCB, 739
7JCB, 740
7JCB, 741
9000 FCRT(A4,I2,9F6.4,3I3,I4,F7.4)


```

      READ (5,9000) LCRYST,LTPE,(BMAX(I),I=1,3),(PUD(I),I=1,3),
2     (ARO(I),I=1,3),(LM(I),I=1,3),KN,FACT
      PUDN=AMAX1(PUD(1),PUD(2),PUD(3))
      PUDM2=PUDN*PUDM
      DC 5 I=1,3
      LF=LM(I)
      READ (5,9010) (FLP(L),L=1,LF)
      PT=0.0
      DC 3 L=1,LF
      PT=PT+FLP(L)
      3   TFL(I)=PT
      SF=ARC(I)/PT
      DC 5 L=1,LF
      FLP(L)=FLP(L)*SF
      5   BM=AMAX1(BMAX(I),BMAX(2),BMAX(3))
      READ (5,9020) IH1
      FCRMAT(2,CA4)
      READ (5,9025) IH3,KMR
      FCNMAT(1,SA4,14)
      READ (5,9030) (APSI(I),I=1,KMR)
      9030 FCRMAT(10,FB8,5)
      READ (5,9030) (BPSI(I),I=1,KMR)
      READ (5,9025) IH4,KMV
      READ (5,9032) (V(I),I=1,20)
      9032 FCNMAT(5F14,5)
      READ (5,9035) (V(I),I=21,KMV)
      9035 FCNMAT(6F1C,5)
      KNVVR=MIN0(KM,KMV,KMR)
      KNVKF=KNVVR+1
      KNVF=KMF+1
      KM=KM-1
      KMF=KM+1
      KFP=KMP
      KND=KM+KM
      DX=0.02
      TDX=3.0*DX
      DXZ=DX*DX
      DXR=1.0*DX
      FK=KMP
      XNV=FK*DX
      HDX=0.5*DX
      DES=0.005
      DESR=1.0*DBS
      9040 FCNMAT(1,CF8,4)
      READ (5,9050) (EA(N),N=11,18),IAH
      9060 FCNMAT(11,0)

```



```

READ(5,9040) (EA(N),N=1,10)
905C FCRMA(5,9060) 4A4
READ(5,9060) JFIT
IF(JFIT)9999,15,10
907C FCRMA(1,6F5,3) 15
10 READ(5,9070) (PSE(J),FIT(J),J=1,JFIT)
908C FCRMA(2F4,0,2F3,0,6X,4A4)
15 READ(5,9080) ZB,ZT,BMAS,EDS,DEC,KEM,NM,RES,DRE,REM,
2 IF(ZB) 999,999,20
2C ACA=AD/0.5*ACA
HACA=0.5*ACA
11 FIT=3
IFIT=3
RLA=FACT*ADA
RCDB=RAYDUS
AM=TMAS/BMAS
BNE=BMAS*CVM/CVE
COM=AM/(1.0+AM)
C ERY=73*5023888
CEC=CCM*ERY
7*28926 = .75*PI*(3*PI**2)**1/3
CCCC=1.0*7.28926*DXT*HBAR/(CVE*CVE)
E1CECC*7.28926*DXT*HBAR/(CVE*CVE)
TCEx=2.0*BM
EC=EOS
ECEV=EOS*1000.
DEC=EV=DEC*1000.
FL=LSKIP
CEL=0.01*FL
CER=1.0/OBL
BML=BMM*RCRA
LML=BML*DBSR
SCB=DBC*DBSK
KLB=PUW*DXR*ROAIP
L2SKIP=LSKIP+LSKIP
L4SKIP=L3SKIP+LSKIP
NE=0
DC=25 1=1,2
XW(1)=ROA*SQRT(BMAX(1)**2+PUD(1)**2)
25 XW(1)=XW(1)*DXR+HDX
KLN=MAX(XK(1),XK(2)),KXM(3)
KLM=MIN(KLM,KM)
KLN=KLM-1
C CC 30 M=1,40
BC (N)=0,C
      MAKE THE RUSSEK ENERGY-ELECTRON PRODUCTION TABLE

```



```

3C LCUT(N)=0.0
NP=NM+1
NM=NM-1
KFLTE(6,9505) 1H2
FCRM(1H1,52X,4A4,///)
BC(1)=NM
EN(1)=EA(1)
EN(1)=EA(1)
EN(1)=EN(1)
LC(4,0,N=2,NM
IF(EN(1)-1,CE-10) 42,42,37
EN(N)=EN(N-1)+EA(1)*EA(N)
FNN(N)=FFN
EN(N)=EN(N)/FFN
J=NP-N
FJ=J
40 BC(N)=FJ*BC(J)/FFN
GC TO 45
42 NM=NM-1
NP=NM+1
NM=NM-1
9510 WRITE(6,9510) 1H1,IAH,LCRYST,AC,KM,DX
FLRAT(27X,20A4,/,20X,4A4,*
9510 LATITICE CONSTANT WAS ,F6.3/,36X,IONIZATION ENERGIES,/,14,*
DC(4,7 M=1,400
3 FC*3, BCHR STEP SIZE ,/,)
47 BCZL(M)=0.C
CREK=1.0/CRE
FUE=(KEM-RES)*DRER+1.001
J=N=FCU
J=N=JUM-1
E(1)=RES
E(1)=1.0/E(1))*NM
CC(50 J=2,JM
E(J)=E(J-1)+DRE
E(N)=1.0/E(J))*NM
DC(200 N=1,NM
NR=NM-N
EN(N,1)=-NR
NRP=NR+
IF(NR-2) 2CC,200,60
CC(100 I=2,NR
FI=1.P-1
FKE=K
BCNI(N,I)=-BCNI(N,I-1)*FK/FI
2CC CCI INUE
2CC 500 L=1,JM

```



```

DC 202 I=1,100
PF(I)=C.0
PZ=1.0
PZT=0.0
FK=E(L)/EN(L)
K=FK
1F(K-NM) 210,210,205
2C5
DC 220 I=1,K
F1=1 PZT+(-1.0**I)*((E(L)-FI*EN(L))**NM)*BC(I)
FZ=PZ+PZT*ERN(L)
DC 440 N=1 NM
1F(LCUT(N)) 400,29C,400
29C 1F(E(L)-ENN(N)) 400,390,300
NP=N+1
FK=(E(L)-ENN(N))/EN(NP)
K=FK
1F(K) 290,390,310
1F(K-NM) 320,320,315
315 K=NM
32C DC 350 I=1,K
F1=1
EF=E(L)-ENN(N)-FI*EN(NP)
1F(EF) 39C,350,350
350 PF(N)=PP(N)+(EF**NM)*BCNI(N,I)
PP(N)=BC(N)*((E(L)-ENN(N))**NM)+PP(N)*ERN(L)
44C CONTINUE
1F(PZ) 410,420,420
41C PZ=C
42C PFT=PZ
DC 430 N=1 NM
1F(PP(N)) 425,430,430
425 PP(N)=0.0
LCC(N)=-1
43C PFT=PFT+PP(N)
PFTR=1.0/PPFT
EL(L)=0
ET(L)=0
CC 440 N=1 NM
PF(N)=PP(N)*PPTR
FFN=PP(N)*FFN
TE=PP(N)*EN(N)
EL(L)=EL(L)+TE
ET(L)=ET(L)+TE*EN(N)
44C CONTINUE
45C

```



```

CE1=E(1)-EA(1)
DE1R=1.0/DE1
FCE1=EL(1)*DE1R
CC650 J=1, JNM
650 GREL(J)=DRER*(EL(J+1)-EL(J))
MAKE THE CROSS SECTION TABLE
K=K/M
K/M=KM/2
K=KMR-KMH
FK=K
K=KMR-FKMP
XMP=UX*FKMP
X=GX*FK
XGX=X*DX
SIG(KM)=0.0
CC700 M=1,KH
K=K-1
XDX=XDX-DX2
SIG(KM)=SIG(KM)+XDX*(APSI(K)+BPSI(K))**EOT
K=KMH
KF=KMH-1
DC750 M=1,KP
XGX=XDX-DX2
J=J-1
K=K-2
SIG(K)=SIG(K+2)+XDX*(APSI(J)+BPSI(J))**EOT
SIG(1)=SIG(2)+0.5*Dx2*(APSI(1)+BPSI(1))**ECT
CC ECO K=3, KMM, 2
SIG(K)=0.5*(SIG(K+1)+SIG(K-1))
800 WRITE(6,6820) (SIG(K),K=1,KMR)
WRITE(6,69820) (V(K),K=1,KMV)
9820 FCHWAT(LX,10F1.5)
MAKE CALCULATIONS FOR A SINGLE ICN ENERGY
1000 WRITE(6,9205) IH2
DC1010 NE=1, KEOV
L=1,1000
E(L)=0.0
RWIN(L)=C.C
EIN(L)=C.C
ELECT(L)=0.0
1010 GCONTINUE
CC LUZO M=1,3
EA(M)=0.0
1020 VC=SQRT(EC*EV*T0BM)
EIF=ELC*VC
ECP=EC*CEC
ECPK=1.0/EOF
LOCATE THE DISTANCE OF CLOSEST APPROACH

```



```

K=KMINP
X=XMV
CC 1050 M=1,KMV
K=K-1
X=X-DX
FN(K)=1.0-ECPRT(V(K)
IF(FN(K)) 1060,1040,1040
RX(X(K))=X
RX2(K)=X**X
RX2(K)=1.0/RX2(K)
104C CUNTINUE
105C CUNTINUE
X=DX
KMIN=1
CC TO 1065
106C KMIN=K
X=X+DX
KMP0=KMIN+1
LC 1070 M=1,KMIN
RX2(M)=0.0
RX2R(M)=0.0
FN(M)=0.0
1070 CUNTINUE
RX(KMIN)=X-DX
DXT=DX
CC 1070 M=1,5
DXT=0.1*DXT
CC 1080 NN=1,10
X=X-DX
PUT=V(K)+(X-RX(K))*DXR*(V(K+1)-V(K))
IF(1.0-ECPRT(POT)) 1080,1080,1080
108C CUNTINUE
109C X=X+DXT
RMIN(1)=X
B(1)=0.0
KSS=KMIN-1
PSI=0.0
C
FSI=0.5*SQRT(FN(KMP0))*SIG(KMP0)
FIC=FSI*(RX(KMP0)-X)*DXR
UC 1100 K=KMP0,KLB
T=S15(K)*SQRT(FN(K))
110C FSI=PSI+T
EIN(1)=EFSI*(PSI+FSI-0.5*T+FIO)
#EIN(1)=CALCULATE THE NUMBER OF ELECTRONS FROM THE RUSSEK MODEL
1110 IF(EIN(1)>DR) 1110,1140,1120,1120,1130
IF(EIN(1)-EA(1)) 1110,1140,1120,1120,1130

```



```

1120 ELEC(1)=0.0
1120 ELEC(1)=1170
1130 ELEC(1)=(EIN(1)-EA(1))*FDEL
1130 ELEC(1)=1150
1140 ELEC(1)=EL(M)+(EIN(1)-E(M))*DREL(M)
1140 ELEC(1)=1130
1150 EAV(1)=ELEC(1)*FLPD(1,1)
1160 EMAX=0.0
1170 LMAX=0
C          THIS IS THE INTEGRAL FOR A SINGLE B(L)
DC 1990 L=2,LML,LSKIP
LS=L          FIND RC FOR GIVEN B(L)
C          B(L)=B(L-LSKIP)+DBL
1171 IF(B(L)-BML) 1171,1171,2000
K=K$+K$TEP
X=RX(K)
E=B(L)*B(L)
DC 1 1/2 M=1,KSTEP
K=K-1
IF(1.0-E*PR*V(K)-B2*RX2R(K)) 1173,1173,1172
CCNTINUE
1172 KSS=X(K+1)
X=RX(K+1)
CC 1 1.75 M=1,3
DXT=0.*DXT
CC 1174 MM=1,10
X=X-DXT
PCT=V(K)+(X-RX(K))*DXR*(V(K+1)-V(K))
IF(1.0-ECPR*POT-B2/(XX)) 1175,1174,1174
CCNTINUE
1174 X=X+DXT
RC=X
RC2=KO*RC
C          FIRST INCREMENT AT SINGULARITY FCR B(L)
KT=KO*DXR*SQRT(PUDM2+B2)
IF(KT-KLNM) 1177,1177,1176
1176 KT=KLNM
RMN(L)=RC
KB=K+2
DXR=0.1*(RX(KB)-RC)
DERR=1.0/CRB
DUC=0.5*RC*DXR
CC=2.0*RC2*DXR
DC=0.5*SQR(DX/R)
PCT=V(K)+(RC-RX(K))*DXR*(V(K+1)-V(K))
SIGR=SIG(K)+(RC-RX(K))*DXR*(SIG(K+1)-SIG(K))

```



```

AL=1.0-ECPR*POT
RN=ECR+DR8
PCT=V(K)+(RN-RX(K))*DXR*(V(K+1)-V(K))
AN=1.0-ECPR*POT
N=C
DUX=(AN-AL)*DRBR
IF(DADX)>2000,1182
PSI=0.2*SQR(AN*DU/SQRT(2.0*(DADX*RCZ*RO+B2)))
1182      INTEGRATE THE REST OF THE FIRST STEP FCR B(L)
C
AN=RO
DC 1190 M=1,10
RN=AN+DR8
AL=AN
DUX=V(K)+(RN-RX(K))*DXR*(V(K+1)-V(K))
AN=1.0-ECPR*POT
C=RC/RN
UZ=L*OT-C
UZ=SQR(UZ)
DL=DXR/SQRT(RN*RN*RN*(RN-RO))
SIG=SIG(K)+(RN-RX(K))*DXR*(SIG(K+1)-SIG(K))
T=SIG*AN*DU/(C*C*SQR(TU2*(AN-AL))/U2+B2*(2.0-U2))
1195      PSI=PSI+T
1195      EIN(L)=E1F*CB*(PSI-0.5*T)
1195      AN=FN(KB)
PSI=0.5*SIG(KB)*AN/SQRT(AN-B2*RX2R(KB))
C
KEP=KB+1
CC 1190 K=KEP*KT
CC 1190 T=SIG(K)*FN(K)/SQRT(FN(K)-B2*RX2R(K))
1290      EIN(L)=EIN(L)+E1F*(PSI-0.5*T)
C
N=EIN(L)*DRER
CALCULATE ELECTRONS FROM RUSSEK MCCEL FOR THIS B(L)
1410      IF(EIN(L)-EA(1)) 1410,1440
1420      ELEC(L)=0.0
GC TO 1600
1430      ELEC(L)=(EIN(L)-EA(1))*FDEL
GC TO 1500
1440      IF(W-JW) 1460,1460,1450
1450      N=JW
1460      ELEC(L)=(EIN(L)-E(M))*DREL(M)+EL(M)
C
1500      CC 1590 1=1,3
IF(B(L)-BMAX(L)) 1510,1510,1590
1510      J=E(L)*DBSR
EAV(I)=EAV(I)+ELEC(L)*FLPD(J,I)*SCB

```



```

311CC DC 3500 I=1,2 JFIT
      FIX=FIT(I,M=1,3)
      DC 3200 M=1,3
      DC 3200 N=1,KEOM
      320C PEL(N,M)=FIX*ELECS(N,M)+PSE(I)
      WRITE(6,9505) 1H2
      WRITE(6,9510) 1H1,IAH,LCRYST,A0,KM,DX
      WRITE(6,9520) 1H1
      9720 FFORMAT(//,//,30X,5H ION,/,30X,4CH ENERGY
      (1,1) (6,5730) (EQLIN(N,M),N=1,3),N=1,KEOM)
      9730 FFORMAT(26X,FL0.0,5X)3E16.5
      974C WRITE(6,9740) PSEL(I)FIT(I)
      974C FFORMAT(//,30X,20H PSE(I)FIT(I)
      35CC 2 14H ELECTRONS/ICN
      9995 CCNTINUE
      GC TO 15
      STCP
      ENCL
      ENCL
      //GC, SYSIN 00

```


LIST OF REFERENCES

1. Medved, D. B., Mahadevan, P., and Layton, J. K., "Potential and Kinetic Electron Ejection from Molybdenum by Argon Ions and Neutral Atoms," Physical Review, v. 129, p. 2086-2087, 1 March 1963.
2. Harrison, D. E., Jr., Carlston, C. E., Magnuson, G. D., "Kinetic Emission of Electrons from Monocrystalline Targets," Physical Review, v. 139, p. A737-A745, 2 August 1968.
3. Carter, G. and Colligon, J. S., Ion Bombardment of Solids, American Elsevier Publishing Co., Inc., 1968.
4. Parilis, E. S., and Kishinevskii, L. M., "The Theory of Ion Electron Emission," Soviet Physics - JETP, v. 3., p. 885-891, October 1960.
5. Firsov, O. B., "A Qualitative Interpretation of the Electron Excitation Energy in Atomic Collisions," Soviet Physics - JETP, v. 36, p. 1076-1080, November 1959.
6. Wolff, P. A., "Theory of Secondary Electron Cascade," Physical Review, v. 95, p. 56, 1954.
7. Harrower, G. A., "Auger Electron Emission in the Energy Spectra of Secondary Electrons from Mo and W," Physical Review, v. 102, p. 340, 1956.
8. Torrens, I. M., Interatomic Potentials, Academic Press, 1972, 247 p.
9. Russek, A., "Ionization Produced by High Energy Atomic Collisions," Physical Review, v. 132, p. 246-261, 1 October 1963.
10. March, N. H., "The Thomas-Fermi Approximation in Quantum Mechanics," Advances in Physics, v. 53, p. 206, 1957.
11. Gombas, P., Die Statische Theorie des Atoms und ihre Anwendungen, Springer-Verlag, 1952.
12. Wedepohl, P. T., "Influence of Electron Distribution on Atomic Interaction Potential," Proc. Phys. Soc., v. 92, p. 79-93, 22 March 1967.
13. Harrison, D. E., "Semiclassical Interaction Potential for Atoms and Ions," Bull. Am. Phys. Soc. II, v. 14, p. 315, 1969.

14. Wilson, W. D., Bisson, C. L., "Inert Gases in Solids: Interatomic Potentials and Their Influence on Rare Gas Mobility," Physical Review, v. 3, p. 3984, 1971.
15. Günther, K., "Über die Existenz eines Maximalprinzips als aquivalente Formulierung des Thomas-Fermi-Dirac Modells und das TFD Wechselwirkungspotential von Atomen," Ann. Physik. (7), v. 14, p. 296, 1964.
16. Herman, F. and Skillman, S., Atomic Structure Calculations, Prentice-Hall, Inc., 1963.
17. Ralston, A. and Wilf, H. S., Mathematical Methods for Digital Computers, v. 2, John Wiley and Sons, p. 249-263, 1968.
18. Conte, S. D and de Boor, C., Elementary Numerical Analysis, 2d. ed., McGraw-Hill Book Co, 1972.
19. Mashkova, E. S., Molchanov, V. A., and Odintsov, D. D., "Anisotropy of the Ion-Electron Emission Coefficient of Single Crystals," Soviet Physics - Doklady, v. 8, p. 806-807, Feb. 1964.
20. Carlson, C. E., Magnuson, G. D., Mahadevan, P. and Harrison, D. E., Jr., "Electron Ejection from Single Crystals due to 1- to 10- Kev Noble Gas Ion Bombardment," Physical Review, v. 139, p. A729-A736, 2 August 1965.
21. Baboux, J. C., Pedrix, M., Goutte, R., and Guillaud, C., "Emission Electronique Secondaire d'un Monocristal de NaCl Bombardé par des Ions de Gaz Rares," J. Phys. Appl. Phys., v. 4, p. 1617-1623, 9 June 1971.
22. Baboux, J. C. and Pedrix, M., unpublished data, private communication.

INITIAL DISTRIBUTION LIST

	No. Copies
1. Defense Documentation Center Cameron Station Alexandria, Virginia 22314	2
2. Library, Code 0212 Naval Postgraduate School Monterey, California 93940	2
3. Professor D. E. Harrison, Codes 61 Hx Department of Physics and Chemistry Naval Postgraduate School Monterey, California 93940	5
4. MM H. Perdrix and J. C. Baboux Institut National des Sciences Appliquees de Lyon 20 Avenue Albert Einstein 69261 Villeurbanne Lyon, France	1
5. Ensign Kristin Lloyd Allen 505 Sweeney Road Virginia Beach, Virginia 23452	1

UNCLASSIFIED

Security Classification

DOCUMENT CONTROL DATA - R & D

(Security classification of title, body of abstract and indexing annotation must be entered when the overall report is classified)

GENERATING ACTIVITY (Corporate author) Naval Postgraduate School Monterey, California 93940	2a. REPORT SECURITY CLASSIFICATION Unclassified
	2b. GROUP

PORT. TITLE Secondary Electron Emission from Monocrystalline Metal and Alkali-Halide Crystals

DESCRIPTIVE NOTES (Type of report and, inclusive dates) Master's Thesis; June 1973

AUTHOR(S) (First name, middle initial, last name) Kristin Lloyd Allen
--

PORT. DATE June 1973	7a. TOTAL NO. OF PAGES 174	7b. NO. OF REFS 22
-------------------------	-------------------------------	-----------------------

CONTRACT OR GRANT NO.	9a. ORIGINATOR'S REPORT NUMBER(S)
-----------------------	-----------------------------------

PROJECT NO.	9b. OTHER REPORT NO(S) (Any other numbers that may be assigned this report)
-------------	--

DISTRIBUTION STATEMENT		
------------------------	--	--

Approved for public release; distribution unlimited

SUPPLEMENTARY NOTES	12. SPONSORING MILITARY ACTIVITY Naval Postgraduate School Monterey, California 93940
---------------------	---

ABSTRACT	
----------	--

This thesis is a computer simulation of secondary electron emission (SEE) from monocrystalline metals and alkali-halides using a modified version of the Harrison, Carlston and Magnuson single collision theory of SEE. Three cases of SEE are investigated: the angular dependence of SEE from Cu bombarded by Ar, the dependence of SEE as a function of energy for rare gas ions normally incident on the (100), (110) and (111) faces of metal single crystals, and the dependence of SEE as a function of energy for Ar and Ne ions normally incident on the (100), (110) and (111) faces of KCl. The theory does not accurately describe the angular dependence of SEE for monocrystalline Cu targets, but does accurately predict the modified $\sec \theta$ dependence found experimentally in polycrystalline studies. For the metal targets, the difference between the theoretical kinetic secondary emission result and the experimental datum is identified as potential secondary emission. The alkali-halide SEE simulation agrees reasonably well with experiment.

UNCLASSIFIED
Security Classification

KEY WORDS

KEY WORDS	LINK A		LINK B		LINK C	
	ROLE	WT	ROLE	WT	ROLE	WT
Secondary						
Electron						
Emission						
Ion						
Bombardment						

15 FEB 77

23882

Thesis

A3778 Allen

c.1

143438

Secondary electron
emission from monocrystal-
line metal and alkali-
halide crystals.

15 FEB 77

23882

Thesis

A3778 Allen

c.1

143438

Secondary electron
emission from monocrystal-
line metal and alkali-
halide crystals.

thesA3778

Secondary electron emission from monocrystalline silicon

3 2768 001 91020 1

DUDELEY KNOX LIBRARY